Figure B.1c Howland Hook Terminal gate –Booth views

The “ceiling” is 15 feet above the road surface and consists of a metal grid (2-ft x 4-ft) that supports non-metallic acoustic tiles (many missing). Above the islands between Lanes C, D, E, and F are piping and blowers that are suspended from the ceiling Figure B.1d. Between Lanes L and M there is an island-to-ceiling masonry structure (possibly a stairwell housing). Between Lanes M and N is a metal-covered wall, with a mixture of chain-link fencing and equipment at the in-bound side.

Figure B.1d. Details of Piping and Blowers in Gate Area

Gate Geometry and Traffic Flow

Figures B.2.a-c show the in-gate geometry and traffic flow. There are total of 20 lanes, 12 of which are in-bound (Lanes E-S), 4 are reversible (Lanes A-D), and four are out-bound lanes in the uncovered area. The blue boxes (figure B.2b-c) represent the booths/clerk houses; the tops of their roofs are typically nine (9) feet above the road surface. The yellow shapes represent piping and blowers located in the ceiling. Yellow triangles mark the beginning of the island. Figure B.2.c shows a green 20-foot container in Lane F, with the e-seal on the back door of the container. In Lane G, there is another 20-foot container, with no e-seal, and is marked in gray.

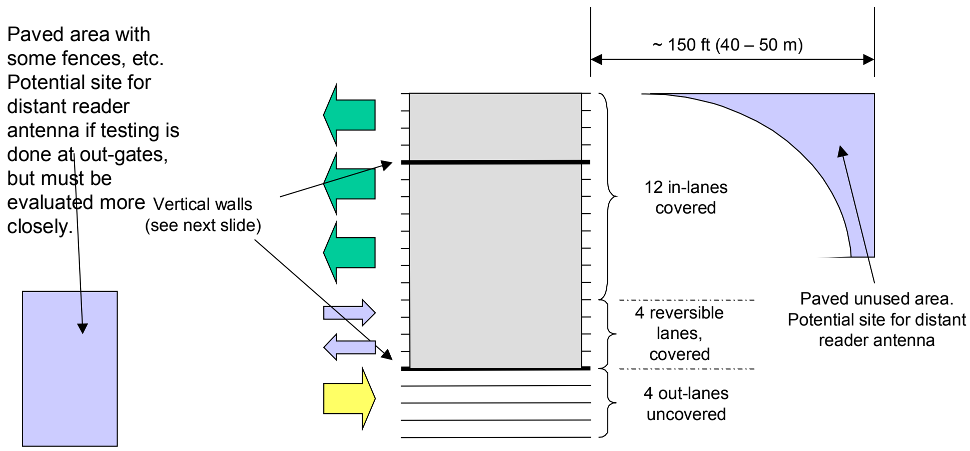

Figure B.2a View of In-gate Area with Traffic Flow

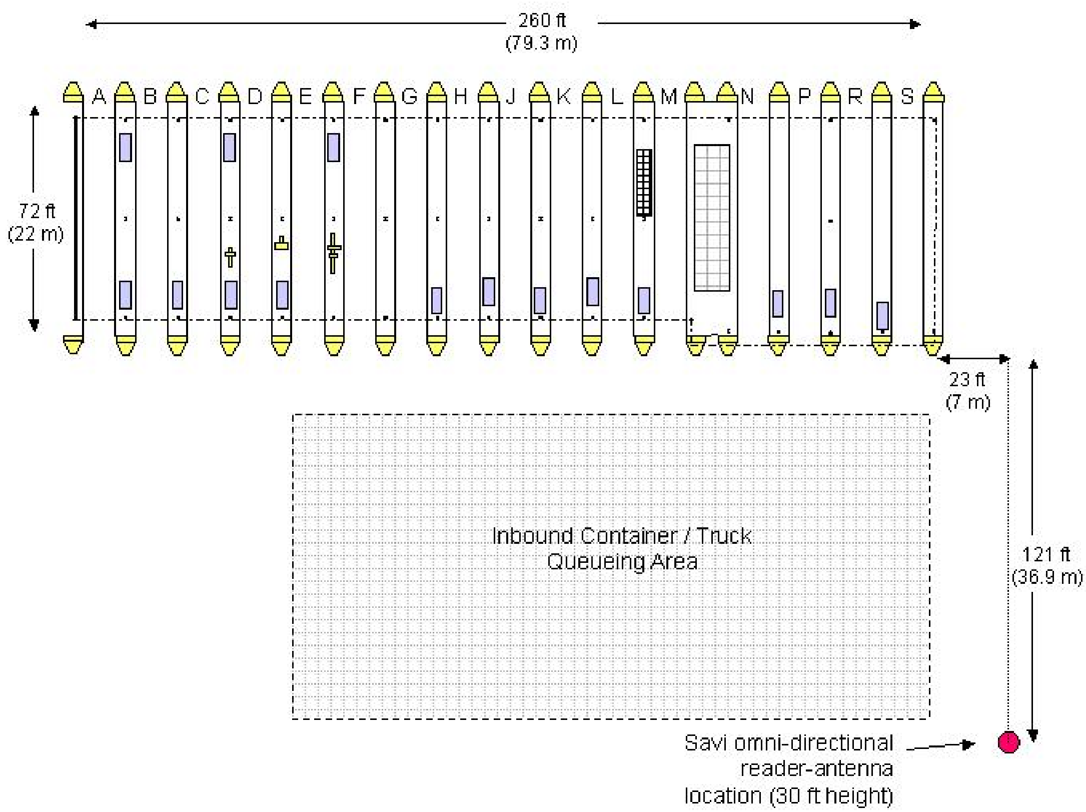

Figure B.2b. View of Gate area with marked position of the Savi Antenna/reader (Lanes A-B are out-lanes)

.

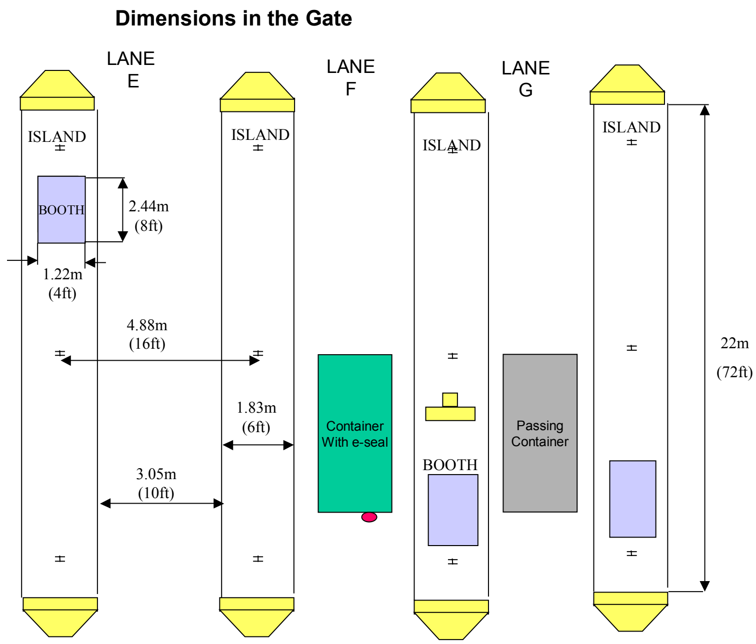

Figure B.2.c In-gate dimensions

Antenna Placement

A vertically-oriented, quarter-wave whip dipole antenna with a circular ground plane was positioned above the E/F island as shown in Figures 3a and 3b. It was placed about 14.5 feet above the road surface, so that its ground plane was slightly below the reflector of a nearby fluorescent lamp. The red circle in Figure B.3b indicates its location. Lanes E and F were selected because they were unused the day of the testing. The lack of clerk houses in islands E/F and F/G minimized large, nearby reflective surfaces. This antenna location was used for testing of Hi-G-Tek, e-Logicity and AllSet seals inside of the gate. Time constraints prevented attempts at optimizing antenna location, which could easily vary among the vendors' systems and would depend on the antenna choice, terminal process requirements, etc. Also, using a longer antenna with a higher gain conceivably could extend the read range. However, the low ceiling and the possible need to place an antenna over a Lane may limit that option. Directional antennae with higher gain are also an option.

Figure B.3a. Antenna Location for e-Logicity and Hi-G-Tek Range Tests

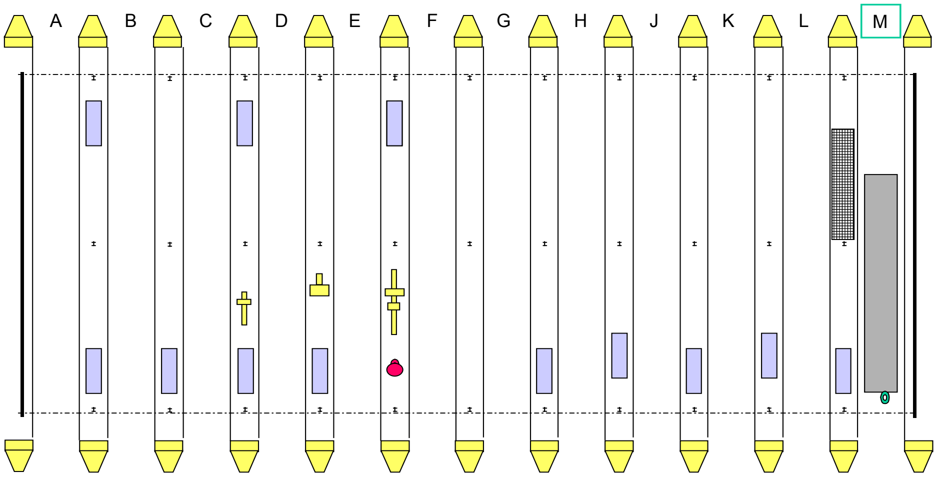

Figure B.3b. Antenna Location for e-Logicity and Hi-G-Tek Range Tests – between Lanes E and F

Savi recommended the external location for their system[1]. Figure B.2b depicts the location of the Savi reader (with integrated antennae) in the gate area – red circle.

[1] There were indications from the other vendors that ranges may be inadequate to reach the in-Lanes if the reader antennae were positioned behind the queuing area. Also, positioning reader antennae inside the gatehouse structure allowed us to examine qualitatively the ability of different wavelengths to travel in a relatively "crowded" environment

B.2 E-LOGICITY TEST RESULTS AND OBSERVATIONS

Gate-Area Readability

As discussed and illustrated in Laboratory test Report (section A.2), in many cases the e-Logicity seal can rotate about its bolt after installation, affecting signal strength and readability.

We tested the seal in three rotational orientations:

- Position 1: Seal face and barcode facing out from door
- Position 2: Seal rotated 90° so that its label faces the right side of the container
- Position 3: Seal rotated 180° so that its label faces the container.

We activated the seal by placing a modified bolt into it. The modification allowed us to place the bolt through the door hasp as would typically be done, but a screw-in plug at the top allowed us to remove the seal and transfer it to another container. (Incidentally, the seal correctly transmitted to the reader that it was "Tampered.") The seal was typically placed on a container as it waited in the queue, and we attempted to read the beaconing seal as the container moved into the gatehouse. Since we were using functional containers during normal gate operations, the containers stopped at various locations. In the queue, the container doors face away from the reader antenna, and no e-Logicity seals were read while in the queue.

Figures 4 and 5 show the results obtained when containers stopped in Lanes M and L, respectively. Several readings (each 10 seconds apart because of the seal's beacon rate) were made with the seal in each rotational position. All readings (except one) for both Lane M and L were successful. For example in figure 4, with container in Lane M, and with the seal in position 1, 5-of-5 reads were successful. In figure 5, with container in Lane L, and seal in position 2, 3-of-3 reads were successful, as another container moved through Lane H. A possible reason that caused one missed read in position one maybe a refraction of the signal from the surrounding structures moving container.

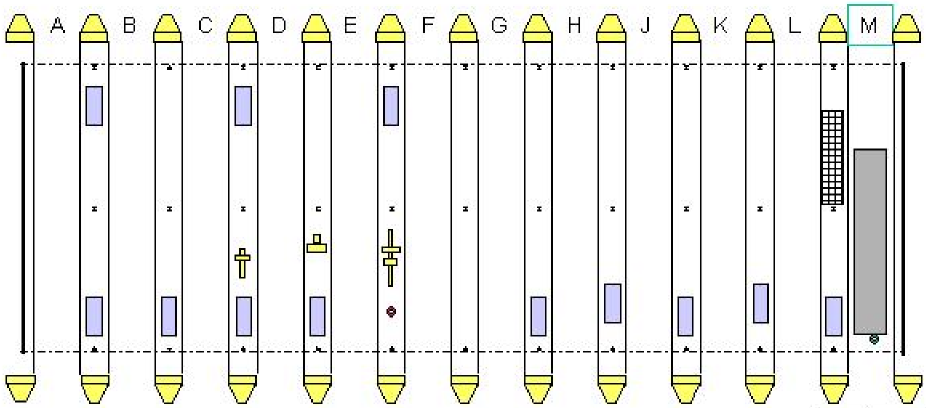

Pos.	Rate
1	5/5
2	7/7
3	4/4

Figure B.4. e-Logicity Seal in Lane M

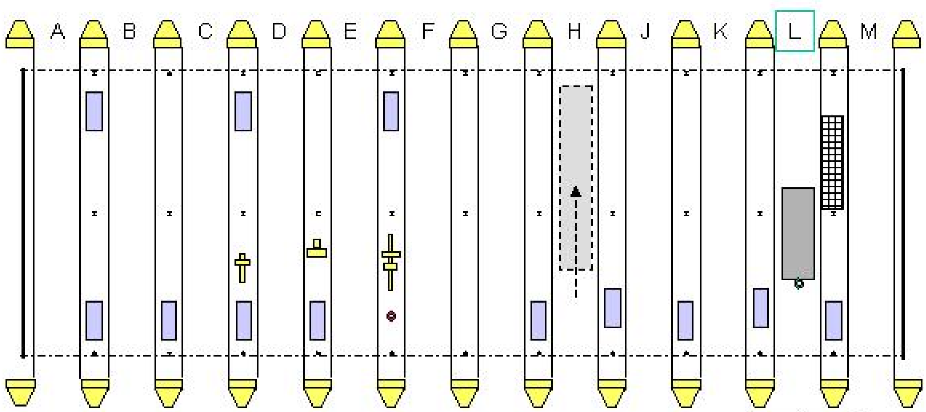

Pos.	Rate
1	12/13
2	3/3
3	3/3

Figure B.5. e-Logicity Seal in Lane L

In Lane K, as shown in Figure B.6, with a container in Lane J and clerk house nearby, reads were only achieved with the seal in Position 2. Lane H contained only a chassis. Also, there was an existing bolt seal in the handle, so our seal was placed in the outboard latch on the right-side door.

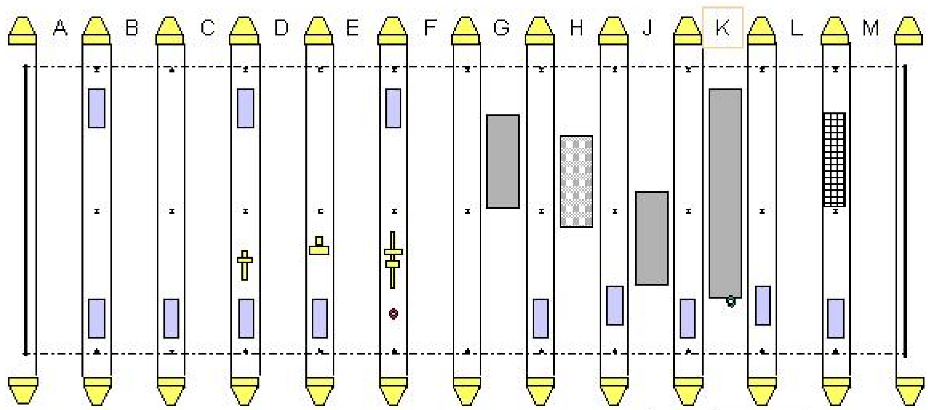

Pos.	Rate
1	No reads
2	4/7
3	No reads

Figure B.6. e-Logicity Seal in Lane K (seal on outboard latch)

Figure B.7 shows consistent reads in all seal positions in Lane H. Because of the proximity to the two clerk houses, there were often drivers walking near the seal; this apparently had no adverse effect.

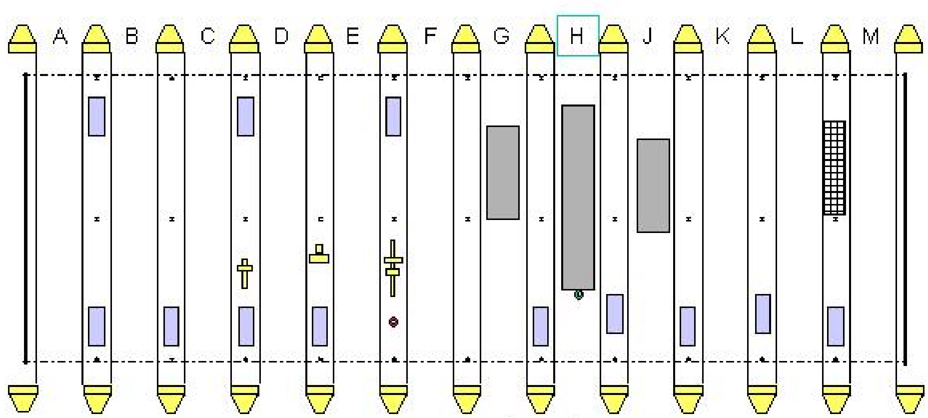

Pos.	Rate
1	3/4
2	4/4
3	6/6

Figure B.7. e-Logicity Seal in Lane H

Containers in Lanes A-D were outbound, so there was never a clear line of sight from the reader antenna to the doors. Figure B.8 shows a container in Lane D that had bolt seals in both right-door latches. So, we tested the seal on the inboard latch of the left-side door. Very good reads were obtained. We then taped the seal into place, hanging from the in-board latch of the right-side door.

No reads were obtained. For comparability, we taped the seal into position on the left-door latch; this still provided good read rates. This door is shown in Figure B.9. The left-door latch is about 27 inches (68 cm or about one wavelength) to the left of the inboard right-door latch.

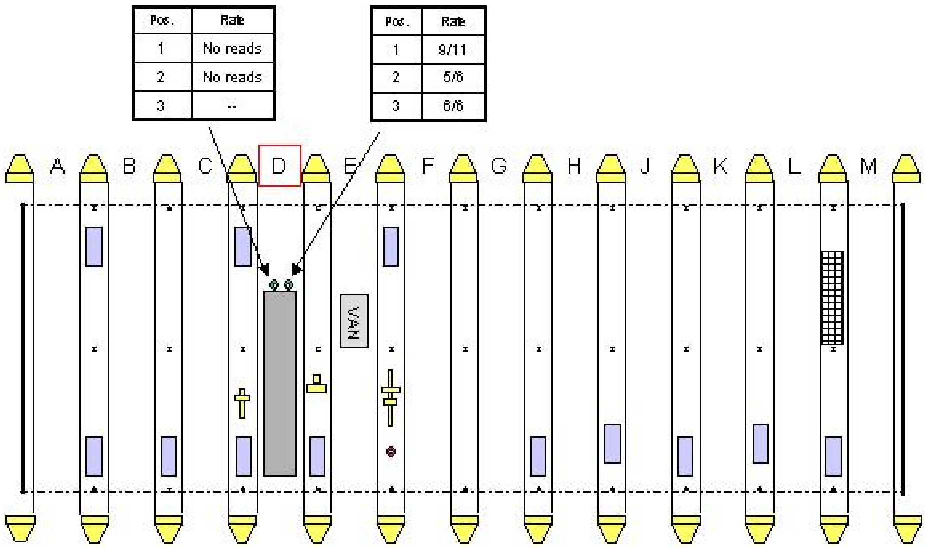

Figure B.8. e-Logicity Seal on Outbound Container in Lane D

Figure B.9. Container Door from Figure B.8 (Lane D)

With no other containers around, a seal in Lane C had to be placed in the outboard, right-door latch. As shown in Figure B.10, no reads were achieved.

When the container pulled forward, so that the seal was past the clerk house as shown in Figure B.11, good reads were achieved. Compared to the case in Figure B.8, the angle from the back left corner of the container to the reader antenna Figure B.11 is not as sharp. This may contribute to the readability from seals placed on the right door.

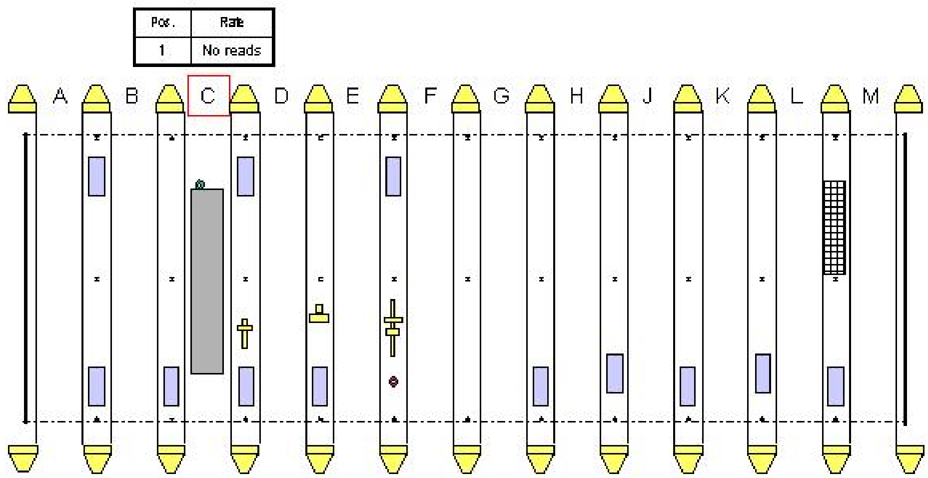

Figure B.10. e-Logicity Seal on Outbound Container in Lane C

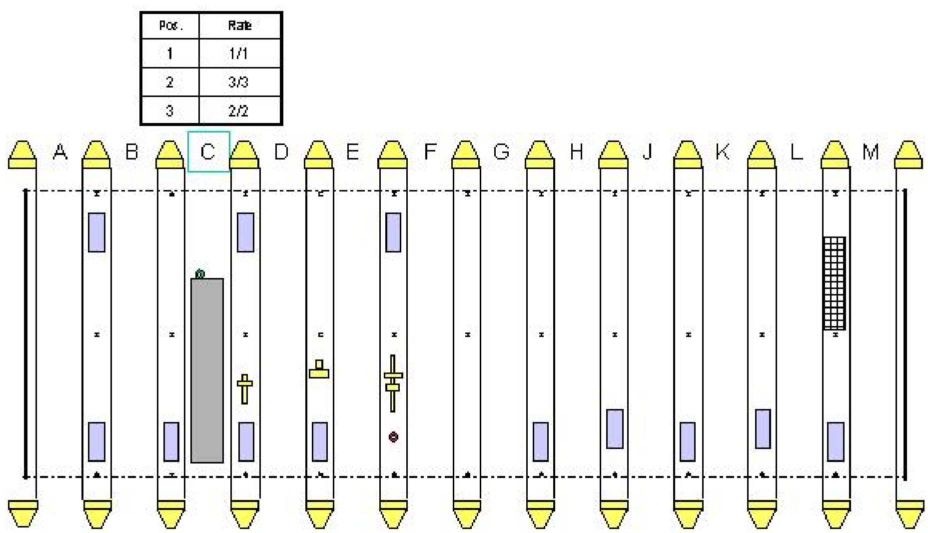

Figure B.11. e-Logicity Seal on Container Pulled Forward in Lane C

Figure B.12 shows a different container in Lane C, with the seal still on the outboard latch. With containers in Lane D and B, good reads were obtained in seal Positions 1 and 2, but reads were inconsistent in Position 3. Because of the proximity to the clerk house, drivers were walking and standing in the general vicinity, though not immediately next to the seal.

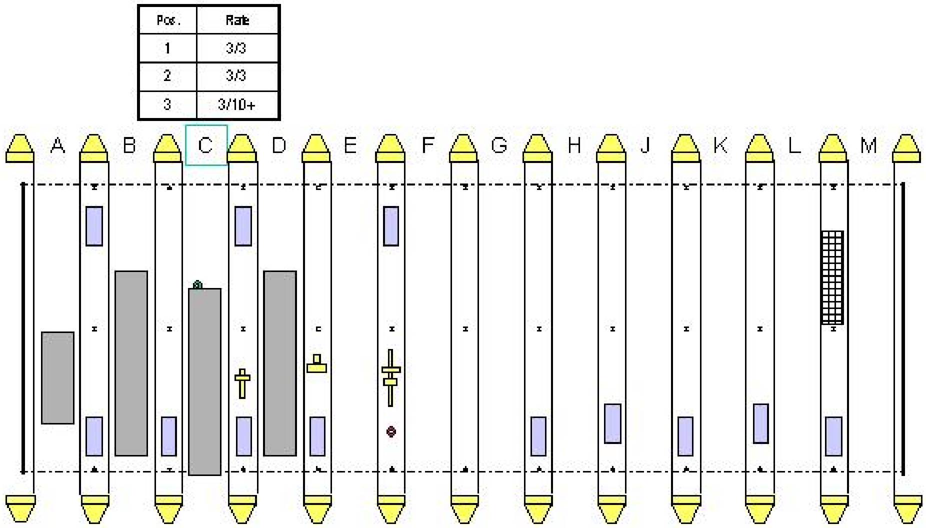

Figure B.12. Containers Surrounding e-Logicity Seal in Lane C

Numerous situations occurred while the seal was on containers in Lane B; these are shown in Figures 13(a) through (e). These results in 13(b) suggest that the presence of a container in Lane D (closer to the reader antenna than Lane C is) may have caused read problems when the seal was in rotational position 2. Also, at least for position 2, reading was more difficult when the container was further back in the Lane (i.e., signals must "turn" a greater amount around the container corner to reach the antenna). In that case (Fig. 13(a)), the I-beam support pillar in island B/C was also near the corner of the sealed container.

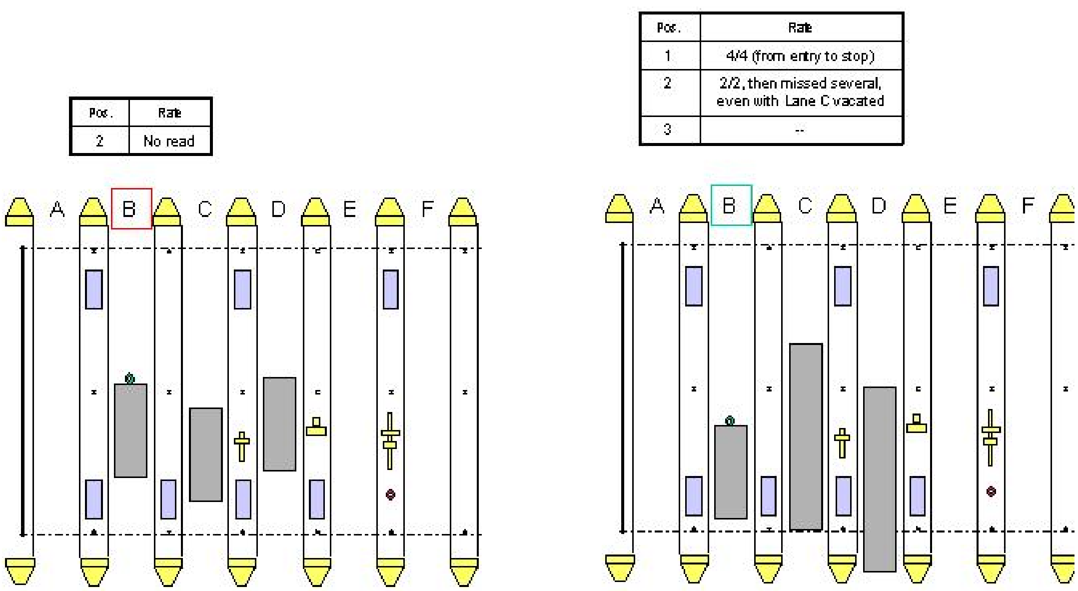

Figures 13(a) and 13(b). Situations with e-Logicity Seal in Lane B

Pos.	Rate
1	--
2	4/4
3	2/4+

Pos.	Rate
1	--
2	3/3
3	--

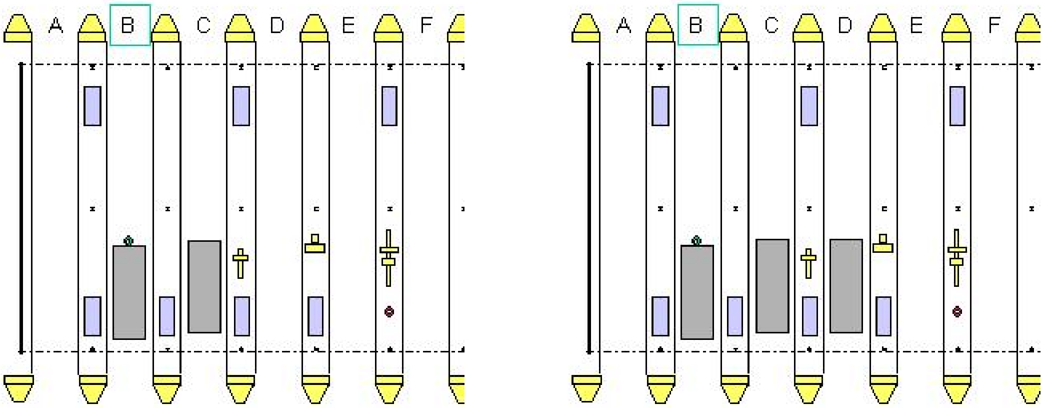

Figures 13(c) and 13(d). More Situations with -Logicity Seal in Lane B

Pos.	Rate
1	--
2	--
3	4/4

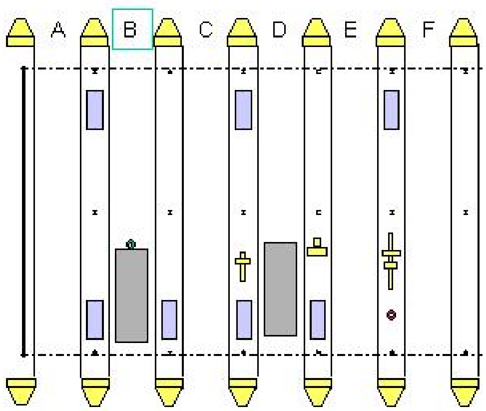

Figure B.13(e). Situation with e-Logicity Seal in Lane B.

Signal Strength

The same seal was placed on a parked container in Lane E, as illustrated in Figure B.14. Using the same antenna as above (quarter-wave dipole with a circular ground plane), field strength measurements were made at a number of lateral locations, at two heights, in two vertical planes, just outside of the gatehouse structure. Figure B.14 shows the locations of these planes (red lines) and locations (red circles).

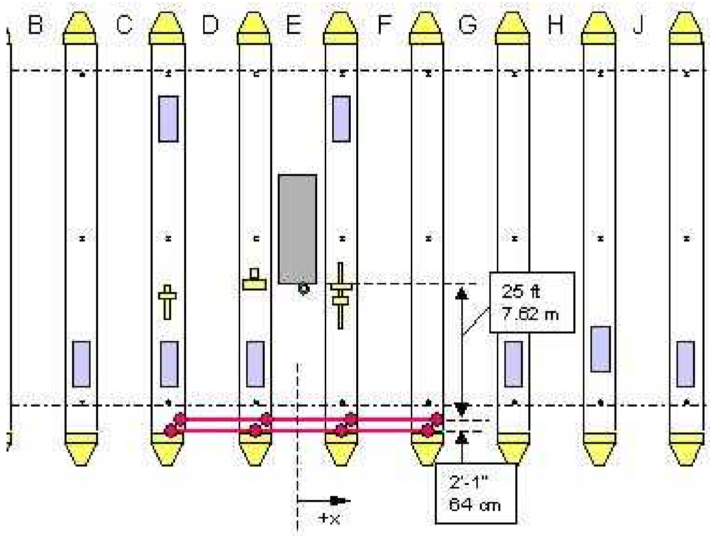

Figure B.14. Schematic of Sealed Container and Field Measurement Points

Figure B.15 shows the antenna in one of these locations. The data are presented in the Table below. They have been corrected for cable losses. Note that there is a different antenna-to-seal elevation angle associated with each measurement point. The antenna may have a somewhat different gain at each such orientation. This must be taken into account in the modeling and in further data reduction. In the Table, Corrected Strength values shown as "32.7" dBμV were actually at the noise floor of the instrumentation; no pulse from the seal was discernible at these points.

Figure B.15. Antenna Outside of Gatehouse Structure

Distance Along Lane (m)	Distance from ctr of Lane E (m)	Height (m)	Seal Orientation	Corrected Strength(dBμV)	Notes
7.62	-6.68	3.91	1	45	
7.62	-6.68	3.91	2	39.7	
7.62	-6.68	3.91	3	44.1	
8.26	-7.32	3.91	1	36.95	Truck in C
8.26	-7.32	3.91	2	32.7	
8.26	-7.32	3.91	3	44	
7.62	-6.68	2.16	1	38.9	
7.62	-6.68	2.16	2	36.7	
7.62	-6.68	2.16	3	42.1	
8.26	-7.32	2.16	1		Truck in the way (D). No data.
8.26	-7.32	2.16	2		Truck in the way (D). No data.
8.26	-7.32	2.16	3		Truck in the way (D). No data.
7.62	-1.802	3.91	1	48.8	53.1 with container 5' past in D
7.62	-1.802	3.91	2	48.8	
7.62	-1.802	3.91	3	49.6	53.2 with container 5' past in D
8.26	-2.442	3.91	1	51.4	
8.26	-2.442	3.91	2	42.4	
8.26	-2.442	3.91	3	32.7	
7.62	-1.802	2.16	1	49.1	
7.62	-1.802	2.16	2	43.2	
7.62	-1.802	2.16	3	51.9	
8.26	-2.442	2.16	1	42.1	
8.26	-2.442	2.16	2	37.2	
8.26	-2.442	2.16	3	39.7	
7.62	3.076	3.91	1	44	
7.62	3.076	3.91	2	43.5	
7.62	3.076	3.91	3	32.7	
8.26	2.436	3.91	1	40.6	
8.26	2.436	3.91	2	36.7	
8.26	2.436	3.91	3	32.7	
7.62	3.076	2.16	1	43.3	
7.62	3.076	2.16	2	42.3	
7.62	3.076	2.16	3	44.4	
8.26	2.436	2.16	1	46.3	
8.26	2.436	2.16	2	44.6	
8.26	2.436	2.16	3	38.5	
7.62	7.954	3.91	1	37.2	
7.62	7.954	3.91	2	38.1	
7.62	7.954	3.91	3	40.5	
8.26	7.314	3.91	1	38.3	
8.26	7.314	3.91	2	42.3	
8.26	7.314	3.91	3	32.7	
7.62	7.954	2.16	1	40.1	
7.62	7.954	2.16	2	40.3	
7.62	7.954	2.16	3	39.5	

8.26	7.314	2.16	1	39.7	
8.26	7.314	2.16	2	41.3	
8.26	7.314	2.16	3	44.3	

Table I. e-Logicity Seal Strength Measurements

B.3 HI-G-TEK TEST RESULTS AND OBSERVATIONS

Gate-Area Readability and Signal Strength

A vertically-oriented, quarter-wave whip dipole antenna with a circular ground plane was positioned above the E/F island as shown in Figures 3a and 16. It was placed about 14.5 feet above the road surface, so that its ground plane was slightly below the reflector of a nearby fluorescent lamp. The red circle in Figure B.16 indicates its location. Lanes E and F were selected because they were unused the day of the testing. The lack of clerk houses in islands E/F and F/G minimized large, nearby reflective surfaces. Time constraints prevented attempts at optimizing antenna location, which could easily vary among the vendors' systems and would depend on the antenna choice, terminal process requirements, etc.

Also, using a longer antenna with a higher gain conceivably could extend the read range. However, the low ceiling and the possible need to place an antenna over a Lane may limit that option. Directional antennae with higher gain are also an option.

The first seal had not been previously used for any extensive testing, and its signal strength had not been measured. After testing with this first seal, we found that its output appeared to be several dB lower than that of the other two seals. So, we conducted additional testing with one of the stronger seals, which we had also used in our laboratory tests. The results with both seals are presented here.

Tests were performed by querying from the reader antenna and waiting for a response from the seal. The query instructed the seal to respond only once.

Immediately prior to testing, a change in the computer used to run the Hi-G-Tek software apparently resulted in losing the ability to vary the reader's output power. This made it difficult to confirm whether the limiting factor was the reader-to-seal link or the seal-to-reader link. Tests were conducted with the reader output power presumably at its default setting (65 on a scale of 0 to 100). Prior laboratory tests had shown that at a power setting of "1," a seal on a door responded at a head-on distance of at least 7 meters (and likely further). Also, a power setting of “60” was found to produce signals about 20 dBμV higher than a setting of “1.” This suggests a head-on range in excess of 70 meters in open space at the default setting; and Hi-G-Tek indicated an expected peak range of about 80 meters in open space.

Figure B.16 shows the seal in Lane M, and shows that the presence of a container in Lane L adversely affects readability. Figure B.17 shows the same seal in Lanes J and L, and indicates that proximity to the clerk houses in islands G/H and H/J may have hurt readability at one location in Lane J.

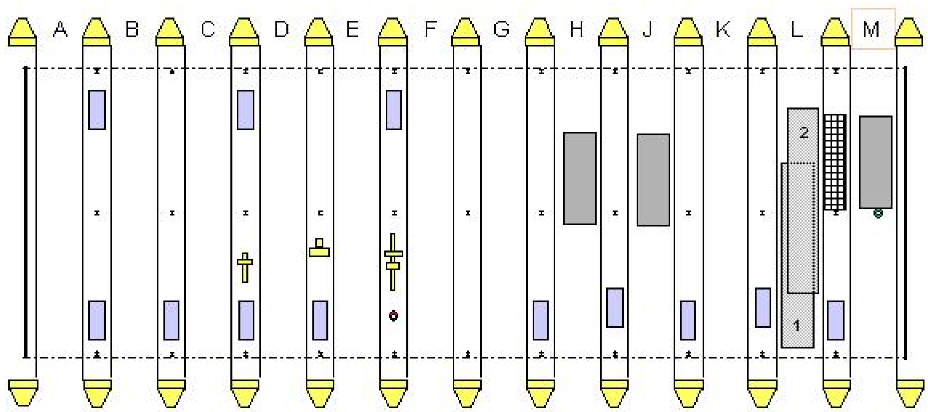

Condition	Rate
No container in L	19/28
Container in L (location 1)	No reads
Container in L (location 2)	No reads

Figure B.16. Hi-G-Tek Seal in Lane M

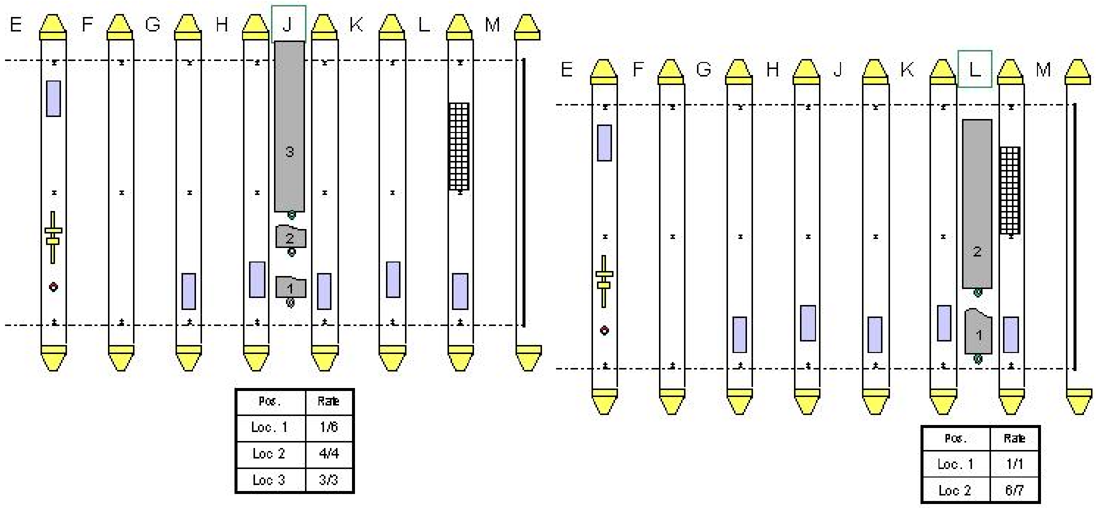

Figure B.17. Hi-G-Tek Seal in Lanes J & L (weaker seal)

Figure B.18 shows seal tested in Lane K. The seal is not in the line-of-site until it the back end of the container is in the gate, hence, there are no reads. Once the back end of the container is in the gate, the reads are registered.

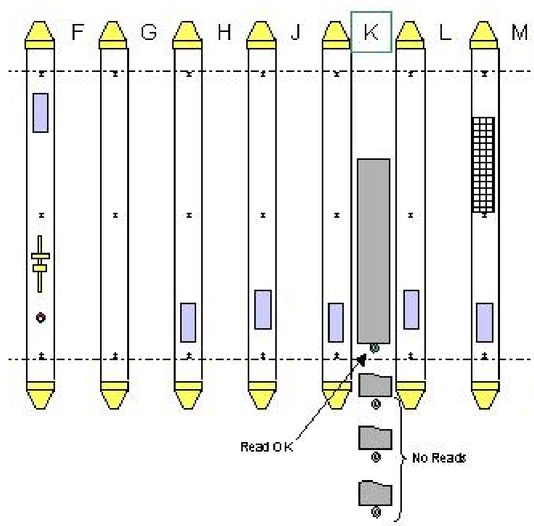

Figure B.18. Hi-G-Tek Seals in Lane K

For outbound containers, with the doors facing “away” from the reader antenna, success was only seen in Lane D with multiple containers arrayed as shown in Figure B.19. However, these tests were conducted with the “weaker” seal. In Lane C, no reads were achieved even with Lane D empty.

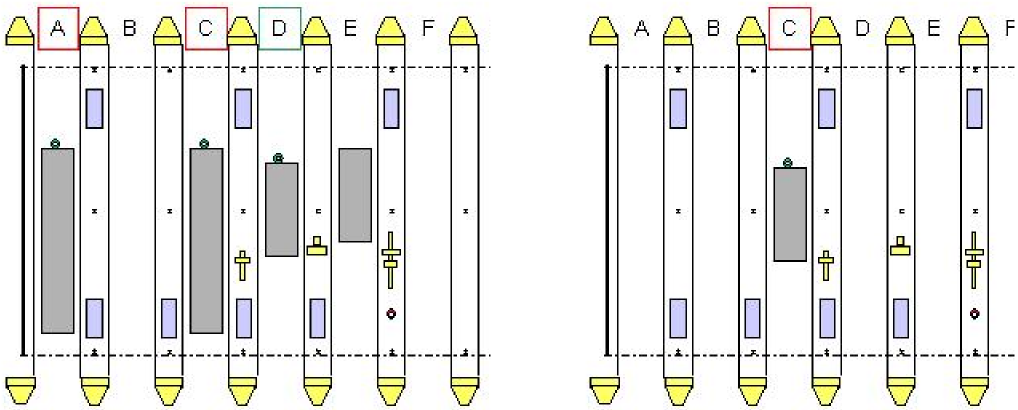

Seal Lane	Rate
A	0/8
B	--
C	0/15
D	9/11

Seal Lane	Rate
C	0/4

Figure B.19. Hi-G-Tek Weaker Seal in Lanes A, C, and D

Hi-G-Tek Updated Gate Testing

Because of the technical difficulties encountered in the earlier testing, we revisited the gate area of the Howland Hook terminal with the same Hi-G-Tek reader and seal. These new tests differed in that:

- The reader output power was better controlled.
- A dipole antenna was connected directly to the reader rather than via a coax cable.
- We located the antenna outside the gate structure. This was to demonstrate the performance of the system in a more likely configuration, rather than to test the performance of 916 MHz transmissions inside the crowded gate structure.

The DataReader, with the vendor-supplied dipole antenna attached, was suspended from a mast at a height of about 25 feet (7.5m). The reader was inverted with the antenna pointing down, so that the casing of the reader would not block signals from below. As shown on Figure B.20 the antenna was placed in Location "A2, "about 61 feet (18.6 m) from the front of the lanes and adjacent to Lane A. Because of the narrow spacing between lanes and the traffic flow, it was not practical to place the antenna out in the queuing area. The A2 location allowed us to test over longer distances than if the antenna was in the middle of the queuing area.

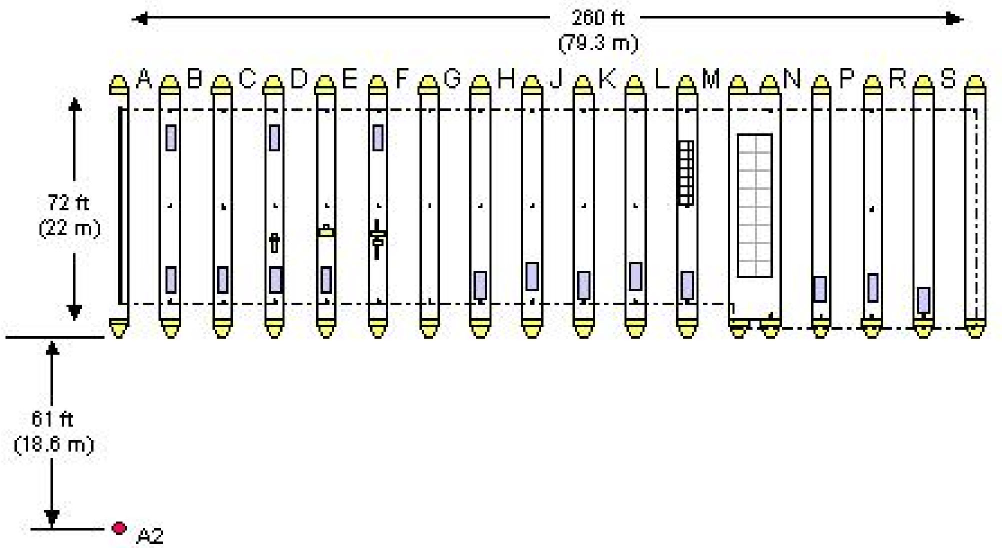

Figure B.20. Location ("A2") of Elevated Hi-G-Tek Antenna and Reader

The reader transmission power was set to "110," which Hi-G-Tek indicated would provide an output power of about 0.75 mW.

In this test, the seal was attached to active but empty containers as they sat in the gate queue and was queried as the containers moved into the gate. The reader interrogation time was set to its default value of 3.06 sec. (Shorter query times require the seals to wake-up and listen for queries more frequently, which reduces battery life proportionately.) The response window was set to a recommended value of 1.68 sec. In this roughly 5 sec period, a container moving at 5 mph (8 km/hr) moves 37 ft (11 m). During the 1.68 sec response window, it moves 12 ft (4 m). So, the moving seal generally receives the query at and transmits its response from different locations. Since the results of each query are displayed after all the seal responses are received, it was not possible to tell precisely where the seal was when it transmitted. It was also not determined whether a failure to read the seal was due to poor communications in the reader-to-seal link or the seal-to-return return link.

With each query, the seal was typically instructed to respond only once during the 1.68 second response window (the number of retries can apparently be set as high as 10 to overcome collisions when multiple seals are responding). If the re-try value were higher, and if there were output-power fluctuations from the seal, we would not know if the reader were detecting all responses or only the strongest. In a multi-seal environment, the stronger signals may be involved in collisions; therefore, one wants to be able to read all of the signals. In some cases, if read rates were low, the number of re-tries was increased to see if this improved performance.

Figure B.21.a shows the results of tests in three lanes, S, P, and M. A seal on a container in Lane S was read on three successive attempts (shown as green circles) as it moved from outside the gatehouse to inside. Trucks with containers were lined up in the queue in Lanes N and P. The seal was read on several more attempts as it sat stationary about halfway down the Lane, as shown. No missed reads occurred. At the furthest point, the distance between the seal and reader was about 280 feet (86 m).

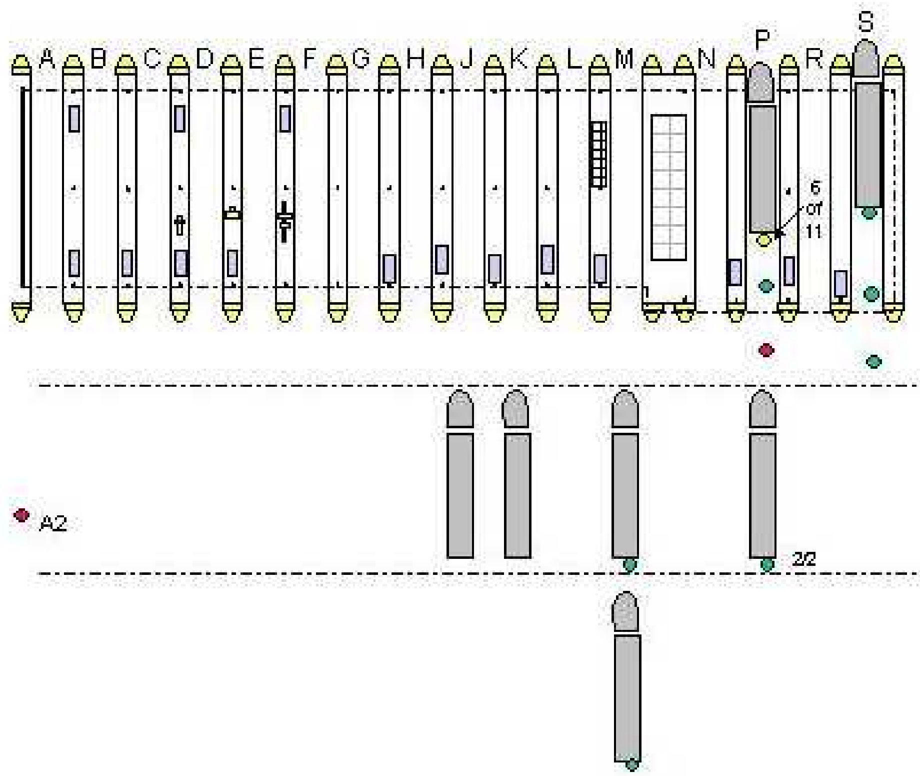

Figure B.21.a. Query Results with Seal in Lanes S, P, and M

In Lane P, the seal was read on two of two attempts as its container sat in the queue. Note that the reader antenna was “ahead” of the plane of the container doors; the signals were effectively wrapping around the container corner. As the seal moved forward into the gatehouse, one read was missed (noted by a red circle). Another truck with a 40’ container sat in the queue in Lane M. It could have been blocking the line-of-sight during the query or response link. Inside the gatehouse, the seal was successfully read while moving. Once it stopped near the location shown, it was read on three of six successive attempts (yellow circle). With the seal and all other containers in the same locations, the seal was instructed to transmit four times for each query. The seal was then read on three of five queries. So, increasing the number of re-tries did not significantly improve the readability of the seal.

In the queue in front of Lane M, the seal was successfully read many times on a container that was next in line (no truck was in the number 2 position). It was also read on a 40’ container that was second in line. The seal-to-reader distance in this position was about 200 feet (63 m), and the reader was about 20° “ahead” of the plane of the doors. The number of re-tries for these cases was set equal to one.

Figure B.21.b shows the results with the seal in Lanes R and L. In both of these cases, a container in the adjacent, intervening lane was also entering the gate, and lagging the sealed container by about one container length. So the front of the intervening container was close to the sealed doors.

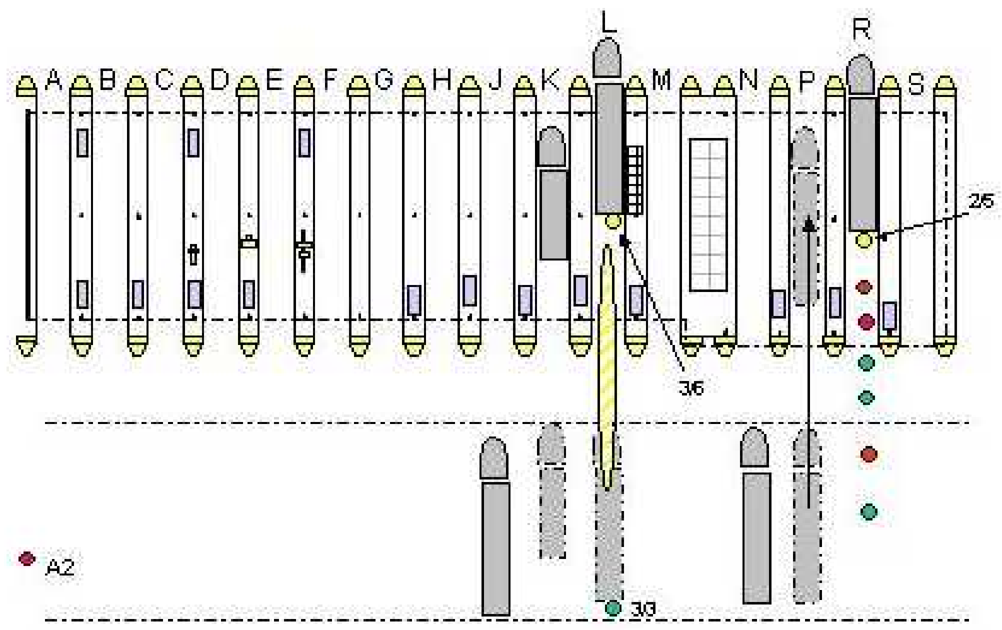

Figure B.21.b Query Results with Seal in Lanes S, P, and M

In Lane R, the seal was read on three of four attempts while it was moving outside the gatehouse. Once inside the gatehouse, and with the adjacent container probably blocking any line-of-sight, two reads failed. Only two of five reads were successful with the container stationary as shown.

With the seal in Lane L, reads were successful while the container sat in the queue. Containers were in Lanes J and K as shown. With the container in Lane K lagging the sealed container, reads were spotty. With the container parked as shown, three of six reads were successful.

Figure B.21.c shows a sealed container in Lane K, with a container in Lane J moving alongside it. A third container sat in the queue for Lane H. Although the seal was read as it sat in the queue, four attempts to read it as it moved toward the gate were unsuccessful (red circles). When it was near the gatehouse structure it was read, but the next attempt failed. The relative positions of the containers in K and J shuffled during this time. But, with the seal stopped in its lane, and with the container in Lane J stopped near the gate entrance as shown, the seal was read successfully on six of six attempts.

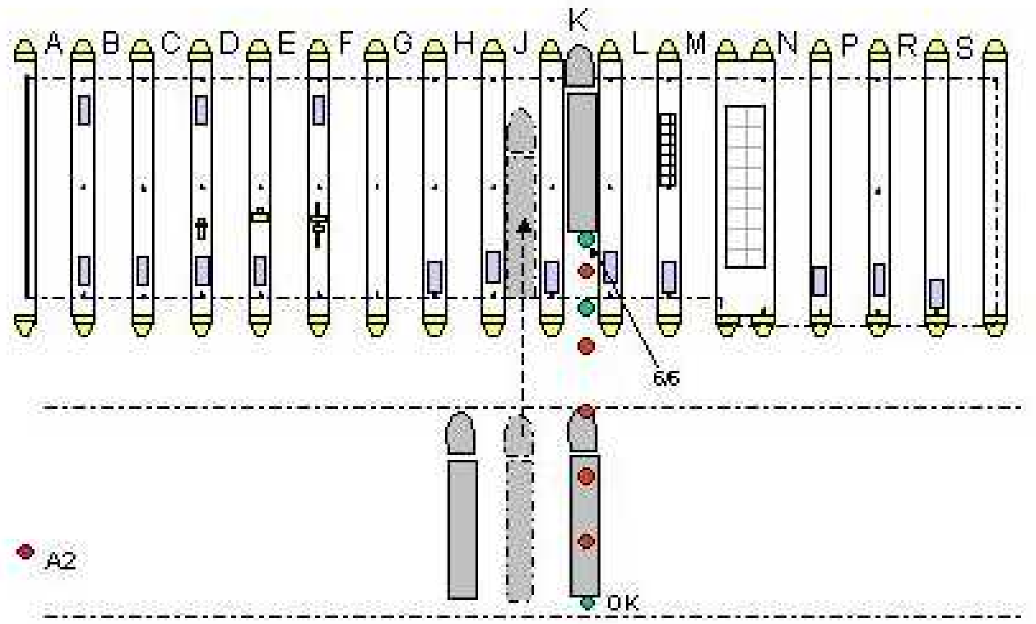

Figure B.21.c. Query Results with Seal in Lane K

When the seal was tested in Lanes E through H, there were no other containers between the seal and the reader antenna. When the seal was in the queue for Lane E, another 40' container was in the queue for Lane F. Likewise, when the seal was in the queue for Lane F, another 40' container was in the queue for Lane G. These adjacent containers may have provided surfaces for reflections as the sealed containers moved forward to the gate. Figure B.22 shows the results for these four lanes.

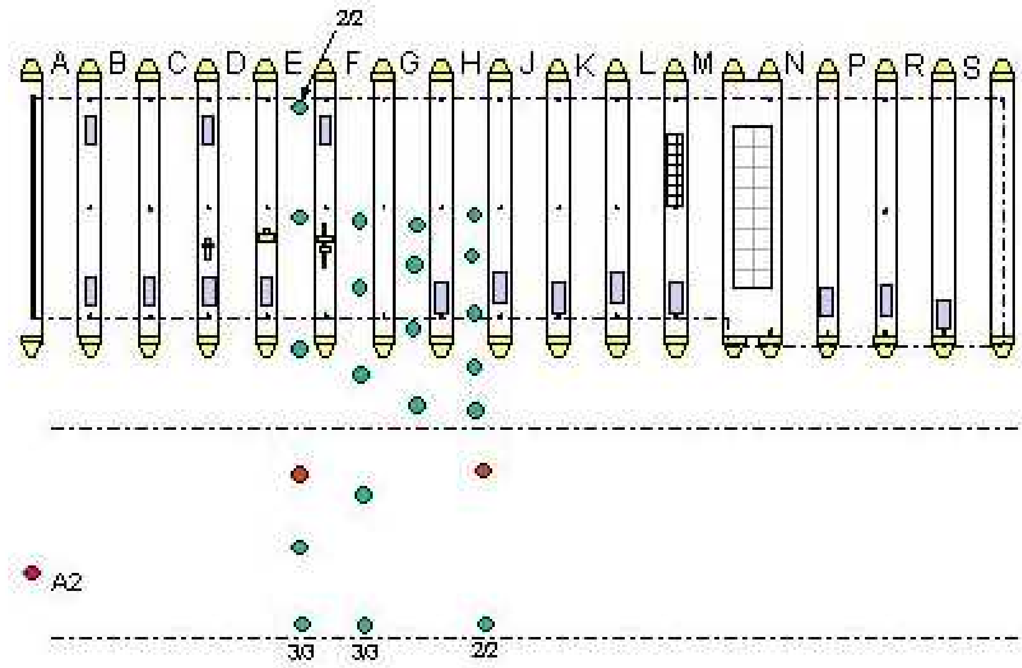

Figure 22. Query Results with Seal in Lanes E, F, G, and H

Of 28 seal locations, only in two positions (once in Lane E and once in H) was a read unsuccessful. Both of these occurred with the seal outside of the gatehouse and in clear view of the antenna. In each lane, the container was stationary for the final query or queries in the locations shown. In Lane E, the truck moved almost completely through the Lane before stopping, so we were able to determine that the seal was readable all the way to the back of the gatehouse.

Overall, the readability of the seals throughout the entire gate structure was good. Read failures usually seemed to be associated with the presence of another container near the sealed container and between the seal and the reader.

With the seal in the near lanes (E through H), there were 11 read attempts made when the seal had a clear line of sight to the reader antenna during both the query and response windows. Reads were unsuccessful in two of these 11 attempts. In one of these, there was a container in an adjacent, further lane; reflections off its surface could have caused a null in the reader or seal area. Reads were achieved at similar view angles from distances that were three times greater, so the read failures are apparently not due to lack of source signal strength.

B.4 SAVI TEST RESULTS AND OBSERVATIONS

Gate-Area Readability and Signal Strength

The location of the Savi reader was shown in Figure B.3. It was elevated about 30 feet above the road surface, within a few meters of a much taller light pole. Four seals with comparable power outputs were typically used simultaneously. Via the reader, we broadcasted a query for all seals in the area to respond. The reader software then reported the ID's and RSSI (received signal strength indicator) from each tag that it read. Since the reader contains two orthogonal antennae to create an omni-directional pattern, the software reported the greater of the two RSSI readings. Savi indicated that for RF-noisy areas, they prefer minimum RSSI values of 60 to 80 to have confidence that reads will be successful. In the low-noise environment of the test terminal, the background RSSI noise was in the range of 25 to 35. We read correct seal ID numbers with RSSI values as low as 51.

We conducted two types of range tests. First, the seals, with their magnetic backings, were attached to various metallic surfaces around the gate structure. To challenge the system, many of these placed on the opposite side of the gatehouse, on surfaces "facing" away from the reader. Many of these were on the flanges of ceiling-support I-beams (10 inches wide). Second, all fours seals were attached to the door of a stationary container being processed in the gate. No bolts were used, so they were not placed directly on the latches.

Figure B.23 shows 11 locations where seals were placed on surfaces other than containers. The results are shown in Table II. At Location 1, no seals were read on one query, an only three of the seals were read on a second query. Table II lists the average for RSSI for this second attempt. In all other cases, all four seals were read.

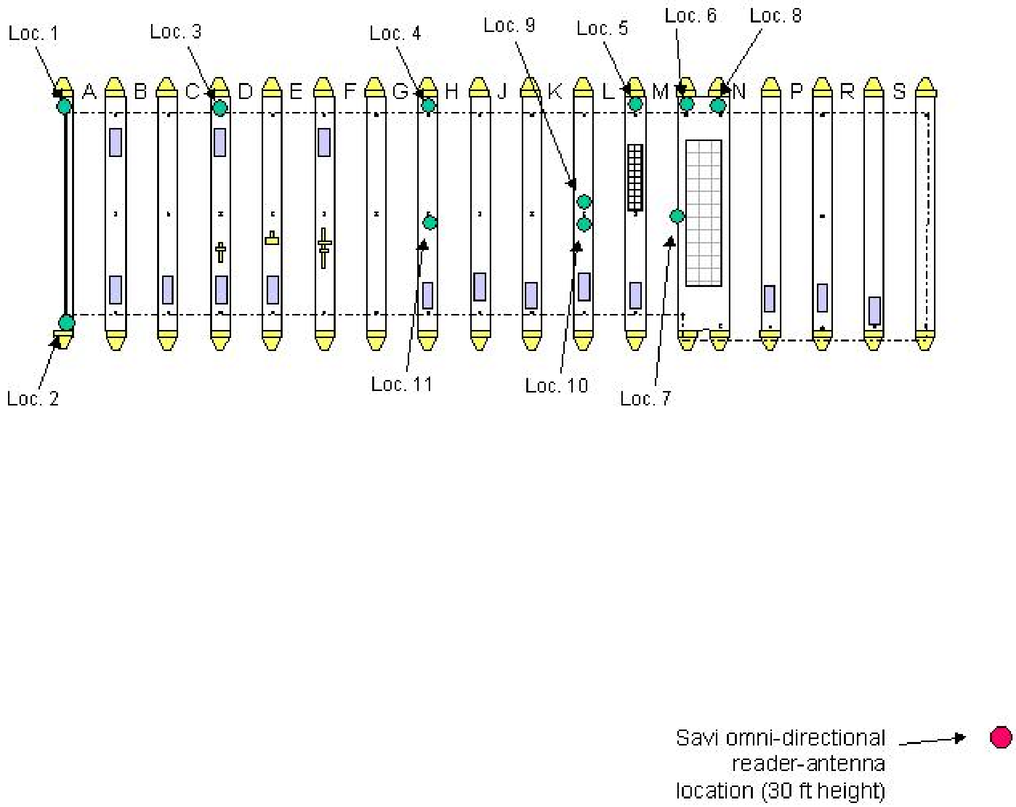

Figure B.23. Savi Seal Locations 1 through 11 in the Gate Area

Location	RSSI (avg)	dBm (avg)
1	52.4	-99.8
2	64.0	-95.2
3	74.1	-91.2
4	76.8	-90.1
5	75.9	-90.4
6	79.0	-89.2
7	78.5	-89.4
8	92.4	-83.9
9	73.3	-91.5
10	101.4	-80.3
11	100.0	-80.8

Table II. Average Signal Strength Measurements for Savi Seals

The average dBm values shown are based on a correlation provided by Savi.

Figure B.24 shows three on-container cases tested. In each case, all four seals were read. Note that this means that the reader-to-seal link and the seal-to-reader link both had an adequate combination of power and gain. The three cases were not simultaneous; they are shown in a single Figure B.for ease of comparison. The signals from the seals in Lane C have an average RSSI of only 65, which Savi may consider marginal in a terminal with higher RF noise at 434 MHz.

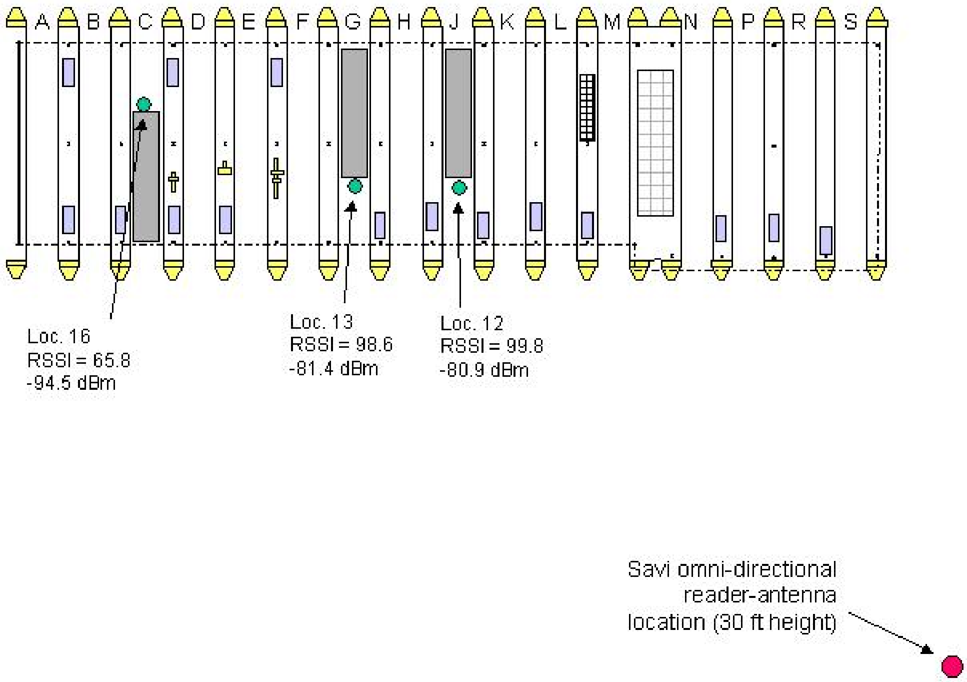

Figure B.24. Results with Savi Seals on Container Doors in Gate Lanes

Figure B.25 shows the other three cases tested. Seals were placed between two 20-ft containers on a single chassis in Lane D. The average signal was as strong as that received from Locations 10 and 11 in Figure B.23, where seals were also at the mid-point of the gatehouse, with a small back-plane (I-beam) but facing the reader antenna. (Note that because of all the containers in the queue and the long distances between the reader and the seals, test personnel were not in visual contact, and the positions of other containers in the gatehouse were not recorded.)

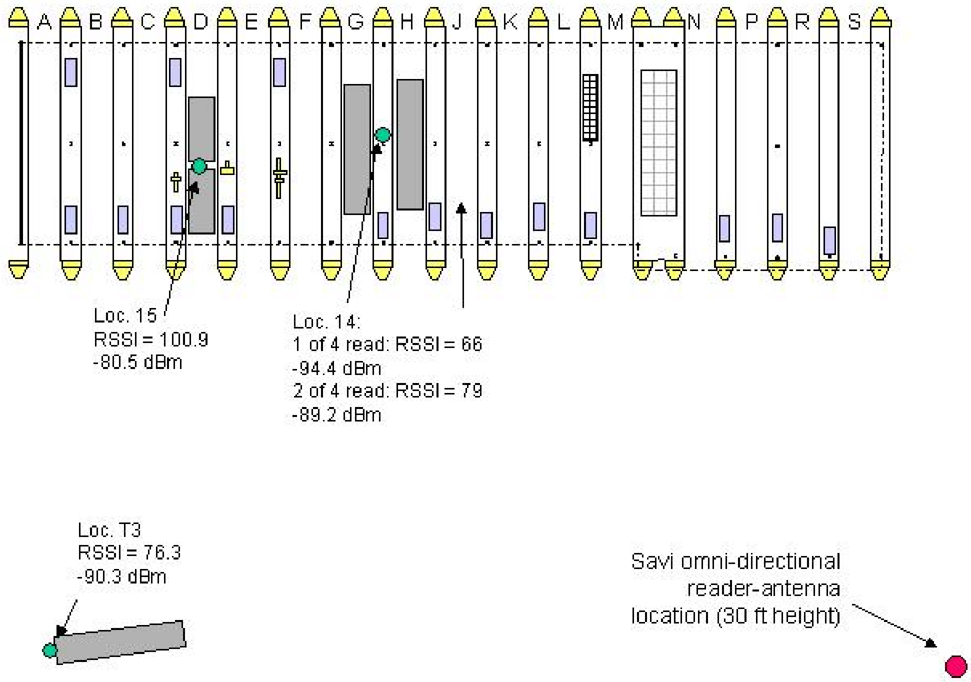

Figure B.25. More Results with Savi Seals in the Gate Area

As shown for Location 14, two containers shielding an away-facing seal reduced the read rate to 37% (these seals were not on a container).

Finally, at Location T3, the four seals were placed on container inside of an entrance tunnel, roughly 100m away from antenna. The seals were queried as the container doors exited the tunnel, with the tractor driving roughly towards the antenna. Four successful reads with an average RSSI of about 76 was recorded. Other measurements with the seals on a light post in that same area gave readings with average values within about 6 dBm of the on-container readings.

B.5 ALL SET TEST RESULTS AND OBSERVATIONS

Gate-Area Readability

For this test, it was impractical to use operating containers as they moved through the gate since the installation/removal of e-seal required opening of the right door of the container. Instead, we installed the seal on a single container and drove that container through various gates.

The reader was positioned above the island between Lanes E and F, as shown in Figure B.26.a, about 10 feet above the road surface. (The tops of the clerk houses were nine feet above the road surface.) The red semicircle and arrow in Figure B.26.a indicates its location and direction. Lanes E and F were selected because they were unused the day of the testing. The lack of clerk houses in islands E/F and F/G minimized large, nearby reflective surfaces. Time constraints prevented attempts at optimizing antenna location, which could easily vary among the vendors' systems and would depend on the antenna choice, terminal process requirements, etc.

The All Set high gain reader includes an integrated, directional, patch antenna with vertical polarization (the low gain reader is omni directional, -9dBd, similar to the AllSeal). Because of its directionality, we performed three sets of tests, each with the reader facing a different direction.

Tests were performed by continuously querying from the reader antenna (scan mode) and waiting for a response from the seal. The process can generate more than one read of the same seal per query. Success rates were measured as the fraction of queries that result in at least one successful read. Because read tests could be run continuously and with intervals of about one second, many of the test conditions allowed us to measure "read zones" as the container was moved slowly through the lanes. In the figures presented below, green-shaded areas mark the approximate regions where the door of the container was, when consistent valid readings were obtained.

In Figure B.26.a, with the reader directed toward Lane M, the seal was read as the container turned to become aligned with the Lane, was lost as the line-of-sight to the reader was blocked by the doors of the container, and was re-acquired as the plane of the doors entered the gatehouse. The read zone extended behind the clerk houses and the intervening containers in Lane L, but readability was lost behind the brick-and-metal, floor-to-ceiling structure between Lanes L and M.

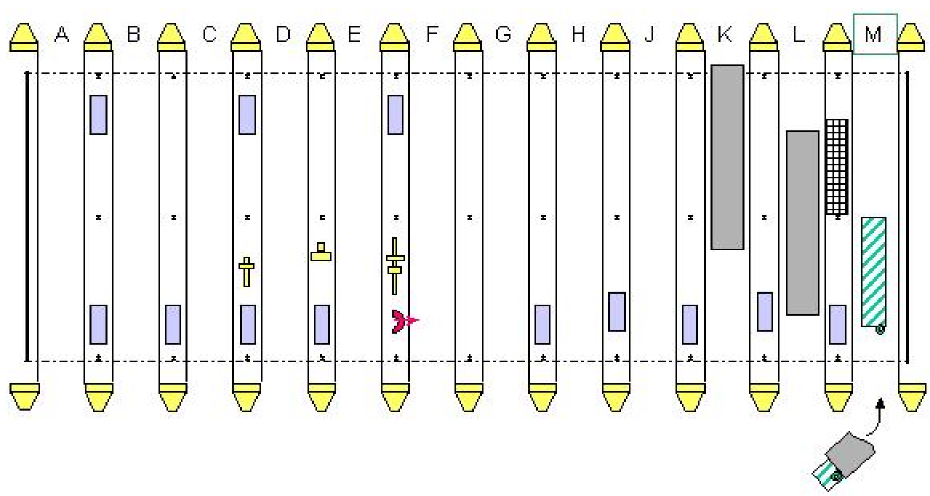

Figure B.26.a. Container with e-seal in Lane M; All Set Directional Reader Aimed Toward Lane M

Figure B.26.b shows the seal in Lane L. The seal was read as it approached the Lane, but once stationary inside, only one read was achieved out of 20 queries. There was no line-of-sight between the reader and seal at that point. Testing while leaving the lane was not performed in this scenario.

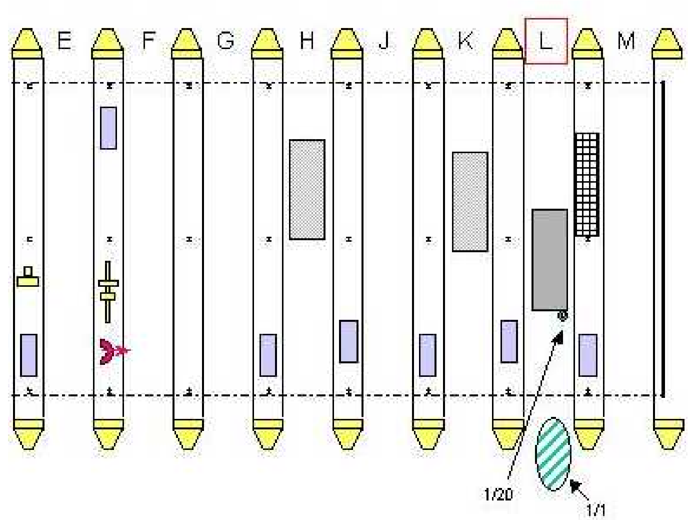

Figure B.26.b. All Set Seal in Lane L, Reader Aimed to Lane M

As shown in Figure B.26.c, the seal was only read in Lane K when it was still outside of the gate structure and approaching the lane. The intervening containers in Lanes G, H, and J, and/or the clerk houses, seem to have provided enough obstacles to prevent a read.

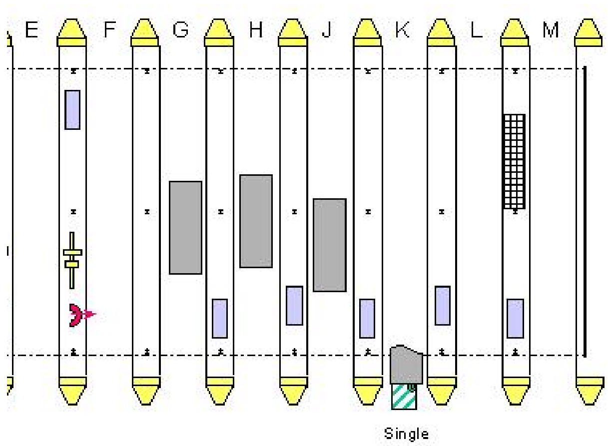

Figure B.26.c. All Set Seal in Lane K, Reader Aimed to Lane M

The seal could be read throughout most of Lane J, even with a container sitting in Lane H, as shown in Figure B.26.d. A container moving through Lane G did not adversely affect readability. A brief region of no reads was observed in the entrance (gap between the two green zones), although reads resumed before the seal moved past the clerk houses.

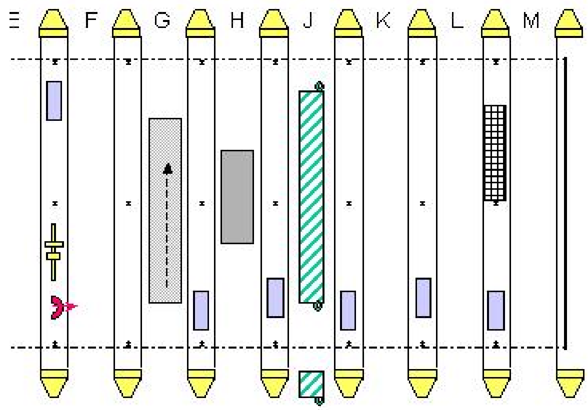

Figure B.26.d. All Set Seal in Lane J, Reader Aimed to Lane M (arrow indicates direction of the container in Lane G)

The results from passes through several lanes are illustrated in Figure B.27.a. In each case, there were no intervening containers between the seal and the reader. As with Lane J, Lane H exhibits a small no-read zone upon entry to the gatehouse structure, but reads resume stops before the seal clears the clerk houses. The reader has a good view of the seal in most of Lanes F, G, and H. The read zone extends further for the more distant Lanes; this is likely due to the sensitivity pattern of the reader patch antenna, which reportedly has a 3-dB full beamwidth of about 65° to 75°, depending on polarization.

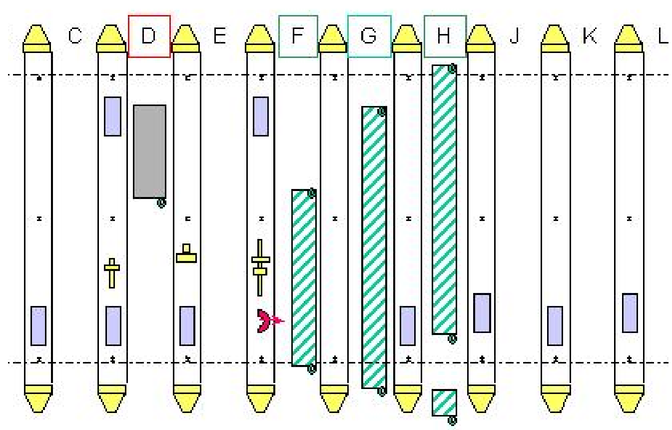

Figure B.27.a. All Set Seal in Lanes D, F, G and H (all inbound)

With the seal stationary in Lane D as shown, no read was achieved. This is to be expected, because of the directionality of the antenna.

Several cases were also tested with the reader antenna aimed toward the container yard, as shown in Figure B.27.b. Note that in Lane D, the seal was not read for most of the passage through the gatehouse, but there was a brief read zone as the seal left the gate. At this point, the seal-to-reader distance and angle appear to be about the same as in Figure B.27.a (seal in Lane D), where no reads were achieved. Three differences may explain these results. First, in Figure B.27.b, the seal has a more open path to the reader; the lip of the container hinge structure prevents line-of-sight from the seal antenna to any reader location on the starboard side of the container. Second, in Figure B.27.a, the seal was stationary, so there may have been a low-signal region that was overcome by moving the seal as in Figure B.27.b. Third, the blower piping and structure suspended from the ceiling may have provided some shielding in Figure B.27.a.

The results for Lanes F and L and Figure B.27.b might be expected based on the results shown for Lanes F, G, and H in Figure B.27.a. The Lane L is far to the side of the directional reader antenna. When the container was driving through Lane F[2], the reader antenna was turned as the container passed by. Good reads were achieved out to some distance beyond the gatehouse. As the container turned to cycle back through Lanes A through D, the seal became readable again, although the seal-to-reader range did not change significantly. This appears to be due to the directionality of the seal's output signal when installed in the hinge area.

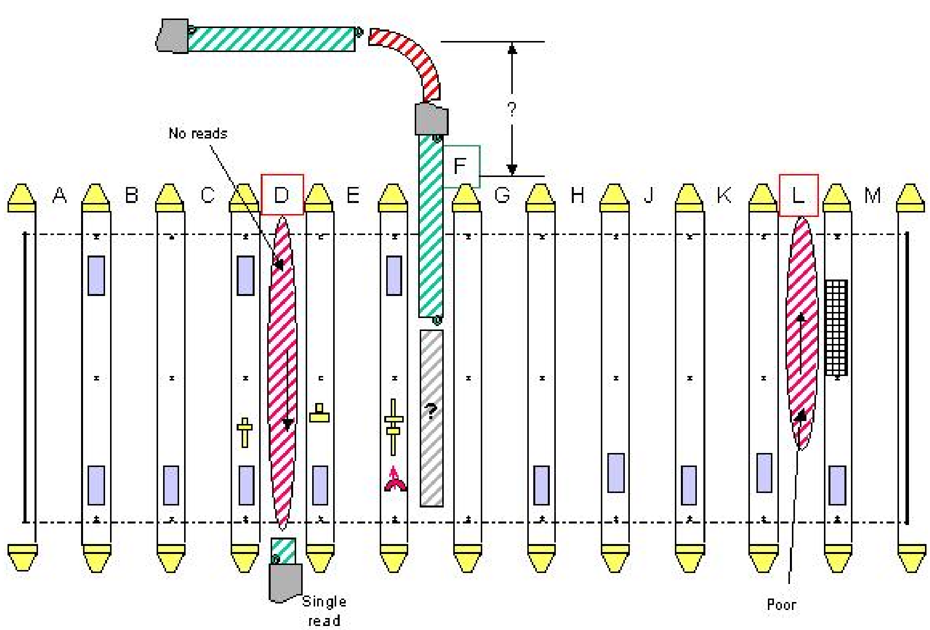

Figure B.27.b. All Set Seal in Lanes D, F, and L, Reader Aimed Toward Yard

---

[2] Note that the read/no-read measurements where not taken as the container was moving through the first half of Lane F, due to other activities. That period is marked as the grey zone.

Figure B.28.a shows the seal in Lane D, with a relatively short view to the reader, with some suspended piping structures in between. Very good readability is obtained until a container moves into Lane E and obstructs the line-of-sight completely. However, when a container is moved into Lane F, it apparently provides a beneficial reflective surface, and readability is restored, even with the container still in Lane E.

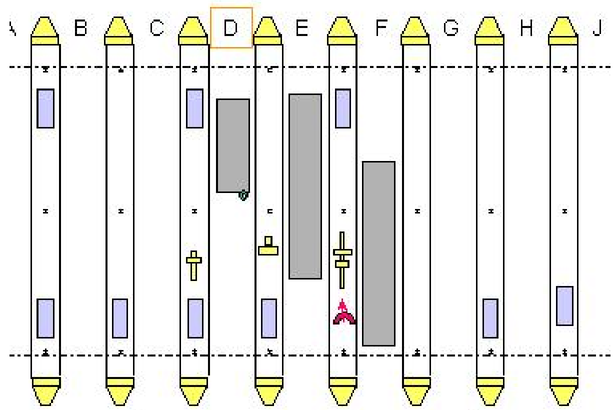

Condition	Readability
Lanes E, F empty	Very good
Container in E as shown	Poor (2/30)
Containers in E, F as shown	Very good

Figure B.28.a. All Set Seal in Lane D (inbound), Reader Aimed to Yard

Figure B.28.b shows the seal in Lane B. For most of its travel through Lane B, the container doors prevent a clear view of the reader. No reads are achieved, even with the intervening Lanes C and D empty. Once the doors were in line with the reader, the seal was behind the clerk house and at a 90° angle to the preferred direction of the reader antenna; no read was achieved. A truck and container pulled into Lane C. As the sealed container exited Lane B, a few reads were obtained. These coincided with a container pulling through Lane G, possibly providing a beneficial reflective surface. These reads were achieved even though the cab of the truck in Lane C blocked the direct line between the seal and the reader, and the reader-to-seal angle was roughly 120° away from the reader antenna's preferred direction.

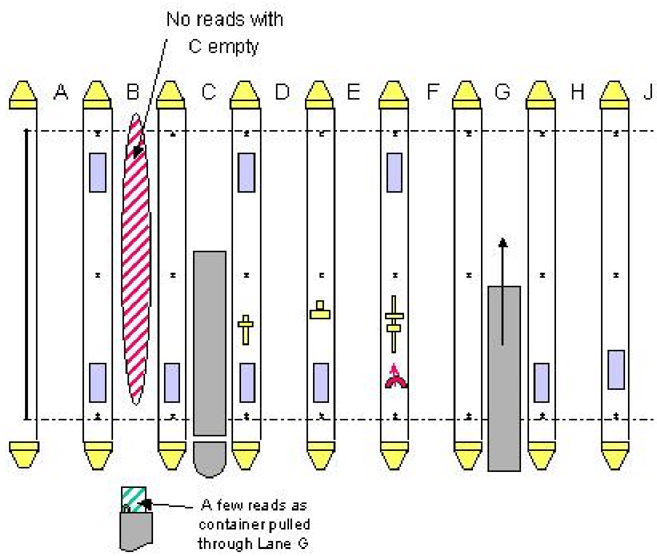

Figure B.28.b. All Set Seal in Lane B (outbound), Reader Aimed to Yard

A few cases were tested with the reader antenna aimed toward Lane A. As shown in Figure B.29.a, with the reader on the starboard side of a container in Lane E, reads begin once the seal is in line with the reader and continue for about 30 feet down the Lane. The stationary container in Lane D (with no container in Lane E) is not read. The angle from the rear left corner of the container to the reader may be too sharp.

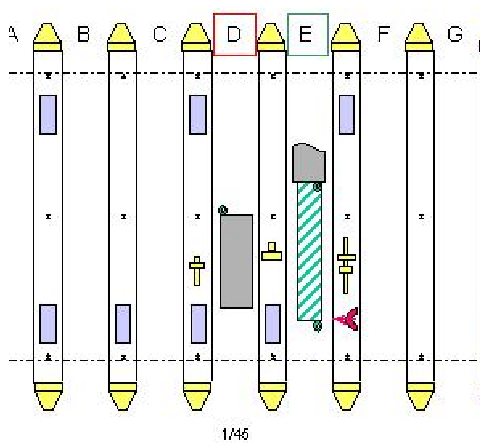

Figure B.29.a. All Set in Lanes D (outbound) and E (inbound), Reader Aimed at Lane A

Figure B.29.b shows the sealed container on two different passes outbound through Lane C. In both passes, there were no containers in Lanes D, E, or F. In the first pass, about two-thirds of the queries produced reads in the yellow[3]-shaded zone shown. In the second pass, reads were not achieved until the

[3]Yellow zone indicates, partial reads (e.g. two out of three queries)

doors had exited the Lane and there was a clear view from the reader antenna to the seal.

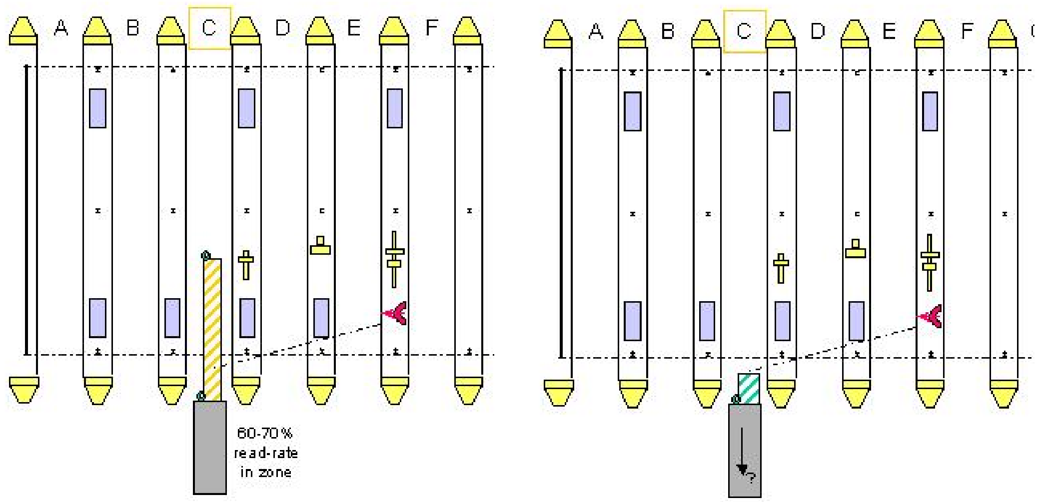

Figure B.29.b All Set in Lane C, Reader Aimed at Lane A

All Set Updated In-Gate Testing

In the initial gate testing, the distance from the All Set reader/antenna to the computer was limited to about 6 feet using RS-232 serial communication cables (this limit was not observe with the e-Logicity and Hi-G-Tek systems). All Set later provided a reader with Ethernet communications. This allowed the reader/antenna to be placed high on a mast, so we revisited the gate area of the Howland Hook terminal with the new reader and two new seals (#0011 and #0021). The antenna was the same as in the earlier tests.

The antenna was tested in three different locations outside the gate structure as shown in Figure B.30.a. In Locations A1 and A2, its height was about 23 feet. In Location F1, it was at about 28 feet. Because of the narrow spacing between lanes and the traffic flow, it was not practical to place the antenna out in the queuing area. Location F1 was as close as the antenna could be placed to the gate without impeding truck traffic. The A1 and A2 locations allowed us to test over longer distances than if the antenna were in the middle of the queuing area.

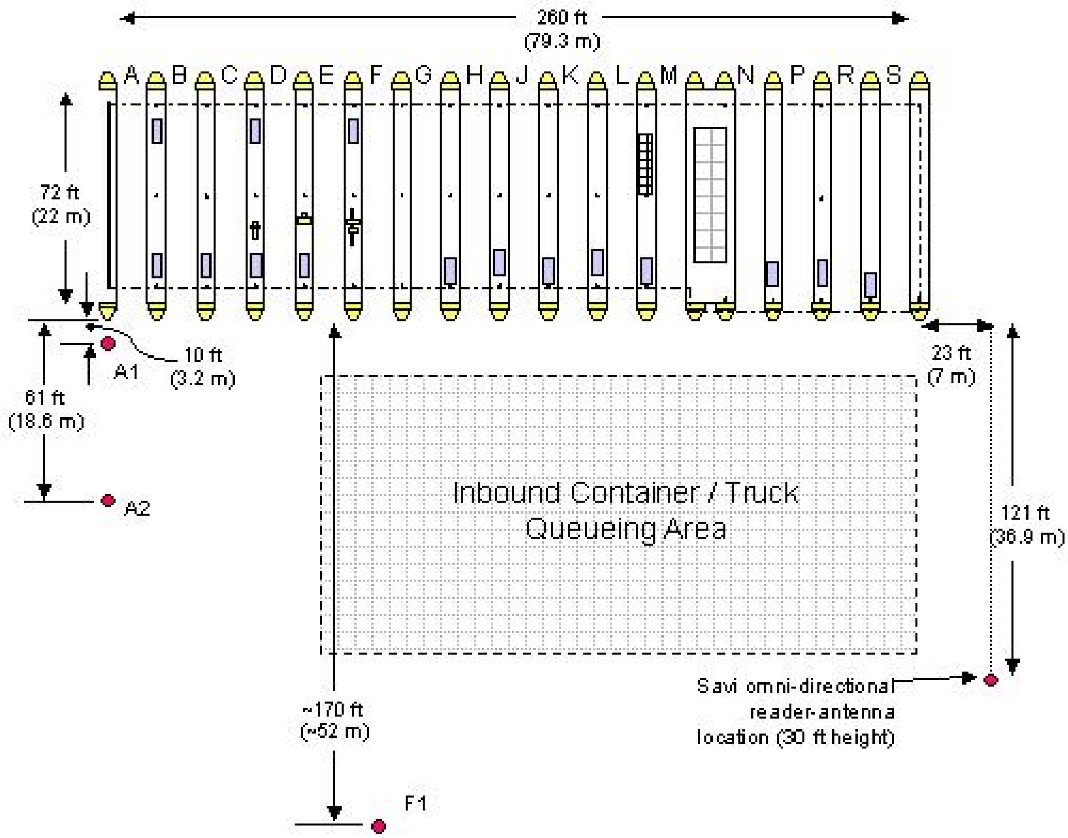

Figure B.30.a. Locations of Elevated All Set Antenna and Reader

The reader/antenna was mounted on a small wooden backing and could be rotated about a horizontal arm on the mast to change its elevation angle. This mounting is shown in Figure B.30.b The aximuthal direction of the antenna was controlled by rotating the mast about the vertical axis. For Location A2, the antenna direction was adjusted into the orientation shown in Figure B.30.c to get the best read performance when seals were held in front of Lanes N and R. The horizontal and vertical full-angle, 3dB beamwidths of this antenna are 75° and 65°, respectively, so we do not expect precise aiming to be critical. The reader was set at an angle of about 20° to the lanes, and given a downtilt of about 10°.

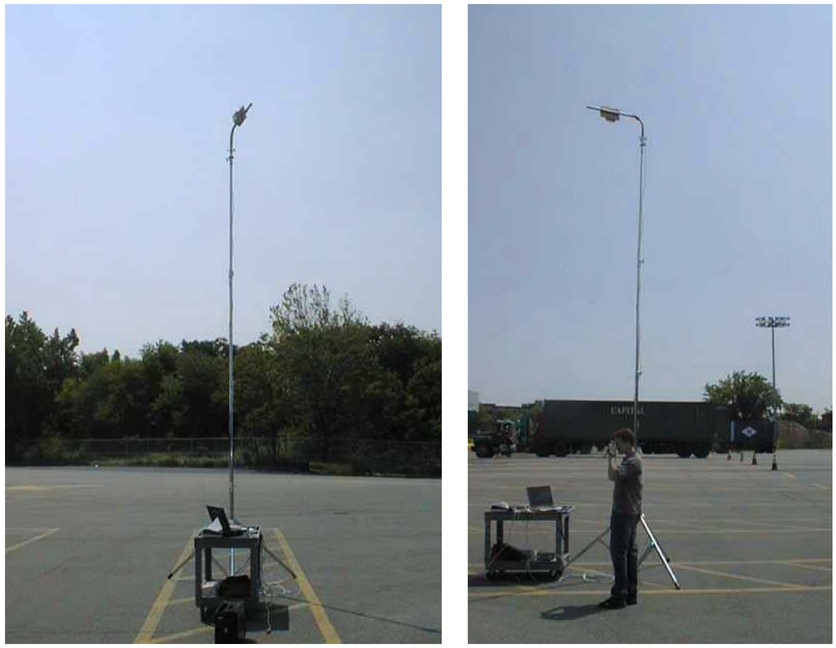

(a) (b)

Figure B.30.b All Set Reader Mounted to Point Down About 10° Below Horizontal

Two seals were installed in an empty 20' container as shown in Figure B.30.c. These were placed in two locations: Seal #21 was placed immediately above the top right door hinge (to optimize line of site), and #11 was placed a few inches above the middle right door hinge.

Figure B.30.c. Seals Mounted on Container Frame

As in the earlier All Set tests, the container was driven slowly (5-10mph, i.e., speed the trucks would normally go through the gate) through various lanes. The demonstration software was run in scanning mode, so it continuously queried for the seals. Once per second, the software reported the last results from the reader, listing the seal ID's that had been read. The software and reader were not synchronized, so occasionally two successful reads by the reader appeared in the software as a "no read" followed by a "double read" of the same seal. Only if the software reported successive "no reads" of a particular seal ID could we be confident that the seal had actually been missed.

<u>Antenna Location A2</u>

Testing was started with the reader mast in Location A2, adjacent to Lane A and about 61 feet (18.6 m) from the lane entrances.

Figure B.31 shows the results of tests in Lanes S and R. The upper seal was read once (green circle) in Lane S but nowhere else inside or immediately outside the gatehouse. The lower (middle-hinge) seal was never read on this pass. Other nearby containers were located as shown. On the pass through Lane R, no containers were in the gatehouse in Lane P or S. The lower seal was read once, then the upper seal was read once. Numerous other attempts (roughly once a second) produced no other reads. It is important to note that the distance from the reader is about 80 meters, which is on the limit of the All Set range, hence, we can not be certain whether no-reads occurred because of obstacles, or because of the noise in the communication channel.

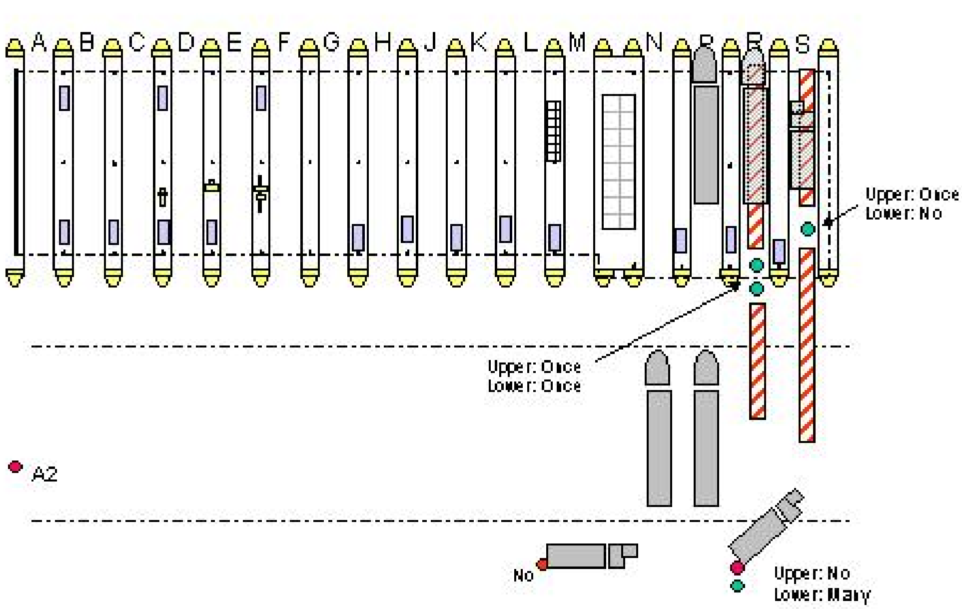

Figure B.31. Query Results with Seals in Lanes R and S

Still referring to Figure B.31, as the container moved behind the queue of trucks, no reads were achieved from the area in front of Lane L. This is expected since we were using directional antenna, and this might have been outside of the antenna lobe. This continued until the container turned to enter the queue for Lane R. At this location, the middle-hinge seal was read repeatedly, but the upper seal was never read. Again, this is most likely because the distance to the lane is at the limit of the All Set dynamic range. The reason why we were getting intermittent reads may have been the result of varying signal/noise levels. The view of the sealed container from the antenna location is shown in Figure B.32.

Figure B.32. Sealed Blue Container Entering Queue for Lane R

Figure B.33 shows the results with the seal in Lanes K, H, G, and F. With a 40' container in the queue for Lane J, the seals were not read outside the gatehouse in Lane K.

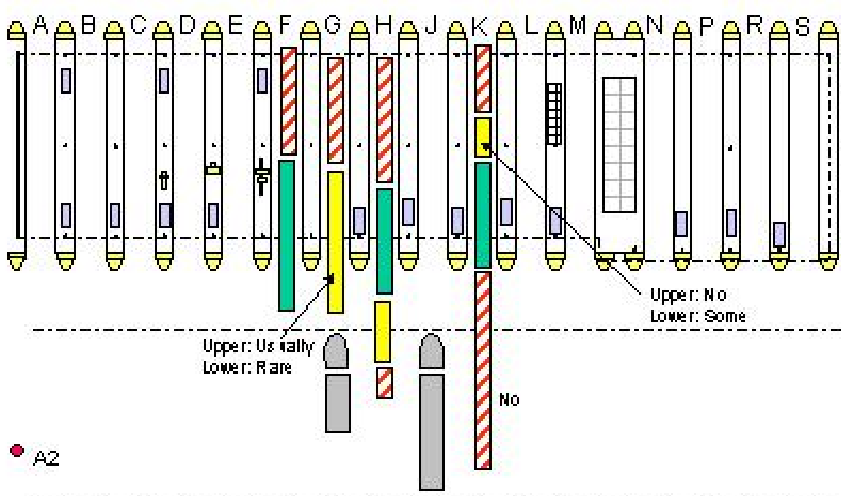

Figure B.33. Query Results with Seals in Lanes G through K

As the seals reached the entrance of the gatehouse in Lane K, each seal was read in roughly half of the query attempts: some queries detected one or both seals, others returned none. Given the short intervals between queries, this is probably satisfactory for determining the presence of the seals in practice. As the seals reached the midpoint of Lane K, the lower seal was still read occasionally – possibly due to random reflections. The upper seal was not read, most likely due to the interference from the ceiling. Therefore, this region is marked yellow instead of green.

In Lane H, the seal was not read in the queue until it moved beyond the 20' container that sat in the queue for Lane G. Results were still spotty, though, with perhaps one-third of the queries producing reads. In the entrance region of Lane H, both seals were read about half of the time, so this region is marked in green.

In Lane G, in the region marked in yellow, the lower seal was rarely read, but the upper seal was usually detected. Beyond this area, no reads were achieved. In front of this area, in the queue, some reads would be expected, but because of the angle at which the truck entered the queue, no data was recorded in this forward area.

For the same reason, no data is recorded in the queue area for Lane F. Outside of and for the first half of Lane F, both seals were read on most of the queries, but not on all. Beyond the midpoint of Lane F, reads stopped.

We estimate that at the entrance to Lane G, the range from the seals to the reader is about 125 feet (38 m), and the seals are off from the aim axis of the reader antenna by 10° or less in both the horizontal and vertical directions.

Lanes A through D are outbound lanes, so the containers move through from top to bottom in the figures shown here. With the antenna in Location A2, the sealed container was driven past in Lane B. With the seals tucked in next to the vertical plate of the container frame, we do not expect good reads to the right side of the container. The lower seal was not read until the doors of the container reached and passed the reader location. At that point, the distance between the seals and reader was about 20 feet (6 m) horizontally and 12 feet (3.6 m) vertically. As the container turned left towards the inbound queue a few seconds later, the upper seal was detected for the first time, and reads from the lower seal became less frequent.

<u>Antenna Location A1</u>

We considered that the poor reads at long distances (Lanes R, S) from Location A2 may have been attributable to poor signal-to-noise ration, i.e., RF-link operate at its limit . The antenna was moved, at the same height, to Location A1. From here, there is an open view to a container just entering the gatehouse as long as there are no intervening containers entering at the same time. The potential disadvantage of this location is that before the seal enters under the gatehouse ceiling, the direct line-of-sight from the seal to reader is at a sharper angle (near parallel with the container door) than for Location A2. The antenna was oriented with the same downtilt as at Location A2, but faced perpendicular to the lanes, parallel to the front face of the gatehouse.

With containers in the queue (but not entering) in Lanes N, P, and R, the sealed container was driven into Lane S. No successful reads of either seal were achieved.

As with the Lane B (out-going) test in Location A2, the sealed container was driven outbound through Lane C with the antenna in Location A1. Both of the seals were read some (< 50%) of the time. Unlike the Lane B test, successful reads were achieved before the doors of the container passed the antenna location.

<u>Antenna Location F1</u>

With Location A1 providing no obvious advantage, we relocated the antenna to Location F1. This, about 170 feet (52 m) from gatehouse, was as close as the antenna could be placed to the gate without impeding truck traffic. Still with a down-tilt of about 10°, the antenna was rotated to face toward the entrance of Lane J. The antenna was elevated to about 30 feet. Figure B.34 shows this placement, the approximate boundaries of the 3dB horizontal beamwidth (37° half-angle), and the test results. This antenna location was chosen because it provided a view of the back of the container as it lined up in the queue. The disadvantages were that:

- the container was usually at least 30 m away from the antenna, and
- with the container passed through the nearer lanes (closer to Lane G), the line-of-sight from the seal to the reader become more perpendicular from the container doors. The seal is partially shielded by the container-frame lip at these angles.

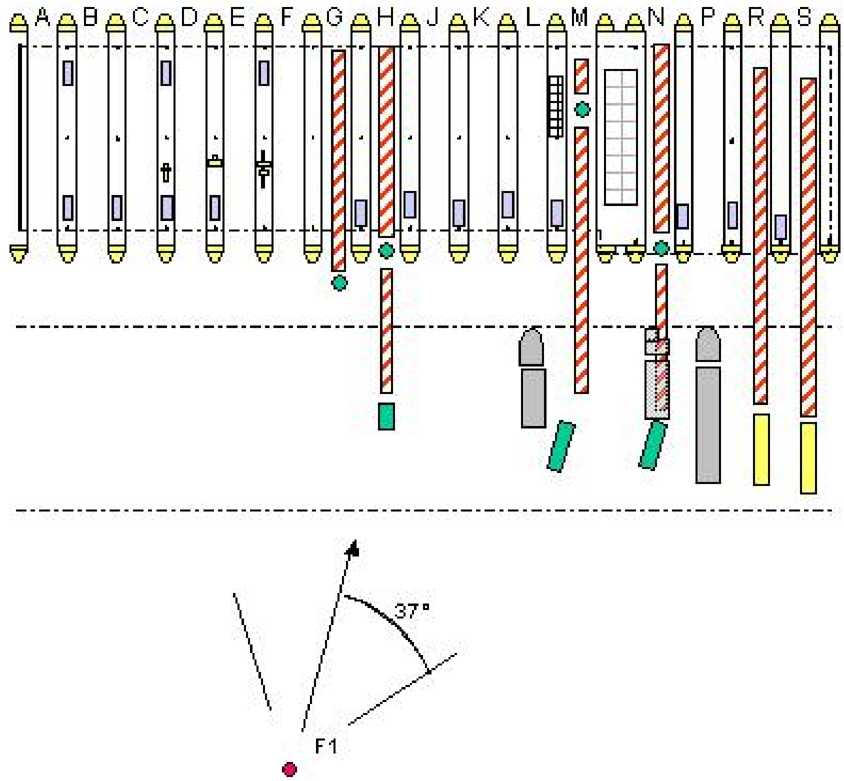

Figure B.34. Query Results with Antenna at Location F1

When the seals were entering the queue in Lane S, the lower seal was read several times in a row, but the upper seal was not read at all. This may again be the result of the RF link being close to its performance limit (76m). As the seals left the yellow-shaded region in Figure B.34 and moved alongside the container in Lane P, neither was read. The opposite was observed in the queue for Lane R: the upper seal was read repeatedly, but the lower seal was not. Moving the antenna slightly did not affect this one-sided behavior; the upper seal remained the only one that could be read.

Both seals were read most of the time as the container turned and entered the queue for Lanes M and N. The read zone was short-lived, however. For the rest of each pass through M and N, the upper seal was read once in each lane, in the approximate locations shown by the green circles. When the successful read of the upper seal in Lane M occurred, it was positioned in a 12-foot (4 m)-wide gap between masonry walls.

In the queue for Lane H, both seals were read most of the time in a brief region. As the container moved forward to the gate, neither seal was read until the seal were near the gate entrance, where the upper seal was read once. In Lane G, the upper seal was read once in a similar position near the gatehouse.

Signal Strength

Signal strengths received by the reader from the seal were measured at various locations using the reader's antenna and the RSSI values reported by the All Set demo software. (There is no firm correlation between RSSI and dBm, but All Set believes that a variation of 3 RSSI units corresponds to about 1 dB, i.e. 200 RSSI is approximately –80dBm but it is not completely linear.) At most measurement locations, the antenna direction was varied as was done for the gate readability tests; that is, it was aimed toward Lane M, Lane A, and/or inward toward the container yard. The reader-antenna height was maintained at 10 feet above the road surface. The 10 measurement locations are shown in Figure B.36.

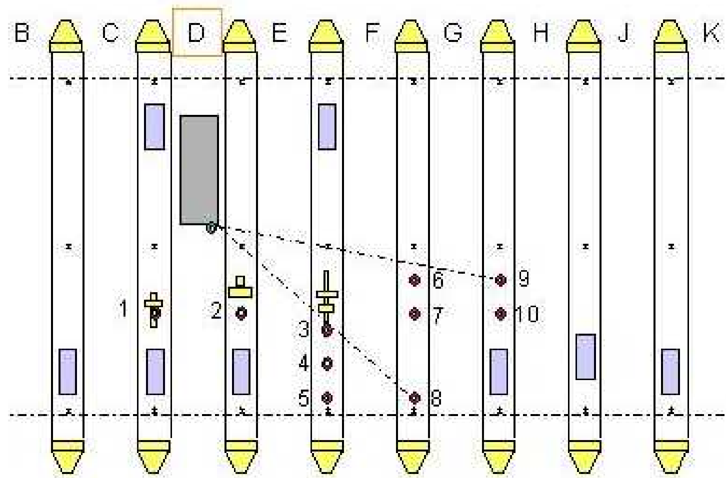

Figure B.36. All Set Measurement Locations in Gatehouse

Note that there is a different antenna-to-seal elevation and azimuthal angle associated with each measurement location and antenna direction. The antenna has a different gain at each such orientation and elevation (the elevation effect may be less for the measurement points selected)[4].

There was traffic in the surrounding Lanes during these measurements. These changes are noted in the following Table, with reference to the locations defined in Figure B.36.

Location	Reader Direction	RSSI values	Notes
1	to Lane A	253	Container in Lane C, many reads
1	" "	No reads	No container in Lane C; container in Lane B

[4] Also the environment will change between different locations. It is hard to make signal strength measurements without using an echo-free room.

1	to yard	242	
1	to Lane M	257	Container in Lane C
2	to Lane A	272	Container in Lane C
2	" "	Rare reads	No container in Lane C
2	to yard	278	Container in Lane C
3	to Lane A	261, 258	Container in Lane C
3	to yard	242	Container in Lane C
4	to Lane A	247, 248	Nothing in Lanes E or F
4	to yard	255	Nothing in Lanes E or F
4	to yard	261	Container moving through F
4	to yard	231	Container in E
4	to Lane M	No reads	Nothing in Lanes E or F
5	to Lane A	259, 250, 274, 272	Container in Lane C, nothing in Lane E. Possible reasons for RSSI changes not observed.
5	to yard	254	Container in Lane C, nothing in Lane E.
6	to Lane A	249	No containers near
7	" "	247, 247	Container in Lane G, rear corner 1-ft past reader, towards container yard
7	" "	247, 248	No container in Lane G
8	" "	233	I-beam on Island D/E is in-line between seal and reader. Intermittent (10%) read rate. As container moved through Lane E, read rate increased at some locations of the moving container, but not at others
9	" "	No reads	Containers in G and H creating "canyon" around reader.
9	" "	239, 244	Container in Lane H. I-beam on Island D/E is in-line between seal and reader.
9	to yard	No reads	Container in Lane H.
10	to Lane A	259	Container in Lane H.

Table III. All Seal Signal Strengths at Various Locations in Gatehouse

APPENDIX C: ON-RAIL TESTING

C.1 INTRODUCTION

The objective of the on-rail test was to determine e-seal readability in the on-rail environment. Testing of all e-seals, except for Savi SmartSeal, was conducted at the Howland Hook Terminal, during the week of March 31, 2003. The weather was fair, with the temperatures in the 40F. On-rail testing of the Savi SmartSeal was performed the week of January 27th, 2003. The temperatures on those days were in the 20F.

The test scenario addressed one of the worst-case scenarios for electronic seals on a railcar. In such a scenario, two twenty-foot containers are placed end-to-end with their doors facing each other. A forty-foot container is placed on top of them. If the containers were placed in a well car, the handle region of the doors may be below the sidewall of the railcar, and there would be a direct line-of-sight to the seal from only a narrow region on the sides of the car. In a slightly less severe scenario, the containers are on a flatcar rather than a well car.

Howland Hook Terminal does not have on-rail facility. Nevertheless, we were able to setup this test with resources available at Howland Hook, and have a test environment that will yield the answers we were looking for[5].

The test setup is shown in Figure C.1. Five empty containers were stacked up. These consisted of four, 20-foot, rag-top containers, with doors facing inward, and a 40-foot container across the top. The seals were applied to the door of one of the upper 20-foot containers (the "Genstar" container on the left of Figure C.1). This arrangement was intended to simulate a double-stack railcar configuration with a 40-foot container atop two 20-foot containers. The lower pair of containers that sat on the ground was used to elevate the sealed container above grade level, as if on a rail bed. A container sitting on a railcar platform is elevated about 4ft from the ground. In our test configuration, e-seal containers are elevated about 8.5ft from the ground, i.e. the height of the container. We

---

[5] The key reasons for selecting Howland Hook Terminal for on-rail test, even though Howland Hook terminal does not have rail facility, were:

- The outlined on-rail test environment can be setup by using additional containers to serve as a railcar platform. Hence, we can achieve almost the same on-rail environment as when the railcar is in the stationary mode.
- Howland Hook management has offered full logistical support to enable this very challenging test setup.
- There was a concern that at the terminal with the rail facility, we will not be able to disrupt the on-rail operational to create the outlined scenario. In the unlikely case that the on-rail facility had additional resources to commit to this test, the cost required to support those resources would have exceed our available budget.

have mitigated the problem of the height difference by adjusting the height of the antenna post.

Figure C.1. Seal Locations on Simulated Rail-Car Double-Stack

The space between the container edges was about 4.5”; the surfaces of the container doors are set back from the container edge, so the distance between the door surfaces varied from about 9.5” to 12.5”. This variation is due to the corrugation features of the doors.

The primary focus of this test was to evaluate readability of e-seals, when they are placed deep between containers with obstructions on all ends, and only a narrow opening that provides line of sight. Therefore, for these tests, the goal was to map the read/write zone around the containers.

Test involving measurements when reader or e-seal platforms are moving where not conducted at this time due to time and resource constraints. The test setup would involve mounting the antenna, reader, and computer systems on a truck and driving past the containers at various speeds. More importantly, to test the velocity angle, it would also require driving at different distances from the container formation. However, based on the communication times for each e-seal system, we can still estimate the maximum speed allowed by these ranges.

C.2 E-LOGICITY TEST RESULTS AND OBSERVATIONS

On-Rail Readability and Signal Strength

Reads were attempted with a log-periodic (directional), low-gain (~ 4.7 dBi) antenna that was moved along a line 6 meters from the container walls at the height of the seal, as shown in Figure C.2. This distance was chosen to simulate a possible rail-side antenna location. At each position along the line, the antenna was aimed toward the gap between the 20-foot containers. This allowed us to maintain the calibrated gain of the antenna at each location.

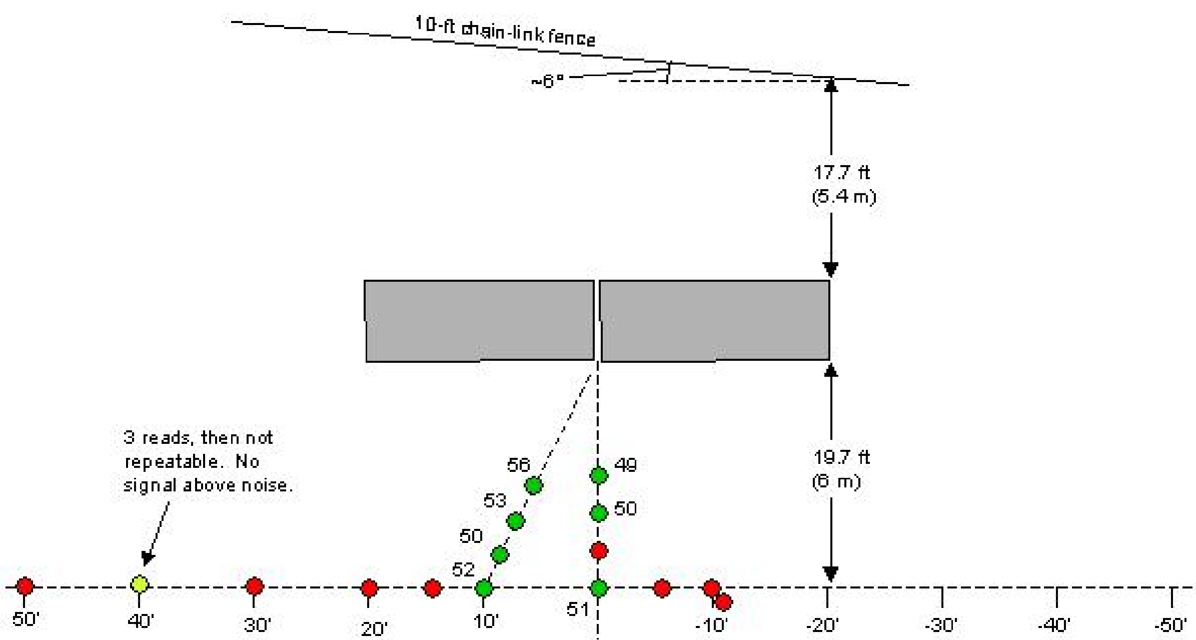

Figure C.2. Successful Read Locations and Signal Strengths (dBμV/m) for e-Seal

Green circles indicate locations where reads were successful and consistent, while red circles indicate locations where reads were non-existent or rare. Note from Figure C.2 that a few intermittent reads were achieved at 40 feet from the container gap, but no signal could be discerned above the noise using the spectrum analyzer, and the reads could not be repeated. The seal was readable in a 10- to 20-foot range near the gap between the containers.

Signal strengths were measured at 1-meter increments within the read zone, as shown in Figure C.2. All measurements were made with the reader antenna vertically polarized.

After testing was completed, it was noticed that the power level of this seal might have been unusually low during this test. The modification made to the bolt to allow it to be removable might have increased the power consumption of the tamper-detection circuit. This may have artificially reduced the read zone. This effect remains to be confirmed. Nonetheless, the output power from the seal was likely constant during this test, so the relative variations in field-strength at various locations should be valid.

C.3 HI-G-TEK TEST RESULTS AND OBSERVATIONS

On-Rail Readability and Signal Strength

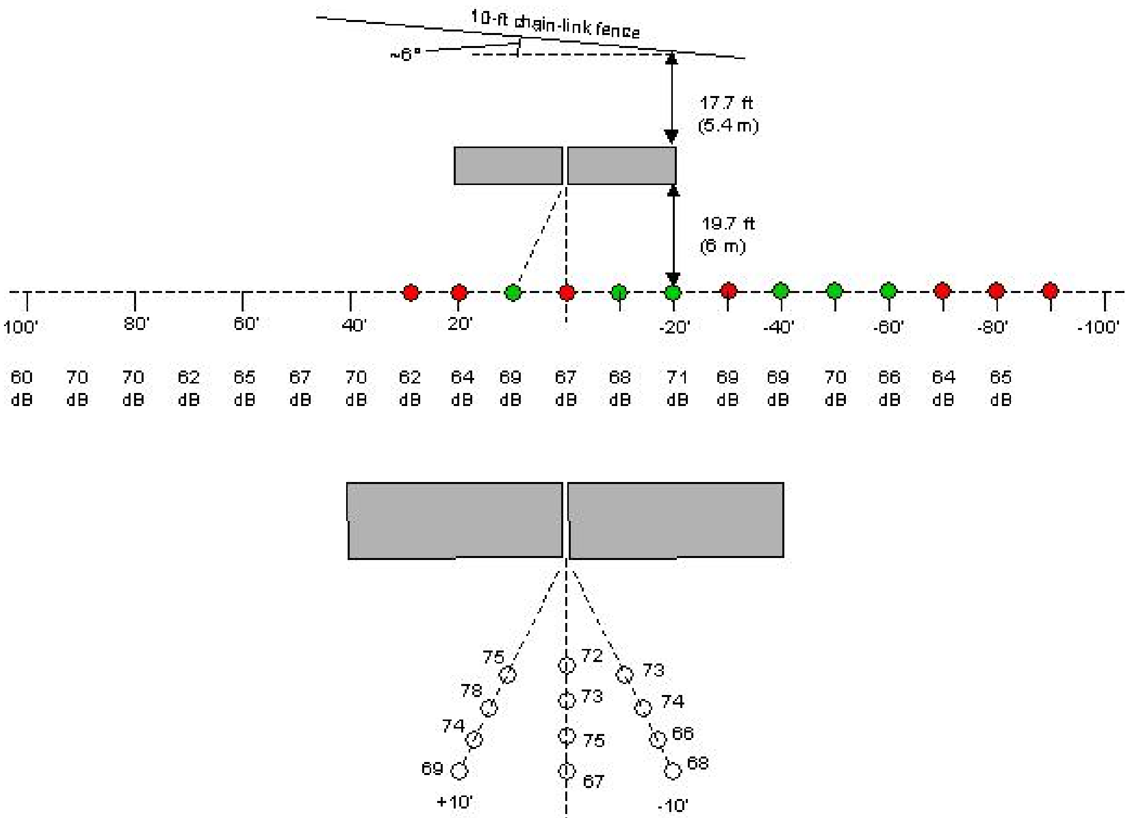

Figure C.3. Successful Read Locations and Signal Strengths (dBμV/m) for DataSeal

Reads were attempted with a log-periodic (directional), low-gain (~ 4.5 dBi) antenna that was moved along a line 6 meters from the container walls at the height of the seal, as shown in Figure C.3. This distance was chosen to simulate a possible rail-side antenna location. At each position along the line, the antenna was aimed toward the gap between the 20-foot containers. This allowed us to maintain the calibrated gain of the antenna at each location. Tests were conducted with the antenna vertically polarized.

Green circles indicate locations where reads were successful and consistent, while red circles indicate locations where reads were non-existent or rare. Figure C.3 shows that readability tends to drop off when the measured signal strength is below about 65 dBμV/m, although some reads were missed where signal strengths measured 67 and 69 dBμV/m. However, readability and signal strength measurements were not simultaneous; if there are strong signal nulls or peaks in these areas, small movements of the antenna could alter the received signal strength and readability.

The lower part of Figure C.3 shows signal strengths increasing by several dB towards the gap between the containers. These were measured at 1-meter increments.

The seal was readable at most measured locations over a 70-foot range, from the +10’ to the –60’ locations. The high signal strengths measured around the +40’ and +90’ locations suggest that those locations may have provided reads. However, the stretches of low-signal regions within these ranges indicates that uninterrupted communications may be a problem at some speeds. Moving the antenna closer to the rail line may raise the minimum signal above the required threshold. Modeling and analysis of specific antennae should provide more guidance.

C.4 SAVI TEST RESULTS AND OBSERVATIONS

On-Rail Readability

The seal was queried and read successfully from a distance of over 374 feet (114 m), with RSSI values in the range of 70 (around –93 dBm). The ultimate range of the Savi SmartSeal in the on-rail simulation was not reached. The distance of 374 feet (114m) was the practical limit for the test space available at the cargo terminal. However, for an environment with more RF noise around 434 MHz than the Howland Hook site exhibited, RSSI values of around 70 may represent a limit to the range at which readability is acceptable.

In this test, the reader was located at a height of about 15 feet. The seal on the container door was at a height of about 10 feet. The reader was moved along a line 6 meters away from, and parallel with, the “rail.” At the long distances involved, the reader ended up being near other containers in the yard, as shown in Figure C.4.

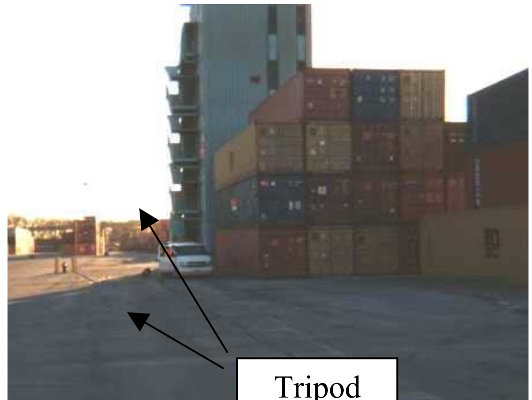

Figure C.4. Reader Antenna Nearing Other Containers (reader is about 200 ft from seal inn photo on right)

The seal was queried several times at each location. With software made available by Savi, we recorded the RSSI values received by both of the orthogonal antennae that are internal to the reader. These values are presented in Table C.1.

Range from Container Gap (ft)	View Angle	RSSI 1	RSSI 2
224	5.1°	79	96
		78	97
		76	97
		67	97
		51	97
		74	98
254	4.5°	89	91
		83	95
		*	*
		89	93
		88	90
		87	92
284	4.0°	89	101
		90	101
		86	104
		88	101
		79	103
314	3.6°	57	99
		61	99
		65	96
		36 / 51 **	99 / 99 **
		57	99
		63	99
		41	97

		49	95
344	3.3°	67	78
		71	82
		61	75
		64	69
		71	70
		70	81
374	3.1°	73	57
		72	52
		75	69
		74	61
		55	78
60	8.2°	120 ***	

* Possible failed query/read.

** RSSI-1 signal fluctuation corresponded to a top-lift driving by, parallel to the "rail," about 30 meters away.

*** See text.

Table C.1. RSSI values for Savi Seal in On-Rail Simulation

The Table also lists the view angle from the container gap back towards the reader. In all cases shown, the angle is very shallow, since the reader-to-seal distance is much greater than the stand-off distance from the reader to the "rail." The last row of data reports a reading taken at a closer point, about 60 feet from the container gap and along a line that was only 2.7 meters from the "rail" edge. This reading was taken with the reader at a height of about 30 feet, rather than 15 feet. In this case, the elevation angle from the seal height to the reader was about 18°, compared to about 1° for the other cases in the table. The measurement did not include a report of which of the two antennae in the reader detected the stronger (120 RSSI) signal.

Signal Strength

During a second set of tests, the Savi SmartSeal was set to beacon at 10-sec intervals. Signal-strength measurements were made with a log-periodic (directional), low-gain (~ 4.7 dBi) antenna that was moved along a line 6 meters from the container walls at the height of the seal, as shown in Figure C.5. This distance was chosen to simulate a possible rail-side antenna location. At each position along the line, the antenna was aimed toward the gap between the 20-foot containers. This allowed us to maintain the calibrated gain of the antenna at each location.

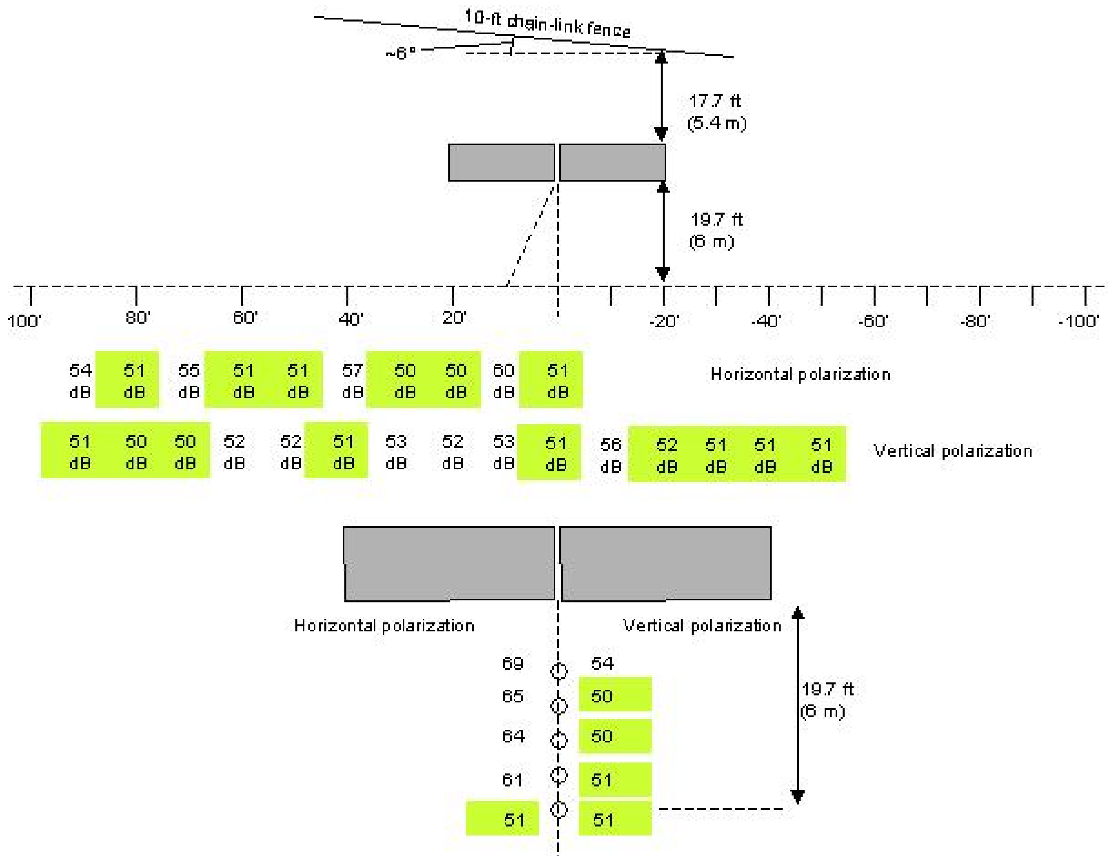

Figure C.5. Signal Strength (dBμV/m) Measured Along Rail Direction for Savi Seal

Two sets of measurements were taken, with the antenna horizontally and vertically polarized. In Figure C.5, signal values shown highlighted, listed at 50 or 51 dBμV/m, were not discernible in the spectrum above the ambient noise. (This does *not* imply that the reader, with its filtering and signal processing capability, could not successfully read or query the seal.) Note that, out to 50 feet along the “rail” direction, the vertical polarization measurements on the “negative” (right) side of Figure C.5 are lower than those on the positive side. A similar trend was seen in the readability of the e-Logicity seal, although its extent toward the positive direction was harder to discern because of the low signal levels.

C.5 ALL SET TEST RESULTS AND OBSERVATIONS

On-Rail Readability

The seal was positioned in the container door, just below the top hinge (a 1” gap between the hinge bottom plate and the top of the seal’s antenna unit). In the container stack, the seal was at a height of 16.5 feet. Reads were attempted by querying the seal from the reader, with its integrated, directional antenna (~ 8 dBi) that was moved along a line 6 meters from the container walls, as shown in Figure C.6. This distance was chosen to simulate a possible rail-side antenna location. The reader was at a height of 8.5’. Reader height was limited by the need to keep the RS-232 no longer than 6 feet for consistent communications between the PC and the reader. Two antenna orientations were used. In one, at each position along the “rail” line, the antenna was aimed toward the gap between the 20-foot containers. This allowed us to know that the gain was consistent at all locations. Because of the asymmetric positioning of the All Set seal (compared to other seals that are placed near the door handles), we also tested with the antenna on the opposite side of the rail, though again always pointing at the gap. The stand-off distance (3.1 m) and lateral extent (30 feet) were limited by the edge of the paved lot and the presence of other containers stacked nearby.

Green circles indicate locations where reads were successful and consistent, while red circles indicate locations where reads were non-existent or rare. Locations of intermittent readability are marked with yellow circles. Along the 6-meter line, consistent reads were obtained along a 55-foot range. After observing the variable performance at the +40’ and +50 locations, we conducted additional tests along a 4-meter line. Performance improved at the 40’ location, but the region of poor or inconsistent reads seemed to be shifted to the 20’ location. This indicates there may be a weak region centered along a line drawn from the gap towards the 35-foot x 6-meter point.

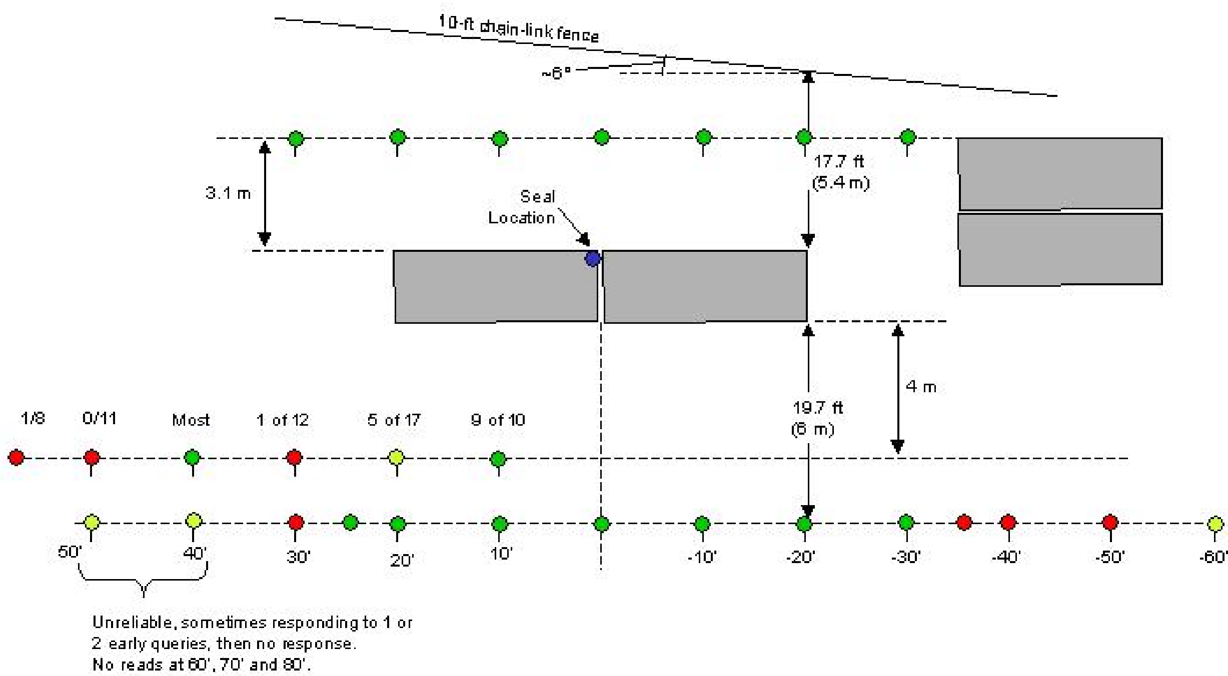

Figure C.6. All Set On-Rail Simulation Results with Reader Aimed at Gap

The second orientation kept the reader facing the lateral sides of the containers, perpendicular to the rail line. This replicates how the integrated antenna would be positioned in an actual application (i.e., fixed). Figure C.7 shows the results with the second reader orientation, perpendicular to the "rail" line. The zone of consistent reads at 6 meters is reduced to about 40', compared to the 55' seen when the antenna is always directed at the gap.

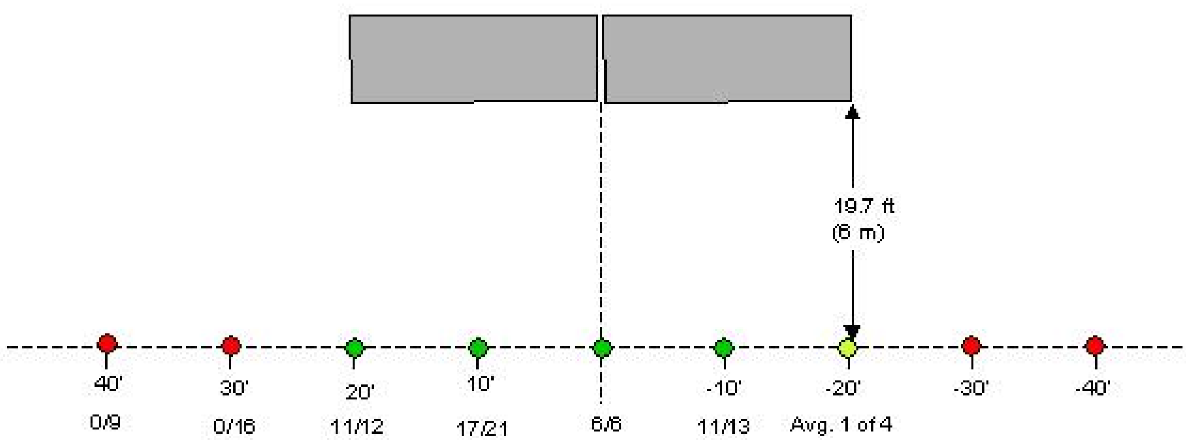

Figure C.7. All Set On-Rail Simulation Results with Reader Aimed Normal to Rail

Signal Strength

Attempts to measure signal strengths were unsuccessful due to ambient RF signals in a band around 2.44 GHz. The seals from the reader and seal could not be distinguished on the spectrum analyzer above the background signals. (Clearly, though, the reader, with its filtering and signal processing capability, could successfully read or query the seal.) These tests were also conducted with recently upgraded software from All Set, and the ability to read RSSI values with that software required the use of an upgraded reader. The new reader arrived the day of the testing, and was not integrated into the test set-ups until the following day. So, no RSSI values were measured in these tests.

APPENDIX D: ON-ROAD AT-SPEED TESTS

D.1 INTRODUCTION

The objective of the on-road tests was to determine e-seal readability and e-seal performance in the on-road environment. Specifically, when the truck is moving at speeds ranging from 5 mph to 30 mph. The findings would enable evaluating the feasibility of security screening of containers without having the trucks to slowdown or stop. If feasible, placing e-seal readers at various check points on the road will improve efficiency of container security checking at the approach to the terminal, boarded points, and various check points on the road.

This section of the report presents the results and observations gathered during the on-road test.

Test Environment

.The On-Road tests were conducted on April 12th, 2003 on the farm in Leesburg, Virginia. The day was partly sunny with the temperatures in the 60F. To simulated container, we had rented a U-Haul truck to simulate a container[6]

The seals were mounted, one at a time, on the roll-up door of the rented truck. Most of the door (the region around the seals) was covered in conductive metal sheeting to provide a large backplane similar to that of a cargo container. Efforts were made to install the seal with a stand-off from the door similar to that observed when installed on a cargo container. For the e-Logicity e-Seal, this involved passing the bolt through a small piece of Styrofoam, and taping the Styrofoam to the door. The e-Logicity seal was installed with its label facing outward from the doors. For the Savi SmartSeal, the backing magnet was held against the door, thereby setting the stand-off distance between the plastic seal housing and the door. This mounting is shown in Figure D.1(a). For the Hi-G-Tek DataSeal, the plastic mounting bracket was held against the door, and the seal inserted into the bracket. For these tests, the keeper-bar was not simulated. This mounting is shown in Figure D.1(b).

---

[6] Simulated "on-road" testing was initially attempted at the cargo terminal test site, but the data presented here were acquired off the terminal, on a lightly used public road, using a roll-door truck in lieu of a container. We opted not to continue these tests at the terminal for a number of reasons. First, in the container yard, there were very limited locations where trucks could be accelerated to 30 mph. Second, the trucks available fore this duty on the terminal had no speedometers, so it was necessary to employ a second "pace" vehicle leading the truck. The truck attempted to match the speed of the pace of the pace vehicle, whose driver radioed to the reader operator when a certain speed was reached. Third, the trucks could not maintain the approximate speed for very long because of space constraints. Finally, the road area available was also used by other two-way truck traffic, which limited the locations at which reader antennae and equipment could be set up.

(a) (b)

Figure D.1 Savi (a) and Hi-G-Tek (b) Seals Attached to Coated Roll-Up Door

The All Set seal was positioned behind a small gusset plate in the lower corner of the door. This area provided structures that were similar (though not identical) to those of an ISO container: a vertical "lip" that blocks the line of sight of the seal from the starboard side of the container, and a gusset plate that provides a some shielding of signals directly rearward of the seal. The roll-up door was opened slightly to allow the seal to be placed in its intended orientation, and then the gap beneath the door was covered with metal sheeting, to restore the reflective backplane. For All Set, the height of the reader antenna was only about 1.5 feet above the height of the installed seal. This is shown in Figure D.2.

Figure D.2. Views of All Set Seal During and After Installation in Door Seam

All the tests were conducted on a narrow, lightly-used, gravel and dirt road. Maximum safe speed was about 30 mph.

D.2 E-LOGICITY ON-ROAD TEST RESULTS AND OBSERVATIONS

Seal #21546 was newly activated by inserting the bolt with a hard push. (Although the bolt felt secure, it reported itself as "tampered," and was later removable with a hard pull.) This initiated the seal beaconing at 10-second intervals.

A directional log-periodic antenna, with a peak gain of about 4.7 dBi at 434 MHz, was aimed down the road at a height of 11 feet above the road surface. The antenna was aimed at about 15° off of parallel to the road (90° would have been looking directly across the road). With the truck traveling "left-to-right, " the reader is on the starboard side of the truck, as it would be if it were on the right shoulder of a U.S. road. With the truck traveling "right-to-left," it passes the reader on its port side, as it would if the reader were on the left shoulder of a U.S. road.

Summary of the e-Logicity on-road test results are shown in Table D.1

Direction of travel	Speed (mph)	Results
Stationary	0	Read range is 170ft
Right-to-left	30	One read
Right-to-left	30	No reads.

Beacon time interval =10sec (preset)

Table D.1. e-Logicity On-Road Summary results

In stationary tests, it was found that the range from the seal to the reader was about 170 feet.

Also, as was found in the gate tests with an omni-directional antenna, the seals are not read as the container is approaching the antenna location, but only once the container doors are nearly in line with the antenna

Multiple passes were made in each direction, at speeds of about 30 mph. Only one successful read was achieved at 30 mph, with the antenna horizontally polarized and the truck moving from right to left. In the 10-second interval between beacons, it is obvious that the seal would pass in less then 10 seconds through a 170-foot region at any speed above about 11 mph. Hence, at container speeds higher then 11mph, the read can be read only if the beacon signal occurs while the seal was in the read zone. As the speed increases, the probability of the beacon signal occurring while the seal is in the read zone is decreasing. During the testing, we were left relying on chance that this would occur, and it rarely did.

D.3 HI-G-TEK DATASEAL ON-ROAD TEST RESULTS AND OBSERVATIONS

A directional log-periodic antenna, with a peak gain of about 4.5 dBi at 916 MHz, was aimed down the road at a height of 11 feet above the road surface. The antenna was aimed at about 20° off of parallel to the road (90° would have been looking directly across the road), in the direction of truck travel so that it would point toward the rear door after the truck passed the antenna. The antenna was oriented with its elements in a vertical plane. With the truck traveling "left-to-right," the reader is on the starboard side of the truck, as it would be if it were on the right shoulder of a U.S. road. With the truck traveling "right-to-left," it passes the reader on its port side, as it would if the reader were on the left shoulder of a U.S. road. The reader transmission power was set to its maximum level (100 on a scale of 0 to 100).

The test results are summarized in table D.2. However, after the testing was completed we had found out from the vendor that the new reader software required different power settings then had been previously specified. Both vendor and testers felt that the incorrect power settings could have resulted in spurious readings. Hence, the obtained results are inconclusive.

Direction of travel	Speed (mph)	Results
Stationary	0	Not measured, 80m - vendor spec
Right-to-left	30	Multiple reads, all successful
Left-to-right	30	Multiple reads, all successful

beacon time interval= 3sec (manually set)

Table D.2. Summary of Hi-G-Tek On-Road Results (Inconclusive)

D.4 SAVI ON-ROAD TEST RESULTS AND OBSERVATIONS

Seal #4000109 was set into beacon mode. In a typical Savi application, a seal may be put into beacon mode by leaving a Signpost area, and read by a distance reader. The seal could then be taken out of beacon mode upon entering a later Signpost area. Querying from the reader and getting a response is not Savi's typical, recommended method for at-speed reading. The reader antenna was positioned on the side of the road, at a height of about 20 feet, and about 10 feet from the center of the lane (which is roughly the seal location).

On-road test results are summarized in Table D.3.

Direction of travel	Speed (mph)	Results
Right-to-left	30	No read
Right-to-left	30	One read, at about 10-15 feet before door reached antenna location
Right-to-left	30 & 25	Two reads. First about 100 feet before door reached antenna location; second about 250 feet beyond antenna. Speed at second read estimated as 25 mph.
Left-to-right	20	One read, about 50 feet before door reached antenna

		location
Left-to-right	30 & 25	Two reads. First about 25 feet before door reached antenna location; second about 400 feet beyond antenna, based on sustained speed of 30 mph.
Left-to-right	30	No read

Beacon interval = 10sec

Table D.3. Summary of Savi On-Road Results

Three passes were made in each direction, at speeds of 20 to 30 mph. With the truck traveling "left-to-right, " the reader is on the starboard side of the truck, as it would be if it were on the right shoulder of a U.S. road. With the truck traveling "right-to-left," it passes the reader on its port side, as it would if the reader were on the left shoulder of a U.S. road.

In the right-to-left direction, one pass resulted in two reads, which were 10 seconds apart (the beacon interval). At an average speed of 27 mph between these reads, the truck would have traveled about 400 feet between reads. This agrees relatively well with the estimated locations of the truck at the times of the two reads. A similar situation occurred in the final left-to-right pass. These results are consistent with the finding (discussed in the Lab Test report) that the seal-to-reader distance, when viewing the seal from the back of the container, is about 550 feet.

D.5 ALL SET ON-ROAD TEST RESULTS AND OBSERVATIONS

The reader, with its directional, integrated, patch antenna, with a peak gain of about 8 dBi at 2.44 GHz, was placed at a height of 4 feet above the road surface. The height of the antenna was limited because the seal was placed unusually low due to the limitations of the truck geometry; we did not want the reader to be artificially high above the seal location. The reader/antenna was located about 10 feet from the center of the lane. Tests were conducted with the reader antenna aimed directly across the lane (90° to the road) and with the antenna aimed at about 25° off of parallel to the road, so that it roughly faces the back of the truck after the truck passes the antenna.

With the truck traveling "left-to-right," the reader is on the starboard side of the truck, as it would be if it were on the right shoulder of a U.S. road. With the truck traveling "right-to-left," it passes the reader on its port side, as it would if the reader were on the left shoulder of a U.S. road.

Summary of the results is shown in table D.4.

Direction of travel	Speed (mph)	Results
Right-to-left	30	Multiple reads until 225 feet

Right-to-left	20	Intermittent as far as 500 feet (150 meters)
Left-to-right	20	
Left-to-right	30	Multiple reads until 70 feet (25m) from reader

Table D.4. Summary of All Set On-Road Results

Results with Reader Aimed Across Lane

The read zone is expected to be smallest with the reader aimed across the lane. The reader queries the seal about every 0.84 seconds. At 30 mph, the truck moves about 37 feet in this amount of time.

With the truck moving in the right-to-left direction at 30 mph, multiple reads were achieved. Some queries resulted in multiple reads. In this direction, the seal is “facing” the reader antenna as it passes, without the edge of the doorframe or the gusset blocking the view.

With the truck moving in the right-to-left direction at 30 mph, multiple reads were again achieved. Successful reads continued until the seal was at a distance of about 75 feet (20 – 25 m) from the reader antenna. When traveling in this direction, the edge of the doorframe is between the seal and the reader when the door is just passing the reader location.

Results with Reader Aimed Along Lane

With the truck moving in the right-to-left direction at 30 mph, multiple reads were achieved. Successful reads continued until the seal was at a distance of about 225 feet (70 m) from the reader antenna. Reads may have continued further except for the truck passing over a crest in the road. The truck travels 225 feet in about 5 seconds at 30 mph, and reads continued with each query during this time.

Some reads were achieved intermittently out to a distance of around 500 feet (150 m) as the truck continued and maintained speeds of over 20 mph.

APPENDIX E: SIMULATION RESULTS

E.1 INTRODUCTION

E.1.1 Purpose and Objective

The purpose of the e-seal field-testing was to collect and analyze e-seal performance data in the operational environment. However, some of the e-seal characteristics (e.g., frequency) and their impact on e-seal performance can be better understood by evaluating e-seal performance in the simulated environment. The primary focus of the e-seal simulation effort was to examine e-seal performance as a function of different frequencies. Of particular interest was evaluating signal patterns and their behavior around complex geometries. Hence, we have used a simulation tool that operates in a frequency domain and predicts resultant signal patterns from antenna sources around complex geometries.

E.1.2 Requirements

Evaluate signal patterns from antenna sources that operate at three frequencies:

- 433MHZ
- 916MHZ
- 2.44GHZ

E.1.3 Reference Documents

- CTLSS (Cold-Test and Large-Signal Simulator) – An Advanced Electromagnetic Simulation Tool for Designing High-Power Microwave Sources, Cook, Mondelli, *et al*, IEEE Transactions On Plasma Science, June 2000
- CTLSS User Manual V 1.1, April 2002, SAIC

E.2 SIMULATION PROCESS & TOOLS

The e-seal simulation was performed using the Cold-Test and Large-Signal Simulator (CTLSS) Tool. The use of CTLSS has been validated for RFID-type devices through past CCDoTT efforts. The Tool was hosted on a PC with a 1.4 GHz AMD Athlon processor. The operating system was Windows 2000.

This section describes in more detail the CTLSS Tool as well as the process used to setup the CTLSS environment and perform simulations.

E.2.1 CTLSS[7] Tool

The CTLSS code is an integrated three-dimensional, large-signal simulation program. It is a general-geometry, frequency-domain, electromagnetic code that predicts resultant signal patterns from antenna sources around complex geometries. CTLSS handles both resonant problems and non-resonant driven-frequency problems. CTLSS models static environments. To examine RF field patterns as components are moving relative to each other, separate simulations must be run, each one representing a “snap-shot” in time.

---

[7] The CTLSS code was created under funding from the Office of Naval Research Modeling and Simulation Program by Science Applications International Corporation (SAIC), and is released through the Vacuum Electronics Branch (Code 6840) at the Naval Research Laboratory.

The CTLSS code has been designed as a coupled cold-test and large-signal model. The entire model is three dimensional (3D), and is intended to handle arbitrary device geometry. The 3D cold-test module is volumetric and operates entirely in the frequency domain. It includes both a resonant (eigen-mode) electromagnetic solver and a non-resonant (driven-frequency) electromagnetic solver. Both solvers are designed to handle complex material properties (permittivity and permeability) with large loss tangents. The driven-frequency solver in this version of CTLSS does not include the capability to process S parameters between ports and between modes. This version is a single-block solver.

CTLSS is an object-oriented program that offers the CTLSS Graphical User Interface (GUI) to write the input file. In addition, CTLSS offers Templates for specific types of devices. Templates are higher-level interfaces that automatically populate the GUI (and hence the CTLSS input file). Often the user will start with a Template that is close to the problem, then edit the problem in the GUI before saving the CTLSS input file. In addition to the setup GUI that creates input files, CTLSS has a run-time GUI that helps to start runs and export data to the viewer and/or the post-processor. After saving the CTLSS input file, the user can call either the CTLSS run-time GUI or the CTLSS viewer interface from the setup GUI and do a setup run to examine the structure in an interactive 3D rendering. When the run is completed, the user can view 3D structures and fields using the either the VTK viewer or the Voyager post-processor. The post-processor creates an ASCII text file of results for import into spreadsheets or other tools.

To set up the simulation environment, CTLSS uses an orthogonal structured grid in either Cartesian or cylindrical coordinates. Structures are automatically broken into discrete elements on the grid using a stair-step representation. The grid is set up separately along each coordinate axis, and may be specified either as a piecewise uniform grid or as a piecewise stretched grid. In both types of setup, the user specifies "critical planes" (usually where the grid needs to align with a structure or feature).

Geometrical structures are placed on the grid using the Boolean combinatorial procedure. The code has a library of basic shapes, or "primitives," with which the user can build up complex structures. When a primitive object is selected, the user specifies its location, its orientation, and its size. The user also specifies the material type (conductor, dielectric, or permeable) and material properties (relative permittivity or relative permeability). The material properties can be specified as complex numbers (i.e., can model loss) and can be diagonal 3x3 tensors. The code then scans the entire grid to determine whether each cell centroid lies inside or outside the primitive object that was selected. The process of filling and carving primitive shapes can generate any geometry on the grid.

E.2.2 Simulation Process

E.2.2.1 Building the Model From a Template

The simulation process starts by selecting from the CTLLS toolbox a template that best models the type of device or problem to be solved. In our case, the problem was to evaluate radiation patterns of e-seal antennas. During the laboratory testing, we had measured antenna patterns for each of the e-seals. Those empirical results served as a guide to select the template that best fits the simulated e-seal antenna.

In general, one needs to perform several simulation runs to identify which template is the best approximation of the modeled e-seal antenna (e.g. vertical dipole antenna, perpendicular dipole, etc). After the first simulation, a new template is selected, and the results are superimposed over those from the first run. This process continues until we develop an e-seal antenna model with a pattern that is almost identical to the empirical results obtained in the lab. This e-seal antenna model is then used in simulation runs. It is important to note that developing an e-seal antenna model can be very time consuming when one wants to have a model that is almost identical to empirical results. In our case, that kind of precision is not necessary, since our objective is not to focus on specific vendor e-seals and their design, but on patterns as results of different frequencies. Hence, a first approximation of the e-seal antenna using a single template is sufficient.

E.2.2.2 Develop Scenarios and Structures

The next step is to develop simulation scenarios and, based on those scenarios, identify the simulation region and develop structures that appear in that region. Again, structure templates are found in the CTLLS toolbox.

E.2.2.3 Simulation Run

The next step is to run the simulation scenario. Note that for this simulation effort the CTLLS code was hosted on a PC with a 1.4 GHz AMD Athlon processor and Windows 2000 operating system. This is a very computationally-intensive simulation, with a run taking roughly 8 to 12 hours of CPU time. However, in the scenarios with the 2.44 GHz e-seal model and a region large enough to contain the structures, the simulation run was almost three times longer, e.g., 31 hours of CPU time. This was because more nodes were needed to handle a simulation with the shorter wavelength.

E.2.2.4 Data Scaling & Methodology

The CTLLS Tool provides as output "energy density (ED)" data. While this output serves as a good starting point to analyze signal strength patterns across different frequencies, one can also further refine these results by calibrating them using signal strength maps obtained during lab testing. This subsection describes the methodology used to calibrate ED data.

First, the locations at which the lab data points were measured must be converted into the coordinate system of the simulation (or vice versa). During e-seal lab testing, seven data points were measured, all at 3m distances from the seal. In the coordinate system of the seal and of the simulation, their locations are:

In the X-Y-Z Plane of the Seal:

	Coordinate System Centered at Seal			Coordinate System of Simulation		
Angular position	X	Y	Z	X	Y	Z
0	3	0	0	3.02	0.20	0.23
30	2.60	-1.50	0	2.62	-1.30	0.23
60	1.50	-2.60	0	1.52	-2.40	0.23
90	0	-3	0	0.02	-2.80	0.23
-90	0	3	0	0.02	3.20	0.23
-60	1.50	2.60	0	1.52	2.80	0.23
-30	2.60	1.50	0	2.62	1.70	0.23

At the 30-degree elevation:

	Coordinate System Centered at Seal			Coordinate System of Simulation		
Angular position	X	Y	Z	X	Y	Z
0	2.60	0	1.50	2.62	0.20	1.73
30	2.25	-1.30	1.50	2.27	-1.10	1.73
60	1.30	-2.25	1.50	1.32	-2.05	1.73
90	0	-2.60	1.50	0.02	-2.40	1.73
-90	0	2.60	1.50	0.02	2.80	1.73
-60	1.30	2.25	1.50	1.32	2.45	1.73
-30	2.25	1.30	1.50	2.27	1.50	1.73

Second, energy density is a scalar value, but field-strength lab data (in dBμV/m) was obtained using a polarized receiving antenna in two orthogonal directions, with its central axis directed at the seal. We make the assumption that the component of the electric field vector along the antenna axis direction was small compared to the other two orthogonal polarizations. Since the antenna was aimed at the seal from four to 24 wavelengths away, this seems reasonable. We perform vector addition on the two orthogonal field-strength values. The square of the resultant vector magnitude is proportional to the local energy density. We perform this conversion for each data point.

Third, we select one point in each data set (the simulation and the lab data) and determine a scaling factor that makes this point the same in each set.

As an example, assume that the selected angular position point is ”0” at the seal level and its value from the lab data is 2.111e9 (uV/m)^2 (or 93.24 dBuV/m). In the simulation results, we select the ED value at a point closest to X = 3.02 m, Y = 0.20, Z = 0.23, which for our case is 0.0003879.

To scale the lab data to match the simulation, we multiply all of the lab data points by (0.0003879 / 2.111e9) = x 1.837e-13. (Such a large negative exponent is not surprising, since one has to convert from μV^2 to V^2, which alone requires a factor of 1e-12.) We apply this factor to all of the lab data points. Alternately, to scale the simulation data to match the lab data, we divide the simulation data by 1.837e-13, and apply this factor to all of the simulation points of interest. An equivalent procedure can be performed if it is desired to work in dB units.

E.2.2.5 Post Processing

When the run is completed, CTLLS will produce output in the form of ASCII data files and a 3D graphical representation of the simulated region. The results in the data file can be scaled using the methodology outlined above, and scaled results graphically presented using CTLSS graphics tool.

E.3 SIMULATION RESULTS

The simulation effort investigated e-seal signal propagation and radiation patterns in in-gate, on-rail and on-road environments. This section presents the results of that investigation.

E.3.1 Modeling

To produce simulations at these frequencies, the modeling tool discretized the simulation region into spatial elements that were only a few centimeters on a side. Memory and processing-time constraints limited the size of the simulation region to about 36 m^3 for the lower frequencies, and about half that for the 2.44-GHz cases. Because of the large dimensions of the containers and gate-structures, the longest dimension of any simulation was about 4.5 m, or about 15 feet.

The seal-antenna location and size was kept the same in all simulations, rather than relocating it to correspond to a particular vendor’s seal at a particular frequency. This allowed comparison among frequencies without the added variable of seal location. The size of the antenna was 12cmx10cmx1cm.

E-seal Modeling
Our first step in the modeling and simulation of the selected e-seals was to examine the radiation patterns obtained in the laboratory environment[8] and select the template from the CTLLS toolbox that was closest to the empirical results. For each e-seal/frequency, a dipole antenna appeared to be the best starting point. Next, to determine dipole direction and orientation, we conducted a number of CTLLS simulation runs, each time changing the direction of the dipole antenna:

- vertical dipole (in Z direction), parallel to the backplane (i.e., container door),
- dipole perpendicular to the plane (in X direction), and
- parallel to the plane but in the horizontal (Y) direction.

For all frequencies and seals, orienting the dipole in the Z direction produced a pattern that fit the lab data better than did the other two orientations. This was mainly because the X- and Y-oriented dipoles each produced stronger variations with elevation (above the x-y plane) than was observed in the data. We further investigated representing each seal as a linear combination of all three dipole orientations, with each dipole contributing in a different proportion in each seal. The results suggest that a well-tuned e-seal model is a superposition of three dipole antennae generated by CTLSS. Additionally, our investigation suggests that the internal structure of the seals and the detailed features of their mounting on the door handles may also need to be modeled to better match the lab data.

However, to converge to this model, one would require finer grid resolution, which would shrink the practical simulation region. Considering that our primary focus was on investigating e-seal performance at different frequencies, rather then particular vendor product, a z-oriented vertical dipole was an adequate representation of an e-seal. Hence, a z-oriented vertical dipole was used for all simulations that follow.

E.3.2 In-Gate Simulation

E.3.2.1 Scenarios and Geometry

<u>In-Gate Scenarios</u>
The objective of the in-gate simulation was to investigate signal propagation and radiation patterns, especially when signals reach obstacles commonly found in the in-gate area, such as booths and other containers.

To accomplish this, we constructed two sets of scenarios. The first set simulated an e-seal on the back of the container with no obstructions in the region.

---

[8] We used the laboratory data that we measured with the seals mounted on a mock-up of a container door.

For each of the three e-seal frequencies, we performed simulation runs in the space with no obstructions. We performed several simulation runs, each time maximizing the X, Y or Z dimension of the simulated space. This approach was needed because of the practical constraints on the size of the simulation region for a single run. The purpose of these runs was to obtain radiation patterns for each of the frequencies and compare them with each other.

The next set of scenarios investigated signal propagation in the environment with obstacles. The objective was to determine how well different frequency signals traveled around objects and the potential impact from signal diffractions. We performed several simulation runs, applying the same structure setup for each e-seal frequency. The structures and regions used for these simulation runs are described below.

Because of the limited simulation region for each run, the results may be more useful when selecting antenna placements within a lane for lane-specific seal reading, rather than when determining the range or antenna placement to read across multiple lanes.

In-Gate Geometry

The key elements that we wanted to investigate in the simulated environment were radiation patterns from the e-seal when there are no obstructions, and changes in those patterns when there are structures in the way. We had setup the simulated region to reflect the e-seal in the in-gate environment. The in-gate geometry and dimensions are shown in Figure 3.2.1a-b. Figure 3.2.1.a shows lanes and islands, and positions of booths and containers. The e-seal that is being simulated is mounted on the container in lane F. There is a booth between lanes F and G, and another container in lane G. Figure 3.2.1.b shows container and booth geometry. The glass windows of the booth are modeled as transparent to RF. For the purpose of the simulation, the e-seal is placed in the lower end of the back door of the container.

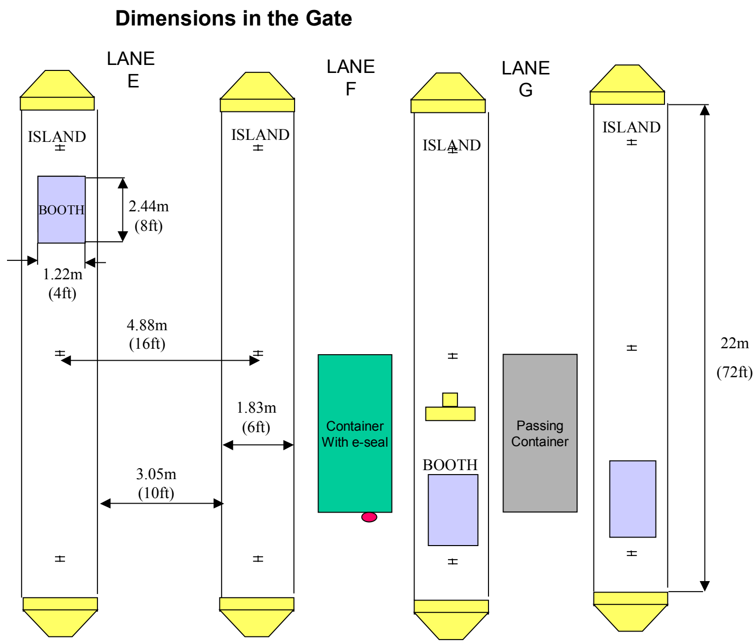

Figure E.3.2.1.a In-gate dimensions and configuration

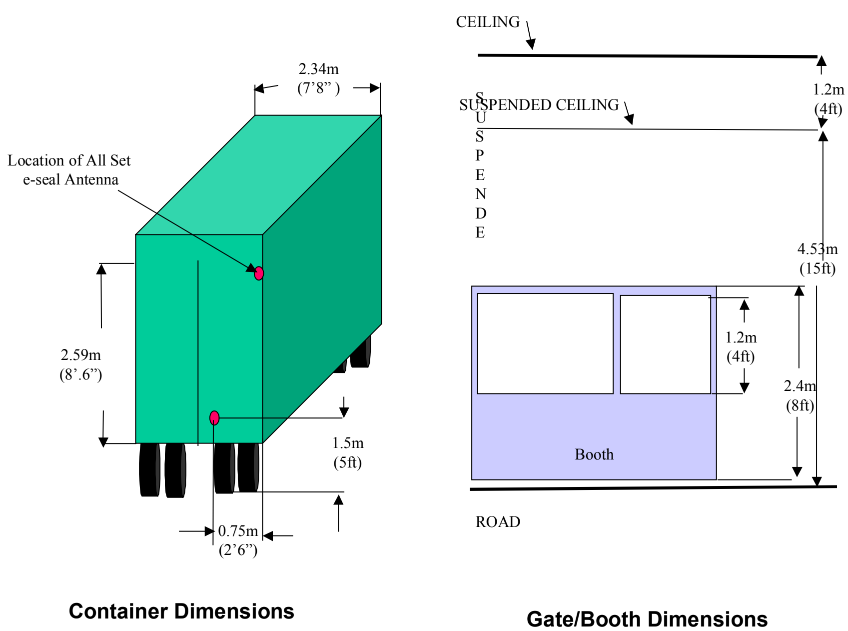

Figure E.3.2.1.b Container and booth dimensions

Simulation Region and Structures

Figure 3.2.1.c is a visual representation of the CTLSS simulation results. All simulation results in this report are presented in this manner. We will use the graphics in Figure 3.2.1.c to show how to interpret each figure.

Each simulation is run in the X-Y-Z space. The typical size of the region that CTLSS can simulate is 2mx3mx6m, and it is dependent on the amount of structures that need to be packed into the region, the wavelength, and the amount of time it will take to run the simulation. Larger regions will require longer times, as will smaller wavelengths. Also, if there are more structures that need to be simulated, those will take up more cells, and reduce the simulation region.

Since the CTLSS simulation region is limited in size, we have limited our simulation runs to only the area immediately around the e-seal. The tower structure shown in the figure below represents a slice of the container around the back door. Further, the structure simulates only the right half of the back door. The region to the left is largely free of reflecting structures; by not simulating that direction, we are able to extend the simulation region further in the other directions.

The figure also shows the radiation pattern in one plane. In this particular case, the selected plane is at a fixed Z coordinate, at the e-seal level, or 1.5m from the lane surface. The color contours show the radiation patterns: areas with the highest electric energy density are shown in red, and areas with the lowest electric density are shown in dark blue. The red dot represents the location of the e-seal. The polygon boundary represents the simulation boundary. It is important to note two items regarding the boundary:

- First, structures cannot be placed right at the simulation boundary, hence, there is an area to the left and behind the tower structure that is not of interest to us. It appears as an open space, when in reality, it should be occupied by a container.

Second, the numerical boundary conditions cause the output graphics to show contour lines that converge near the boundary. This is an artifact of the simulation technique. To avoid RF reflection from the boundary (i.e. to simulate an “open” boundary of RF propagation, boundary layers are constructed with heavy loss properties to absorb the incoming RF energy. As such, energy density of RF decreases exponentially in the boundary layers, which is shown by the concentration of color contours. For practical purpose, values in this thin boundary region near the simulation border should be ignore.

Other notes regarding interpretation of the figures are:

- The energy density values cannot be compared across frequencies, as the values are not normalized to a common power output.
- Instead, it is valid to consider the drop in energy density within a set of figures at the same frequency and with the same structural geometry.

- The values shown are derived from the formula “20*log(energy density).” This makes them proportional to dB (V/m). Note that they are not normalized to a common field strength.
- All seals are modeled at the same location on the container. The 2.44-GHz seal is not located in the upper hinge region where All Set’s 2.44-GHz seal is typically placed.
- From the seal to the region boundary in the X (perpendicular) direction is only about 1 meter. This is less than two wavelengths for the 433-MHz seal and about twice as much for the 916-MHz seal. Therefore, the RF pattern in front of the seal may include near-field effects in its structure.

Figure 3.2.1.d shows various structures used in in-gate simulation runs to represent obstacles to signal propagation, such as a booth and a container in another lane. Again we have simulated only the sections of those structures that are within the simulation region. In the 2.44 GHz case, i.e., short wavelength, we have reduced the size of the region by half, and correspondingly, only the upper portions of the booth and container structures are modeled. This was necessary to fit the computational requirements of a very short wavelength. Hence, the bottom two pictures in Figure 3.2.1.d show structures used for 2.44GHz simulation runs, and represent only the top portion of structures used for 433MHz and 916MHz simulation runs (top two pictures).

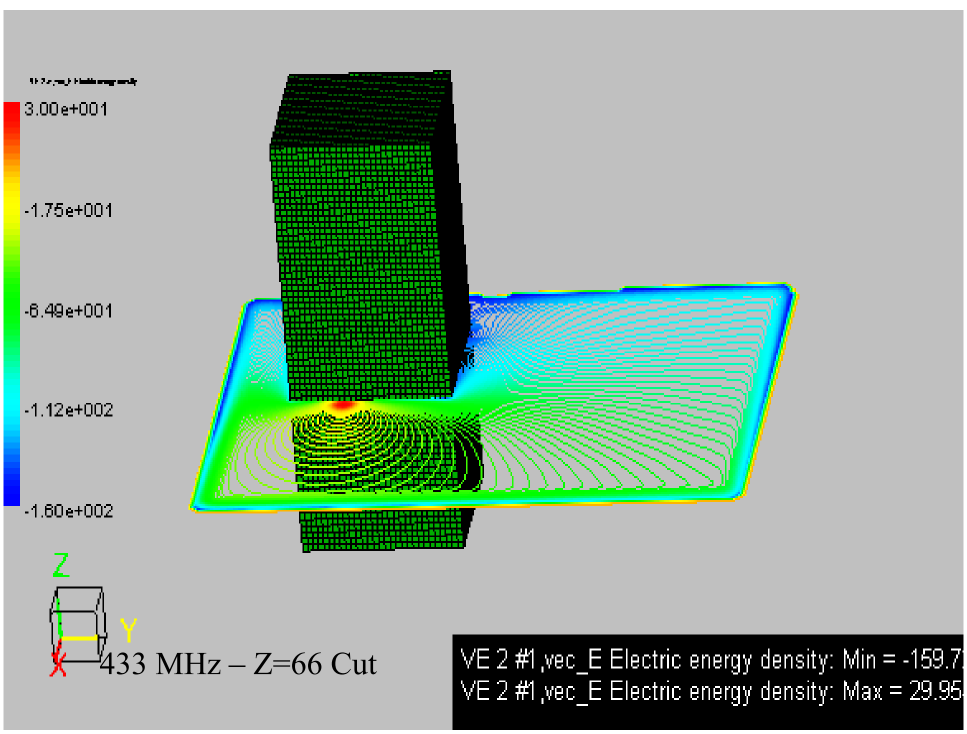

Figure E.3.2.1.c Simulation Region

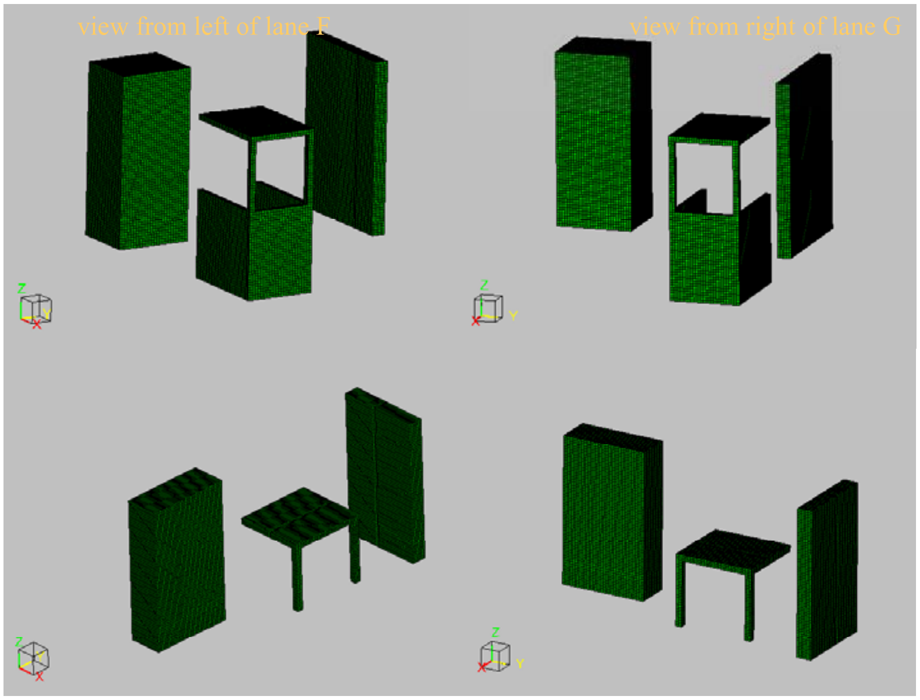

Figure E.3.2.1.d Simulated structures in the In-gate environment

E.3.2.2 In-Gate Simulation Results

This section presents results of our in-gate simulation effort. As mentioned before all the simulation results were obtained by running the CTLSS tool. This was a very computationally-intensive effort. A typical CTLSS run took roughly 8 to 12 CPU hours, and in the case of 2.44 GHz frequency runs with obstacles, it took over 30 CPU hours.

Note that figures shown in this section are only a subset of the data and figures generated during this simulation effort. This subset best conveys the insights obtained during the simulations. Further post-processing of all the obtained data can be done if needed.

<u>In-Gate Scenario: Region around Container Backdoor - Y, X cut Planes</u>

Figures 3.2.2. a-c and 3.2.3.a-c show radiation patterns and signal propagation in the space around the container door. Figures 3.2.2 and 3.2.3 show the radiation patterns in vertical cut planes that pass through the e-seal. In Figure 3.2.2, the cut is perpendicular to the door (normal to the Y axis), and in Figure 3.2.3 the cut is parallel to the door (an “X” cut normal to the X axis). The structure represents the full height of the right-side of the container door, with the structure extending about a foot back.

All figures have a red area representing the e-seal - the source of the radiation. Examining the radiation patterns that spread from the source, we can see that in the case of the 433MHz signal (Figures 3.2.2.a and 3.2.3.a), with the longest wavelength (69 cm), contours are uniform oval lines evolving around the e-seal.

On the other hand, for 2.44GHz (short wavelength -12cm), the contours evolving around e-seal are not uniform but have directional lobes. One reason is the reflection from the container door (backplane). The dipole has all three dimensions comparable to the wavelength and is offset from the container door by a few centimeters. This sets up a reflected "image" RF source that behaves as if it were "behind" the door. The combined radiation from the image source and the actual source can set up interference patterns, i.e., radial nodes of high and low signal strength.

In the areas on the top and bottom of the container, for all three frequencies signal drops off as it travels away from the back door. This drop seems to happen somewhat faster in the case of 2.44GHz frequency

In general, signals at higher frequencies are more directional, and as the frequency increases, there is higher likelihood that there will be regions with higher signal drop off. Looking at figures 3.2.2.a-c one can observe that signal strength in front of the e-seal, i.e., line-of-sight is good for 433MHz and 916MHz frequencies. For 2.44GHz there are gaps between signal lobes that may cause no-reads. A rule of thumb in communication systems is that operating effectiveness decreases by only 5%-10% as frequency increases from 433MHz – 2.44GHz.

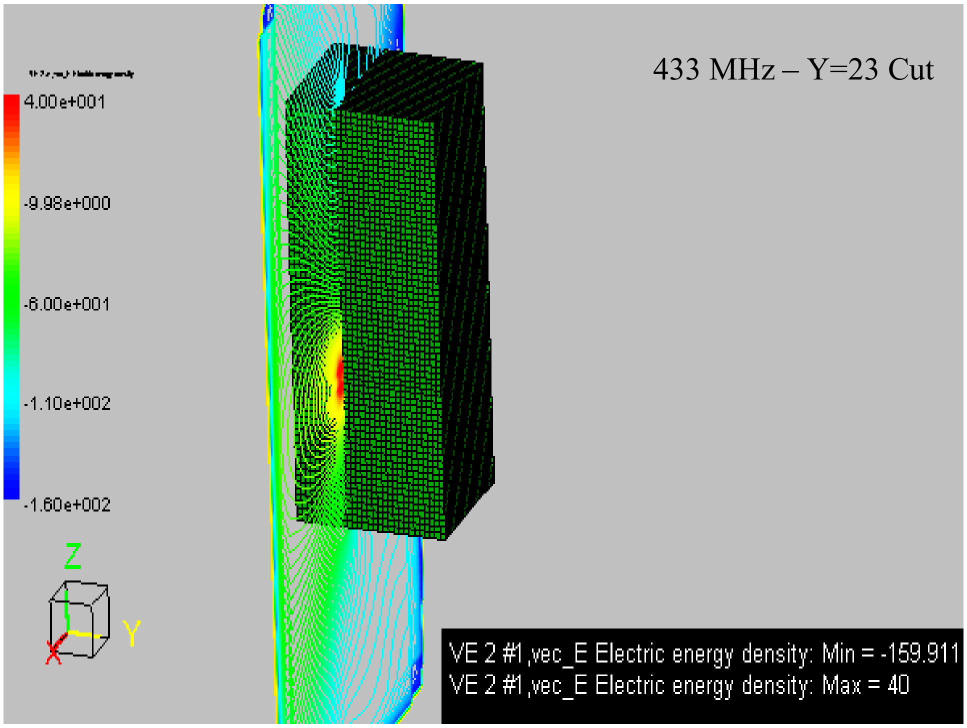

Figure E.3.2.2.a E-seal frequency = 433MHz, Y cut in e-seal plane

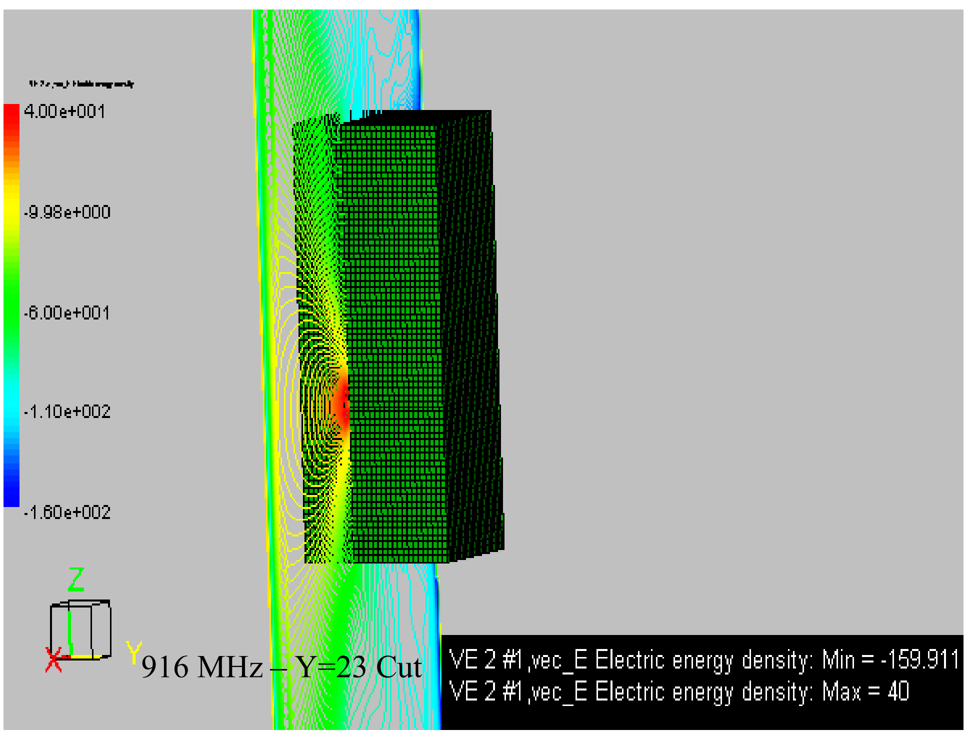

Figure E.3.2.2.b E-seal frequency = 916MHz, Y cut in e-seal plane

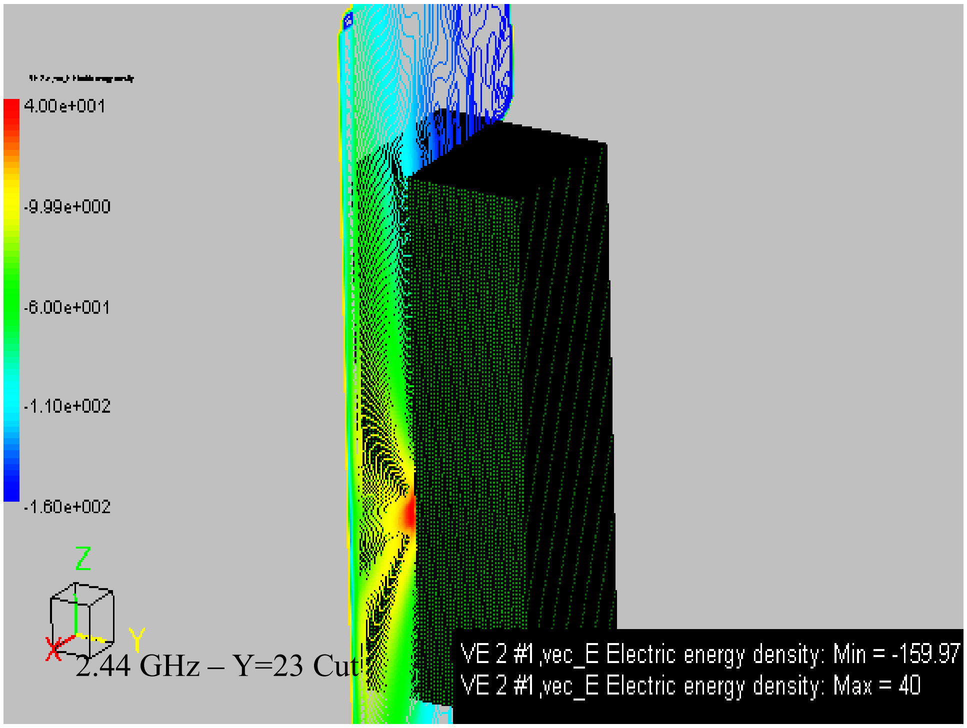

Figure E.3.2.2.c E-seal frequency = 2.44GHz, Y cut in e-seal plane

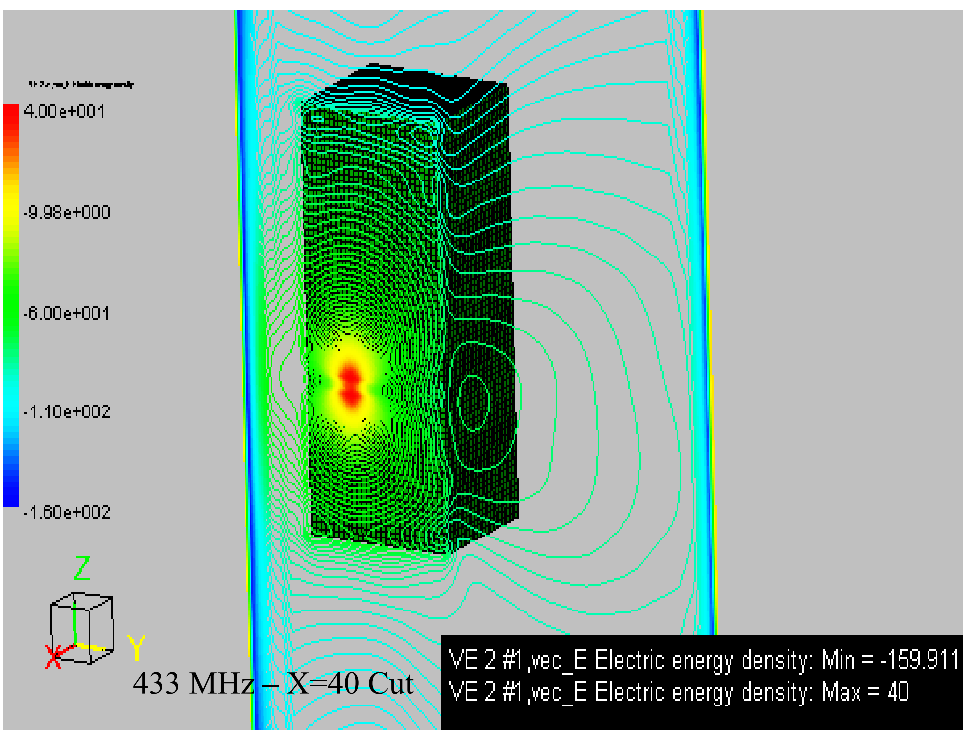

Figure E.3.2.3.a E-seal frequency = 433MHZ, X cut in e-seal plane

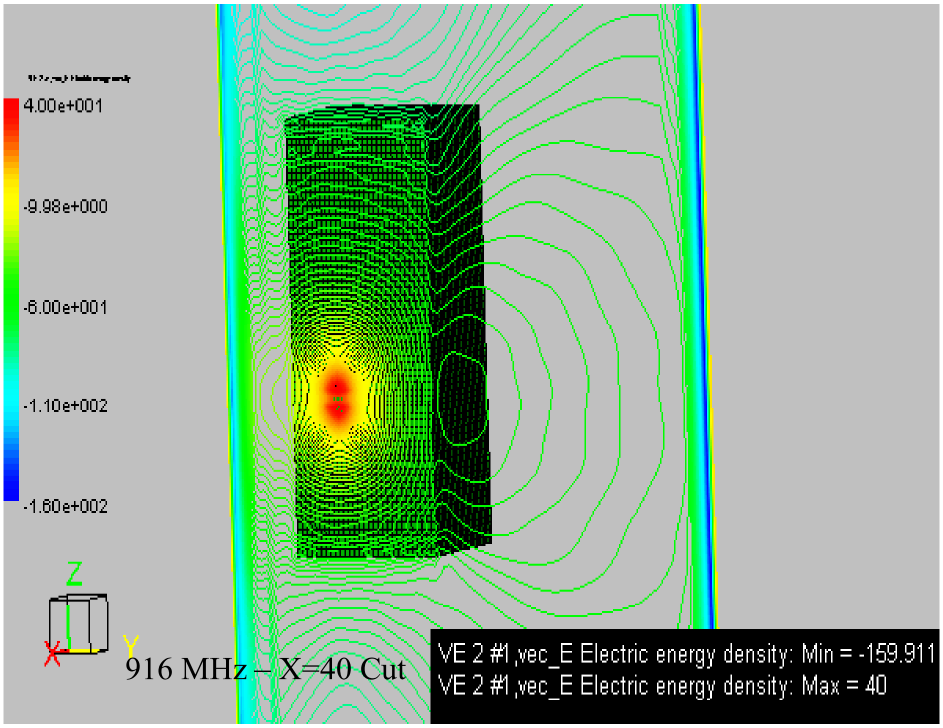

Figure E.3.2.3.b E-seal frequency = 916MHZ, X cut in e-seal plane

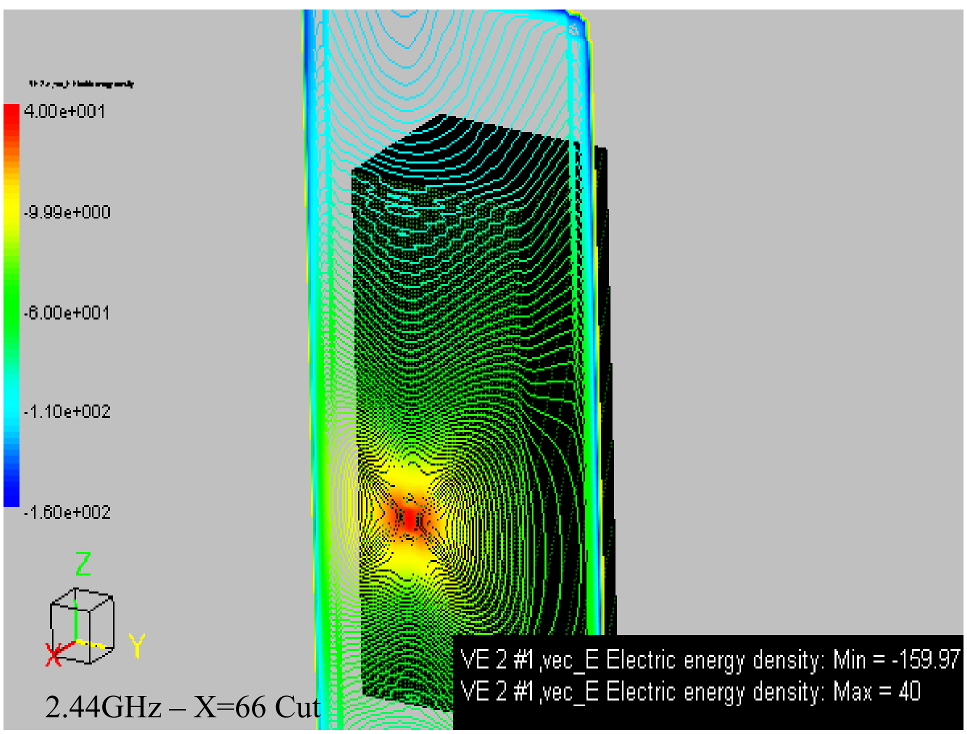

Figure E.3.2.3.c E-seal frequency = 2.44GHZ, X cut in e-seal plane

<u>In-Gate Scenario: With Booth, Container Obstructions Z-cut Planes</u>

In this scenario we examined signal propagation and radiation patterns when there are other structures in the area surrounding the container with e-seal. We examined the region in the back and to the right of the container. For the purpose of the simulation we placed a booth to the right of the container, and another container in the lane to the right of the booth. Figures E.3.2.4 – Figure E.3.2.7 show the results of our simulation runs in the Z cut planes. Note that the simulated region for 2.44GHz frequency was reduced to the top half of the region defined for 433MHz and 916MHz frequencies. Hence, figures E.3.2.4 and E.3.2.5 do not have 2.44GHz results since the simulation in the lower region was not performed for 2.44GHz frequency.

For all selected planes one can see that the contours for all three frequencies are not as uniform as the contours in the open space (Figures E.3.2.2, E.3.2.3 and E.3.4.1). This is largely due to superposition and cancellation with signals that are reflecting from structures in the region. However, the resultant radiation patterns are somewhat similar, suggesting that operational efficiency for all three frequencies is not much different.

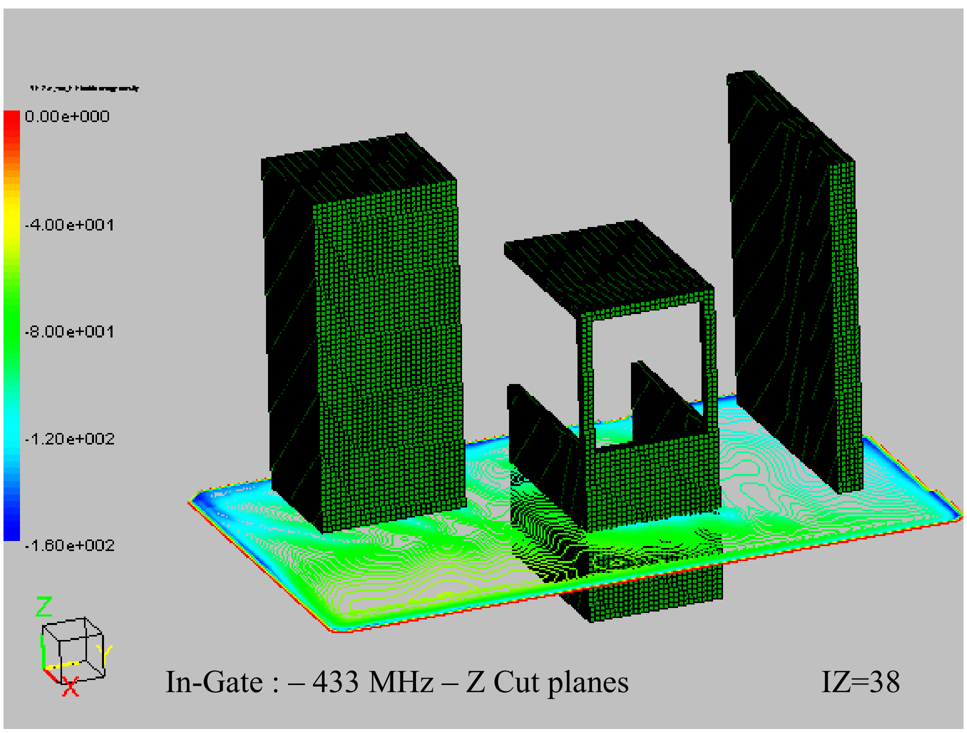

Figure E.3.2.4.a E-seal radiation patterns around obstacles
(frequency = 433MHZ, Z plane cut at 38)

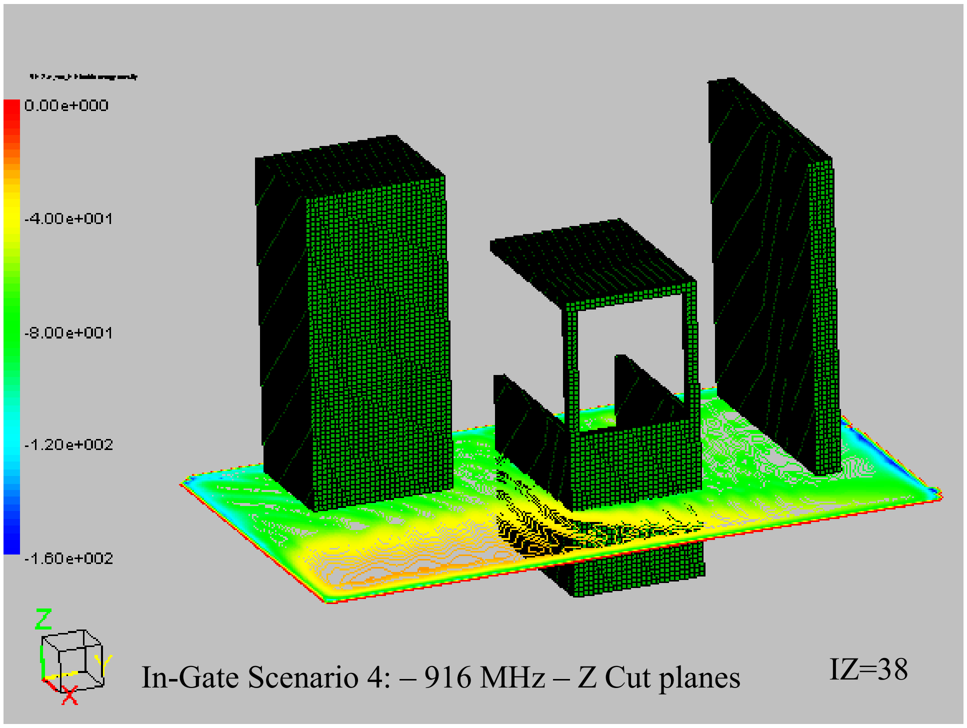

Figure E.3.2.4.b E-seal radiation patterns around obstacles
(frequency = 916MHZ, Z plane cut at 38)

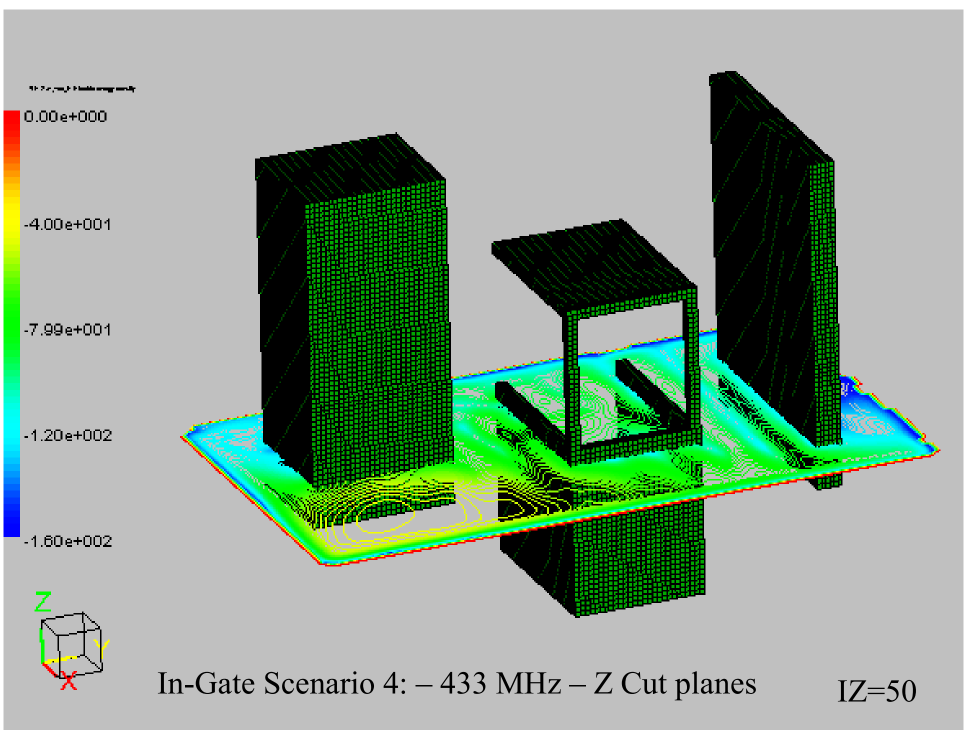

Figure E.3.2.5.a E-seal radiation patterns around obstacles
(frequency = 433MHZ, Z plane cut at 50)

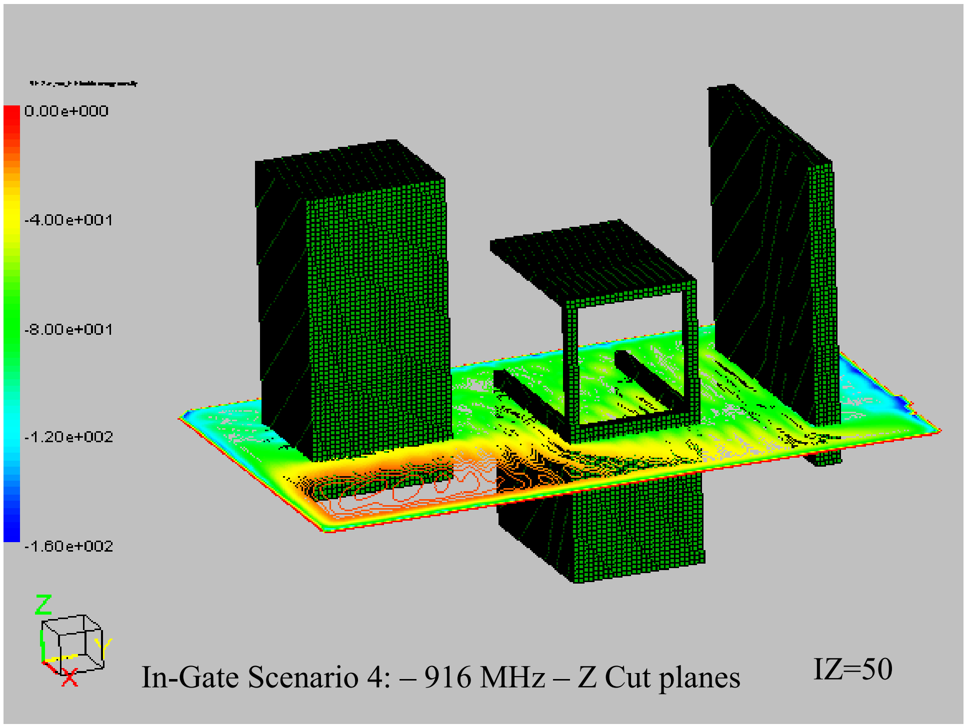

Figure E.3.2.5.b E-seal radiation patterns around obstacles
(frequency = 916MHZ, Z plane cut at 50)

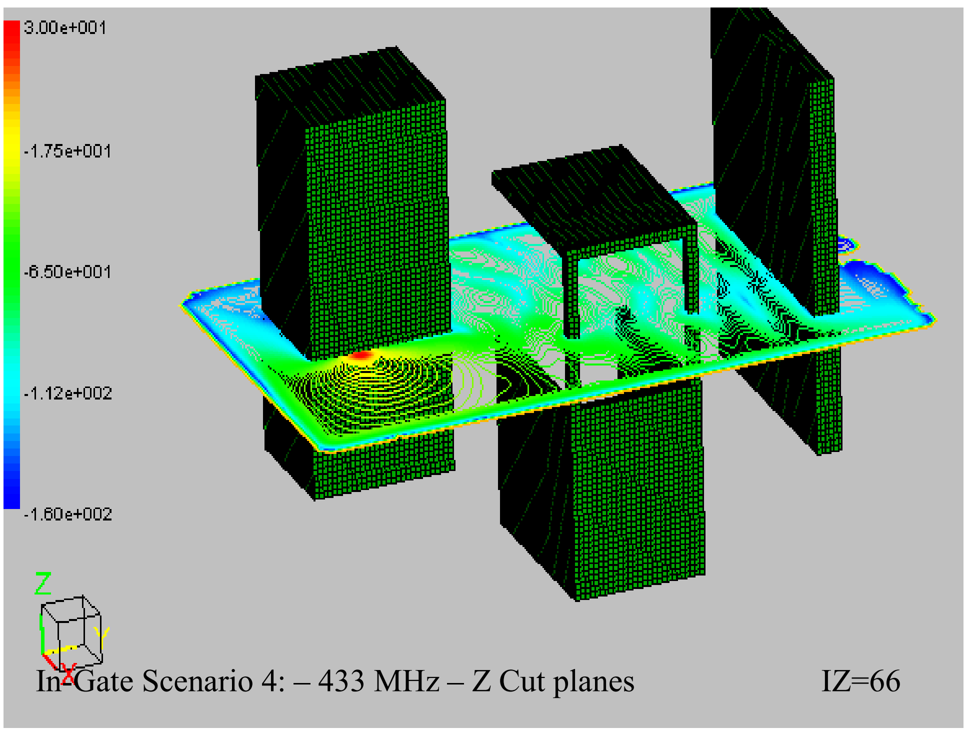

Figure E.3.2.6.a E-seal radiation patterns around obstacles
(frequency = 433MHZ, Z plane cut at 66)

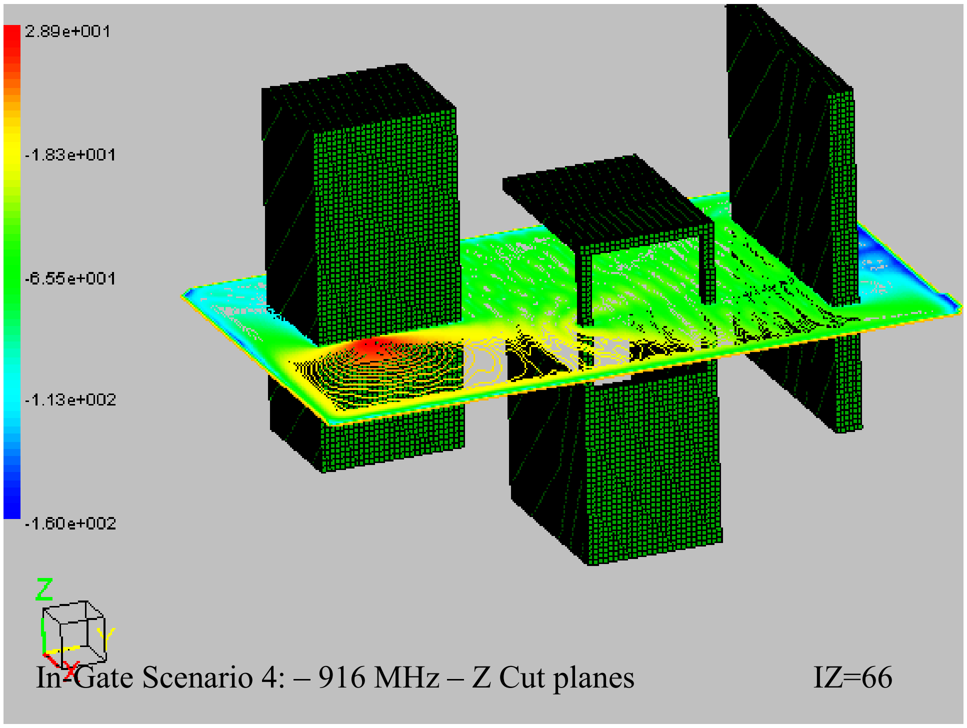

Figure E.3.2.6.b E-seal radiation patterns around obstacles
(frequency = 916MHZ, Z plane cut at 66)

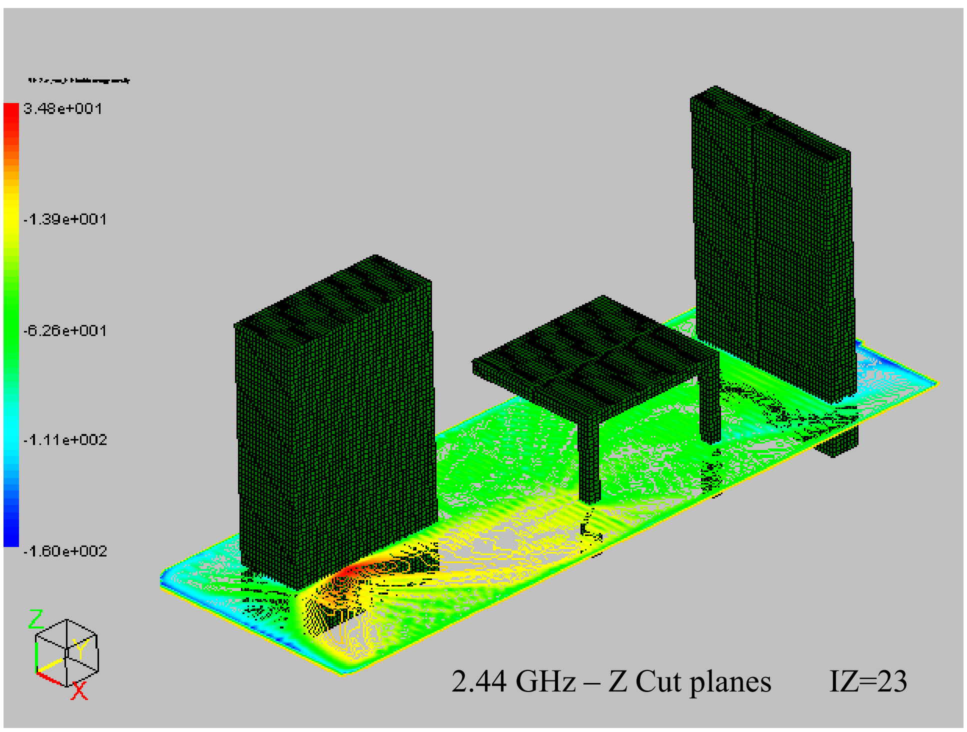

Figure E.3.2.6.c E-seal radiation patterns around obstacles
(frequency = 2.44GHZ, Z plane cut at 23 or 66 level from ground)

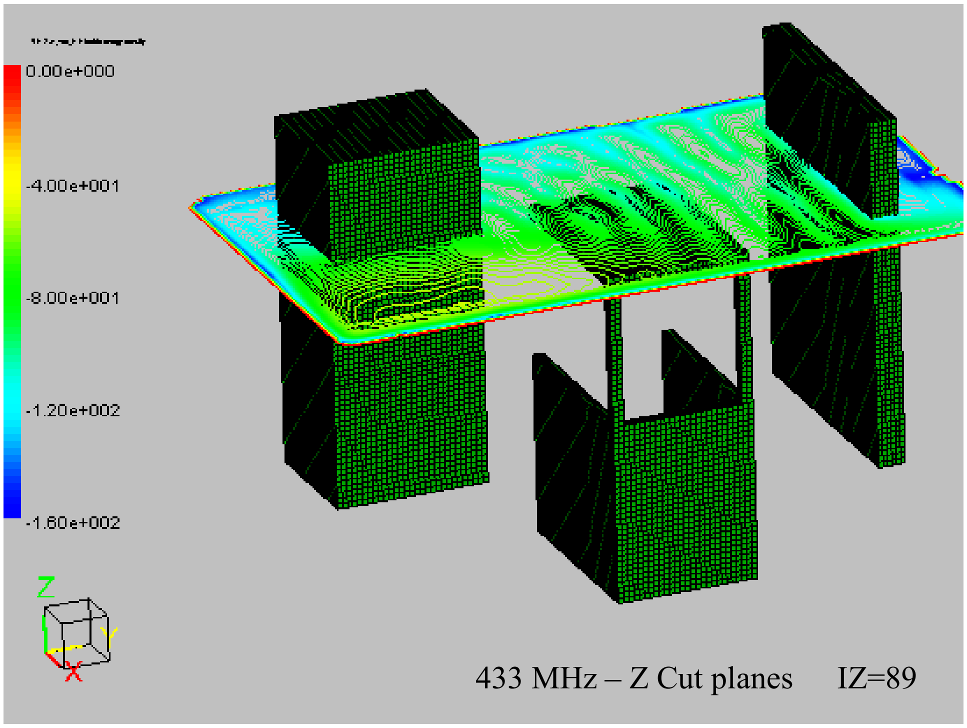

Figure E.3.2.7.a E-seal radiation patterns around obstacles
(frequency = 433MHz, Z plane cut at 89)

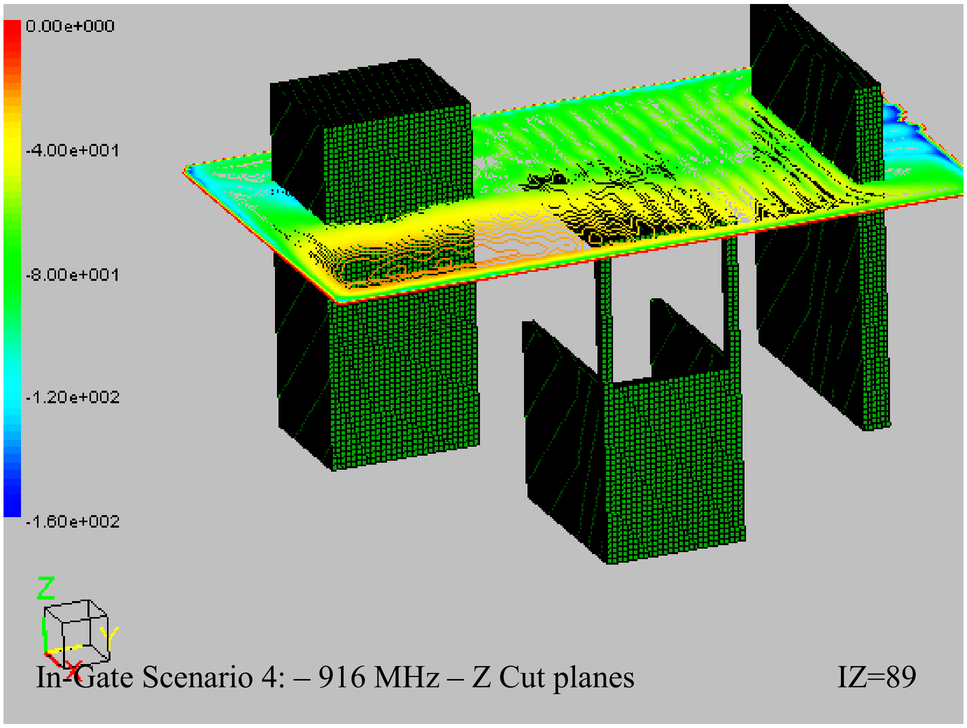

Figure E.3.2.7.b E-seal radiation patterns around obstacles
(frequency = 916MHZ, Z plane cut at 89)

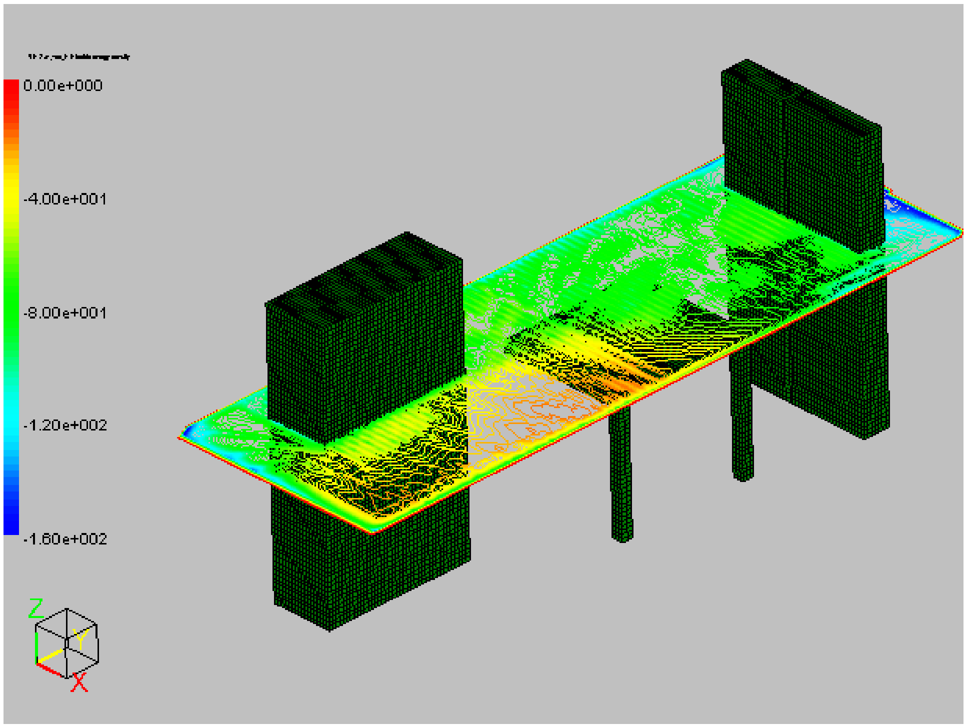

Figure E.3.2.7.c E-seal radiation patterns around obstacles
(frequency = 2.44GHZ, Z plane cut at 54)

<u>In-Gate Scenario: With Booth, Container Obstructions Y-cut Planes</u>

The Y cut in the e-seal plane can be compared with the same Y cuts in open space (Figure E.3.2.2). Again we can see that contours are not as uniform, and this is the result of signals reflected from surrounding structures.

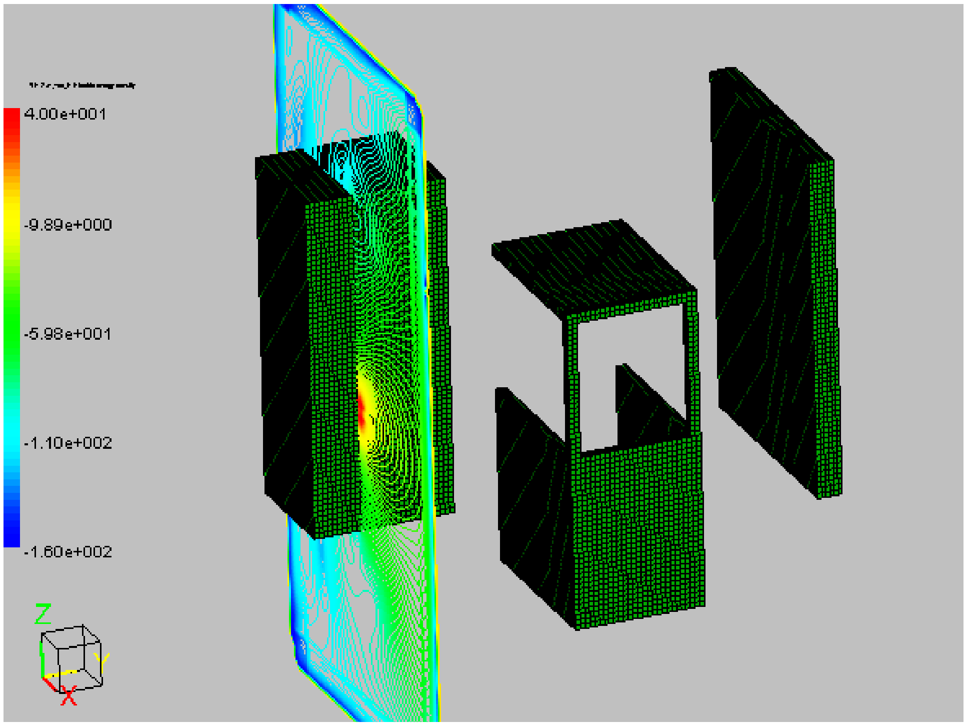

Figure E.3.2.8.a E-seal radiation patterns around obstacles
(frequency = 433MHZ, Y plane cut at 23)

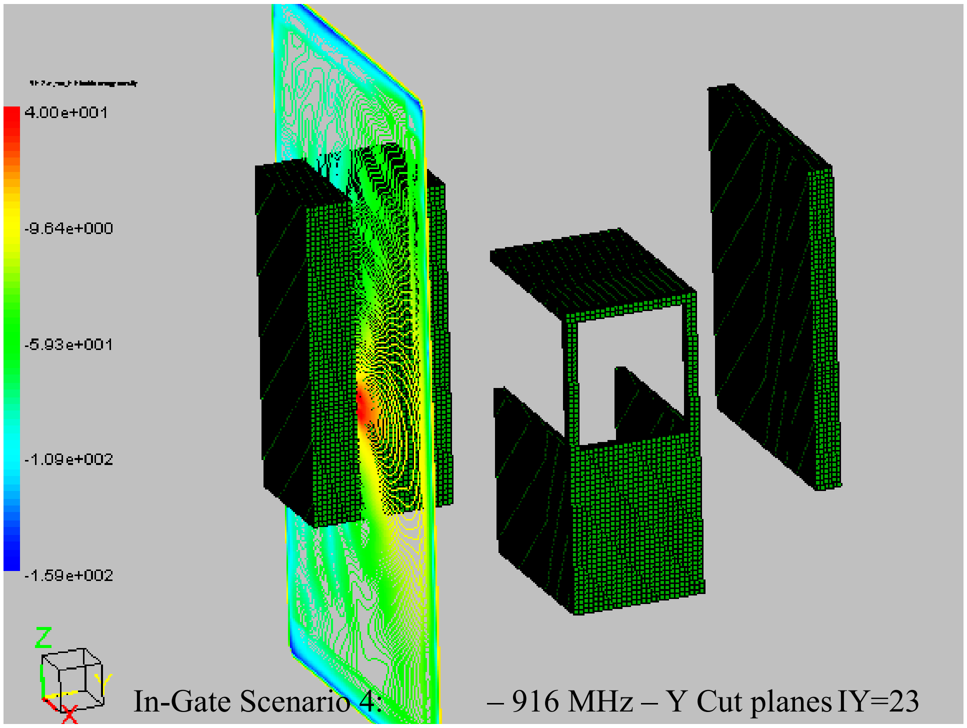

Figure E.3.2.8.b E-seal radiation patterns around obstacles
(frequency = 916MHZ, Y plane cut at 23)

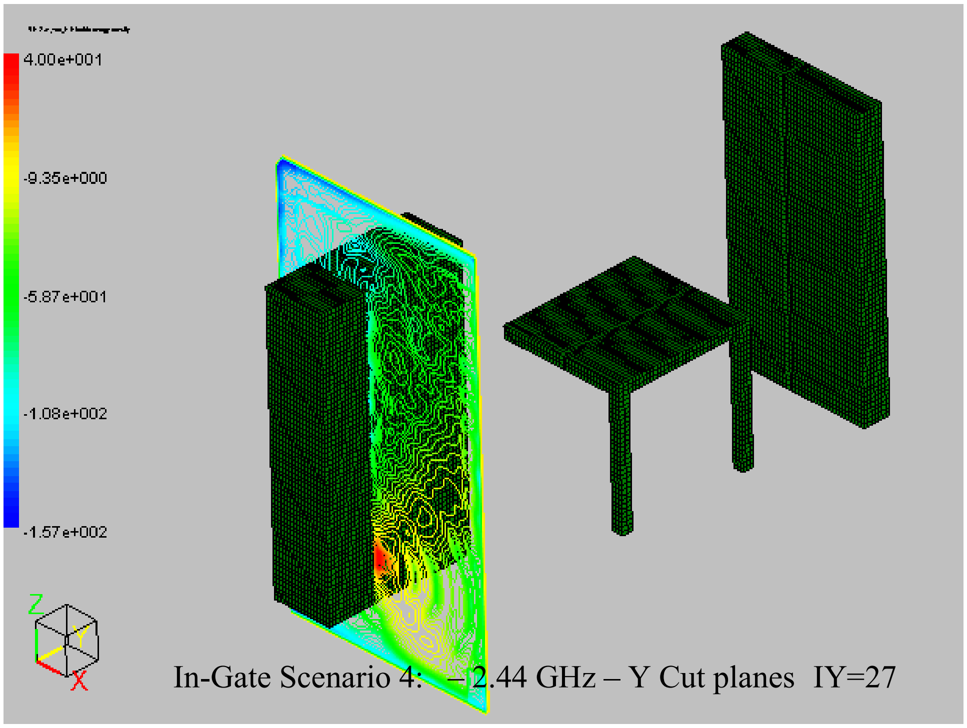

Figure E.3.2.8.c E-seal radiation patterns around obstacles
(frequency = 2.44GHZ, Y plane cut at 27)

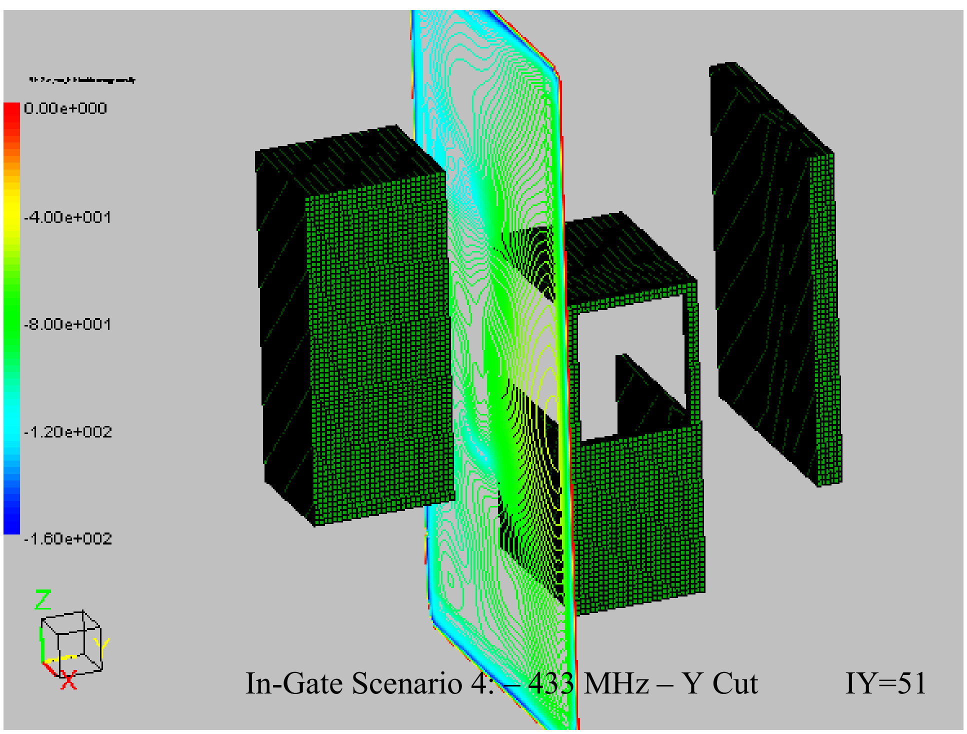

Figure E.3.2.9.a E-seal radiation patterns around obstacles
(frequency = 433MHZ, Y plane cut at 51)

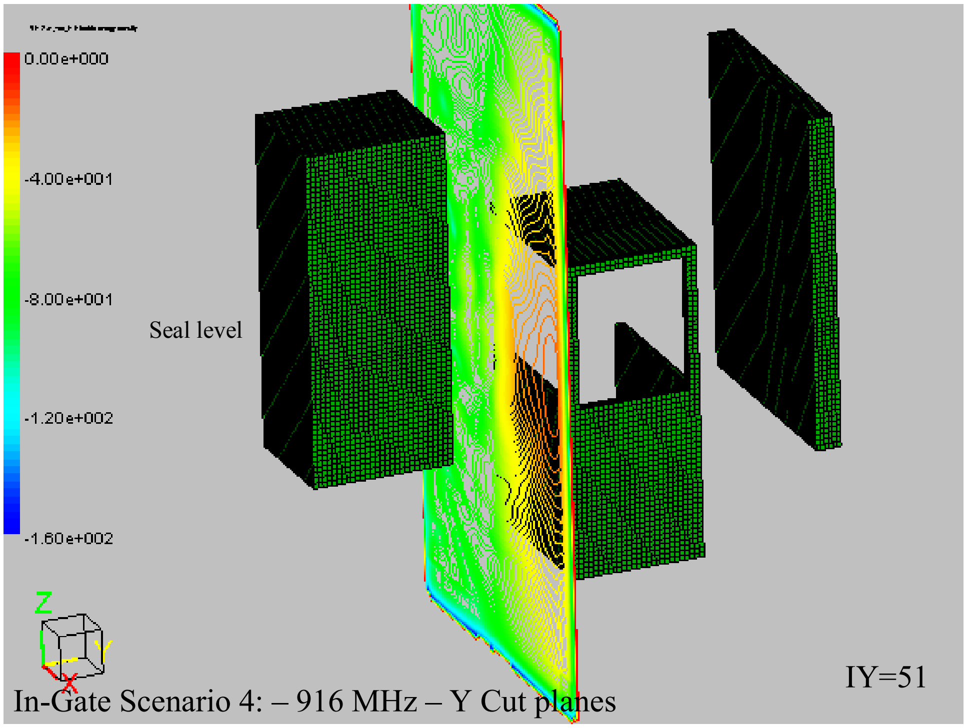

Figure E.3.2.9.b E-seal radiation patterns around obstacles
(frequency = 916MHZ, Y plane cut at 51)

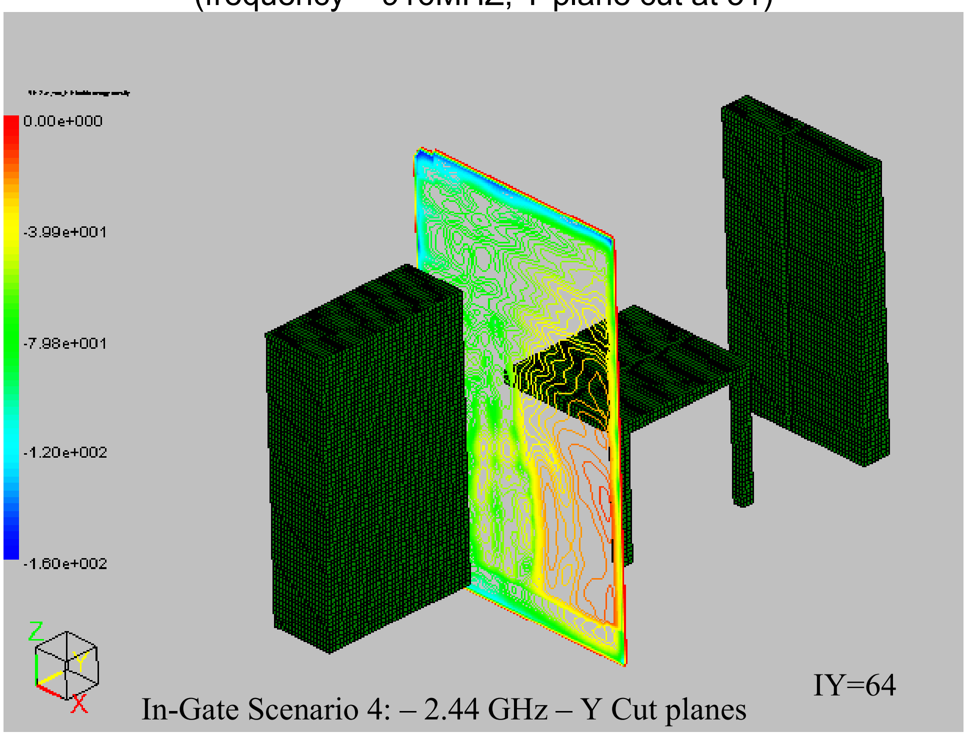

Figure E.3.2.9.c E-seal radiation patterns around obstacles
(frequency = 2.44GHZ, Y plane cut at 64)

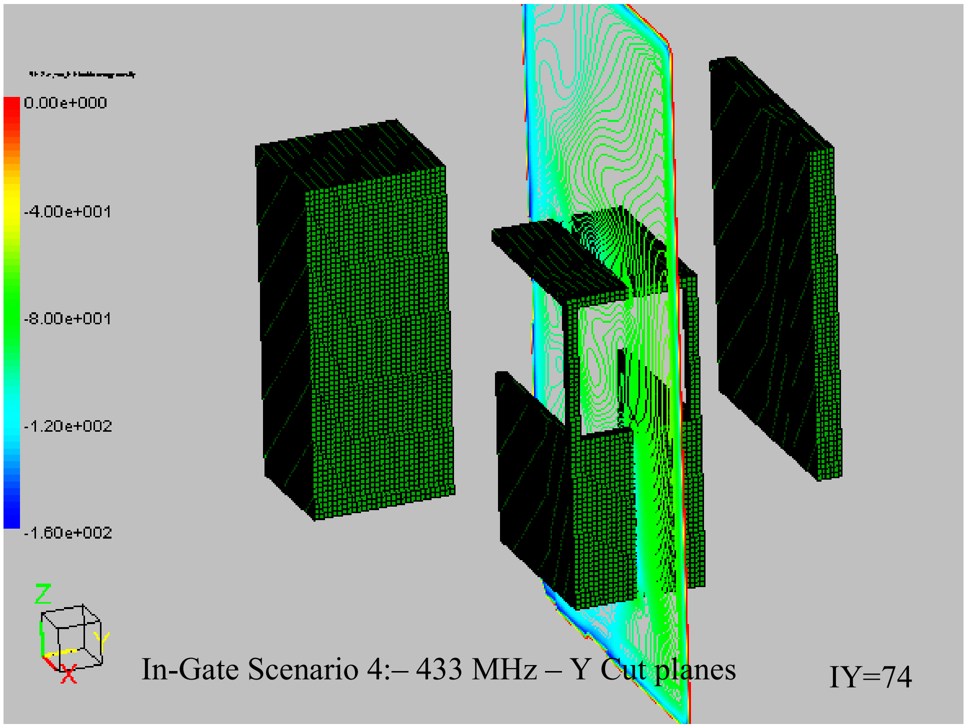

Figure E.3.2.10.a E-seal radiation patterns around obstacles
(frequency = 433MHZ, Y plane cut at 74)

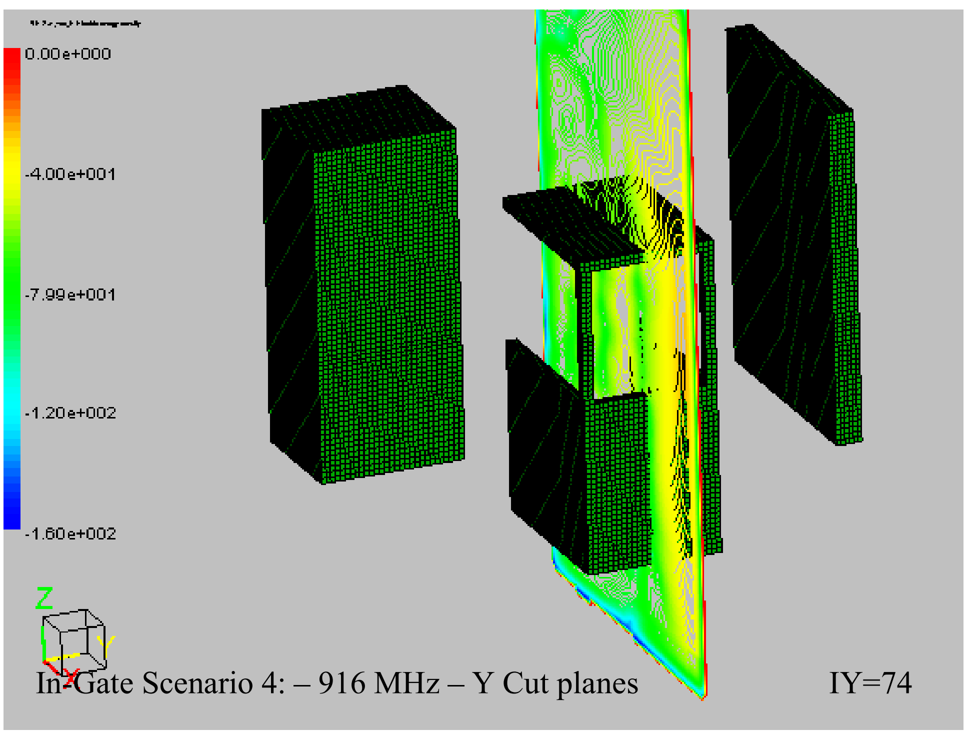

Figure E.3.2.10.b E-seal radiation patterns around obstacles
(frequency = 916MHZ, Y plane cut at 74)

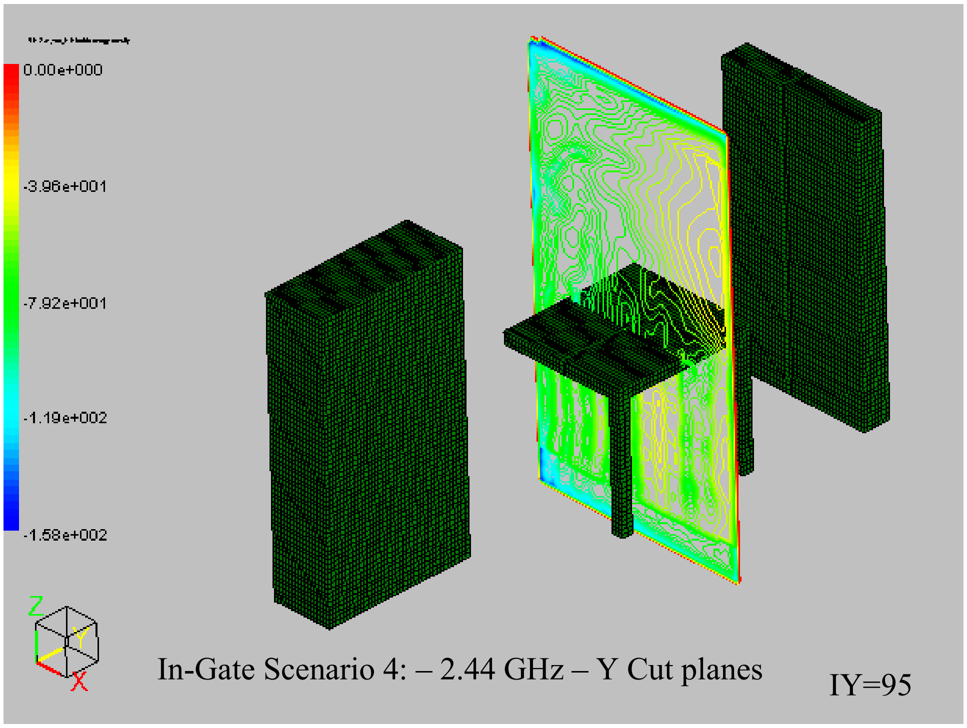

Figure E.3.2.10.c E-seal radiation patterns around obstacles
(frequency = 2.44GHZ, Y plane cut at 95)

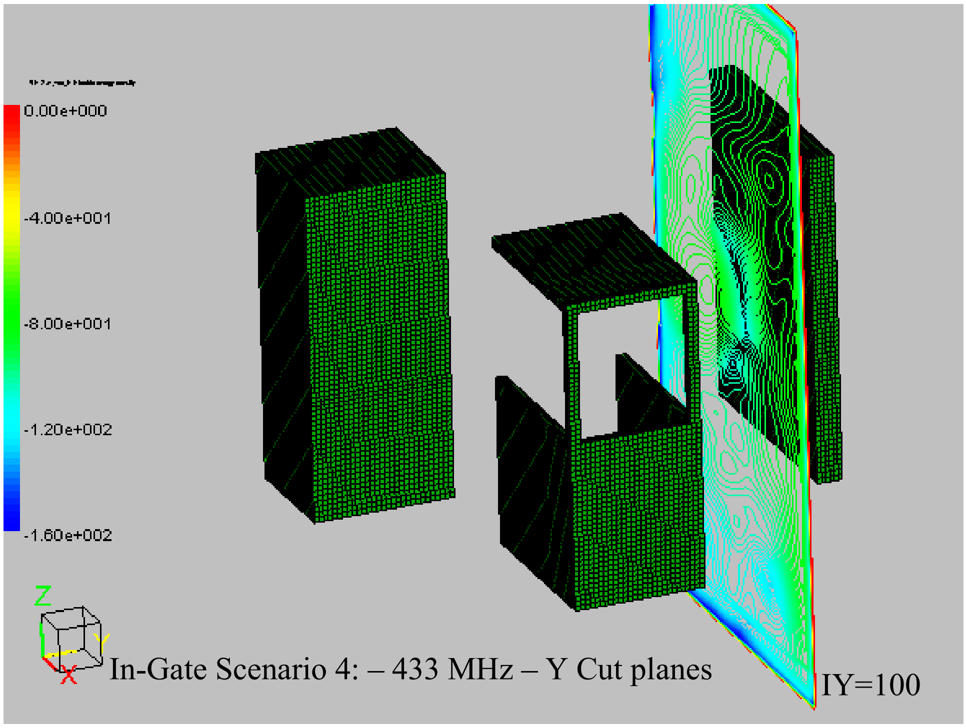

Figure E.3.2.11.a E-seal radiation patterns around obstacles
(frequency = 433MHZ, Y plane cut at 100)

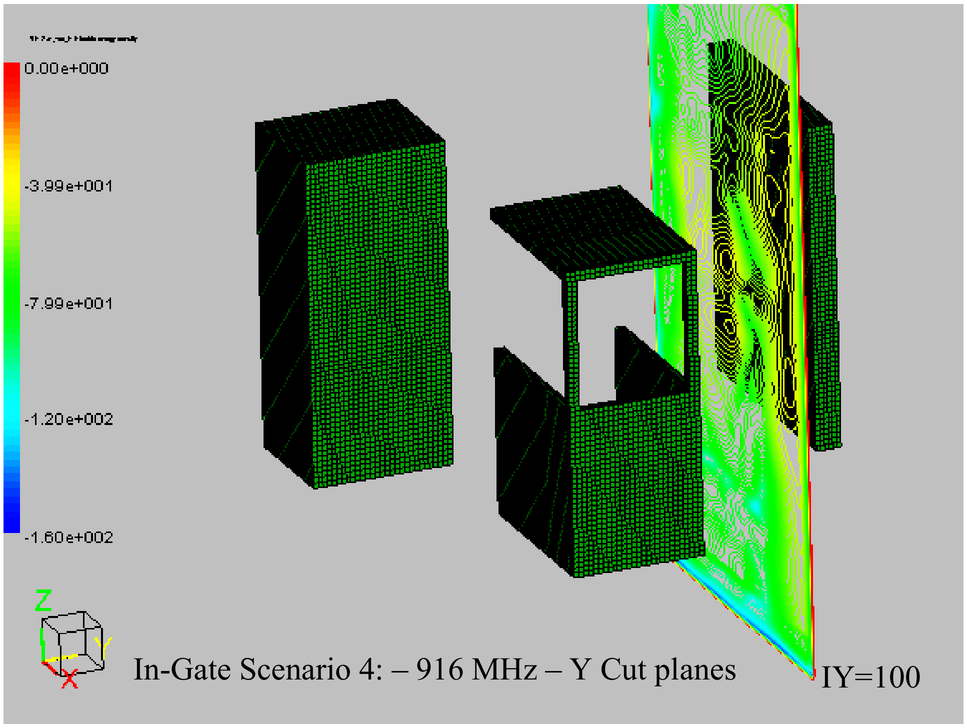

Figure E.3.2.11.b E-seal radiation patterns around obstacles
(frequency = 916MHZ, Y plane cut at 100)

E.3.2.3 In-Gate Simulation Conclusions

The objective of the in-gate simulation was to investigate signal propagation in the in-gate environment, and in particular signal propagation and radiation patterns when signals reach obstacles commonly found in the in-gate area, such as booths and other containers. To accomplish this, we constructed two sets of scenarios. The first set simulated an e-seal on the back of the container in the region with no obstructions. The second set investigated signal propagation in the environment with obstacles. The objective was to determine how well signals of different frequencies traveled around objects and the potential impact from signal diffractions.

In the case when there are no obstructions in the region, the simulation results show that signal strength contours for 433MHz frequencies, with 69-cm wavelength, are fairly uniform, and signals wrap somewhat better around the edges then do 916MHz and 2.44GHz signals. For 916MHz signals, radiation contours are less uniform. Finally, for 2.44GHz, with 12cm wavelength), the contours evolving around e-seal are not uniform but have directional lobes. One reason is the reflection from the container door (backplane). The dipole has all three dimensions comparable to the wavelength and is offset from the container door by a few centimeters. This sets up a reflected "image" RF source that behaves as if it were "behind" the door. The combined radiation from the image source and the actual source can set up interference patterns, i.e., radial nodes of high and low signal strength . This directivity may create gaps where signal drops off sharply, and may result in regions with no-reads.

The patterns produced in the environment with structures are not as uniform as the patterns in the case where there are no obstructions. Pattern of RF intensity exhibits wave-like variations, which is typical of interference due to superposition with reflected signals from all the structures. However, examining the patterns one can conclude that their propagation characteristics are somewhat similar.

E.3.3 On-Rail Simulation

E.3.3.1 Scenario and Configuration

Figure E.3.3.1.a shows the challenging e-seal environment of containers stacked in a well car. The objective of the on-rail simulations was to examine the effectiveness of e-seals in transmitting RF signals to the reader when the e-seal is in the gap between stacked-up containers. The model geometry was intended to simulate the situation where a 40' container was placed atop two 20' containers on a flat railcar, rather than in a well car.

The model was also based on the experimental configuration used in the terminal testing. This configuration is shown in Figure E.3.3.1.b. In this configuration, a 40' container was placed atop two 20' containers, which in turn were elevated to represent their placement on a railcar and rail bed. There is a 4.5" gap between the end surfaces of the two 20' containers. E-seals of various frequencies were modeled on the back door of the container as shown in Figures E.3.3.1.b-c.

Figure E.3.3.1.a On-Rail Scenario

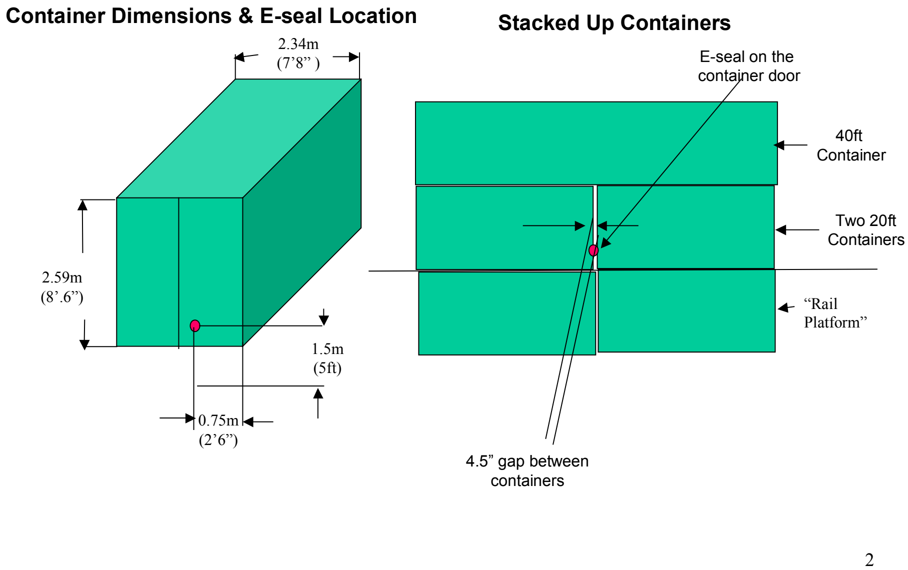

Figure E.3.3.1.b On-rail geometry and dimensions

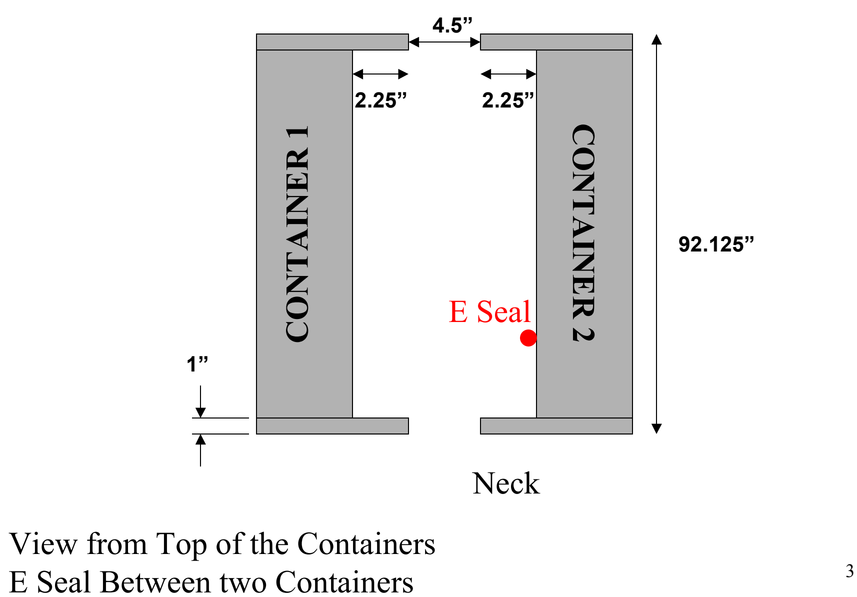

Figure E.3.3.1.c On Rail Container geometry and dimensions

CTLSS Simulation Setup

CTLSS simulation was conducted by placing an RF dipole antenna at the location of the e-seal in the gap between two containers. A top view of the gap structure is illustrated in Figure E.3.3.1.c. The gap is enclosed by end surfaces of two containers, with two necks of 2.25” sticking out from either side separated by a 4.5” space in the middle. The container on the top and the railcar on the bottom also enclose it vertically. Therefore, the gap space can act as an RF cavity with slots on both sides. The cavity structures in the simulation are illustrated in Figure E.3.3.2. The X direction is along the rail, the Y direction is horizontal along the container door, and the Z direction is vertically upward.

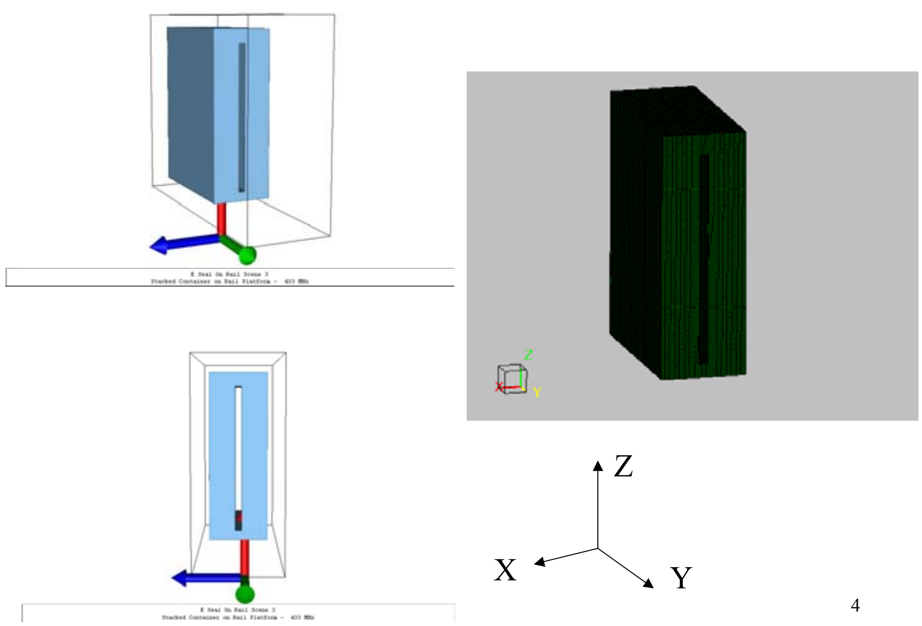

Figure E.3.3.2 On Rail Simulation Structure (e-seal in the slot)

E.3.3.2 Simulation Results

<u>E-seal at 433 MHz Frequency</u>

The first case shown is the simulation of an e-seal at 433 MHz with a dipole antenna oriented in the X direction. In Figure E.3.3.3, contour plots of signal intensity at the X=0 cut plane are shown passing through in the middle of the gap. One can see that there are "lumps" vertically along the slot. This is the result of the e-seal effectively being in a microwave resonant cavity. I.e., the empty space between two containers is a microwave cavity with side slots that allow microwave/RF signals to leak to the outside. With the e-seal acting like a microwave antenna within the cavity, certain cavity modes are excited that have distinct mode patterns (the "lumps") within the cavity. Figure E.3.3.4 shows the RF pattern in a cut plane along the side of the container (normal to the Y axis); this view shows the same lumpy structures. Such a lumpy intensity spectrum may also be viewed as the "diffraction" pattern of the RF waves as they emerge from the cavity slot on the sidewall. Since signal propagation is lumpy in nature outside the gap space, the overall radiation pattern around the container will not be uniformly distributed. This may create no-read regions.

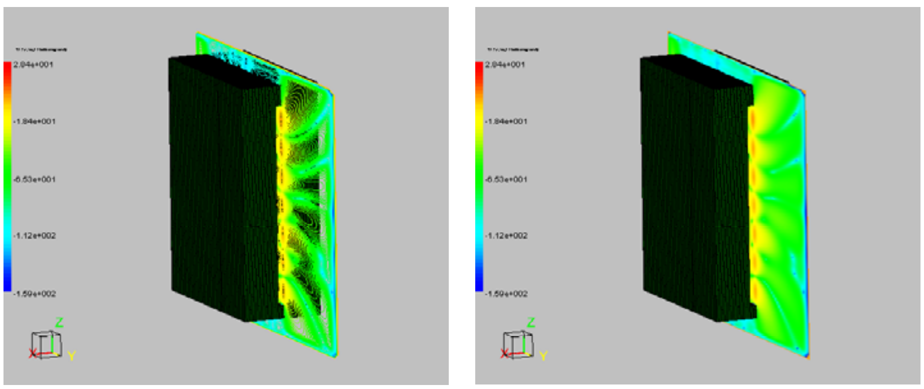

433 MHz – Dipole in X – X=40 plane Cut 5

Figure E.3.3.3 E-seal frequency=433MHz X cut at 40

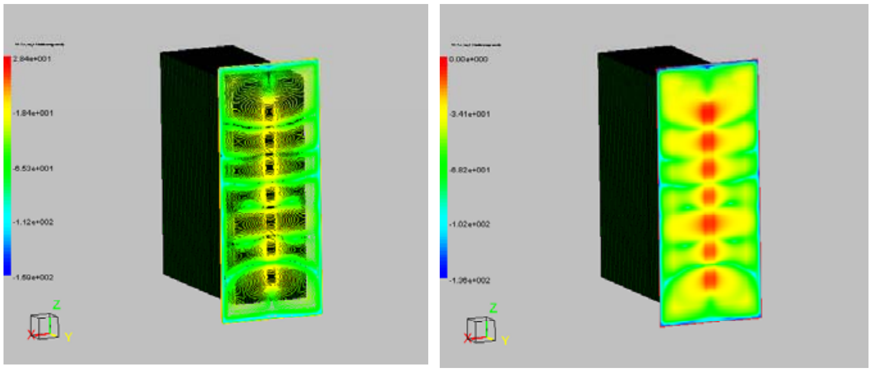

433 MHz – Dipole in X – Y=54 plane Cut 6

Figure E.3.3.4 E-seal frequency=433MHz Y cut at 54

To further illustrate the effect of non-uniform spatial distribution of RF signals, CTLSS simulations of larger space (up to 3 meters) along the container wall are conducted. In the larger simulation, the gap is modeled as a simple rectangular slot without the presence of detailed neck structures. The Y cut plane up to 3 m in X length along the container surface is illustrated in Figure E.3.3.5. Again, the color contours of signal strength contain striation patterns that are similar to the plots in the previous figures. It is worthwhile to note that the striation pattern diminishes as the distance from the slot along container surface increases. Beyond 2 m from the slot along the surface (along X), the intensity map shows uniform intensity distribution, albeit at a much lower signal strength level. Figure E.3.3.6 shows the same cut plane as in Figure E.3.3.5 (parallel to container surface), but at 1 m distance away from the container surface. Again, signal intensity striations persist up to 2 m along the surface from the slot position. These findings need to be compared and validated with read results obtained during terminal testing.

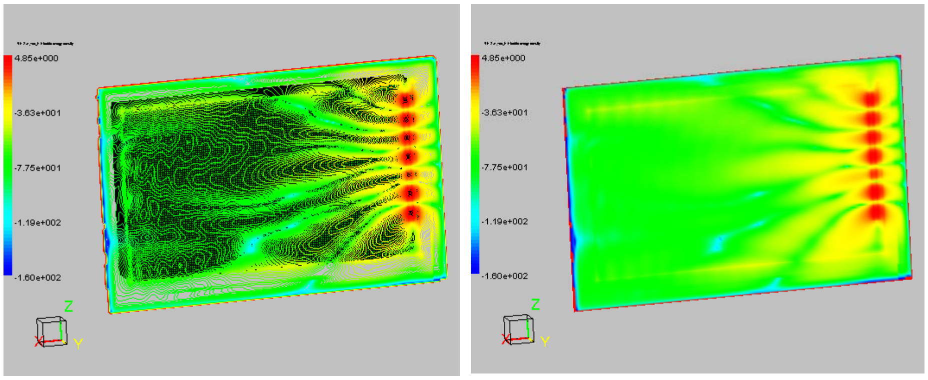

433 MHz – Dipole in X – Larger X region -Y=39 plane Cut 7

Figure E.3.3.5 E-seal frequency=433MHz Y cut at 39

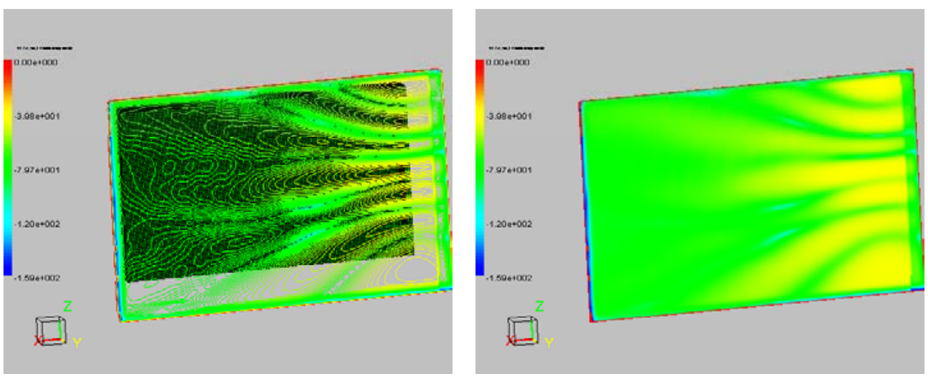

433 MHz – Dipole in X – Larger X region -Y=66 plane Cut 8

Figure E.3.3.6 E-seal frequency=433MHz Y cut at 66

CTLSS simulations have also been conducted by placing a dipole antenna along both Y and Z directions (i.e. along the surface of container backdoor, in two orientations). In both cases, the RF signals are strongly attenuated within the gap. In fact, the attenuation is so severe that there is no presence of RF signals outside the gap. Apparently, for these two dipole orientations, the 433 MHz frequency is below the cut-off frequency of the specific cavity/waveguide modes that the antenna is intended to excite. Therefore, RF signals do not propagate out of the microwave cavity/waveguide. Radiating elements in the e-seal may contain all three dipole components. Non-propagation of two dipole components in the gap implies added power loss, and therefore a less efficient link between the e-seal in the gap and the reader outside the gap.

<u>E-seal at 916MHz Frequency</u>

For this frequency, the CTLSS simulation was performed by placing an X-oriented dipole antenna in the gap. Figure E.3.3.8, shows signal intensity contours on the plane passing through the gap (X cut). The RF pattern is similar to that of the 433 MHz. However, there are more "lumps" of intensity peaks than the 433 MHz case, indicating that higher order waveguide modes are excited by the e-seal at higher frequency. Figure E.3.3.9 shows contour plots of signal intensity, i.e., lumpy RF structures, in Y cut plane outside the cavity slot. Figures E.3.3.10 and E.3.3.11 are contour plots of RF intensity at Y cut planes that are parallel to the container wall. These plots contain an enlarged simulation region in X. Comparing these plots with those of the 433 MHz in Figures E.3.3.5 and 3.3.6, one can observe that there are more striations with smaller spatial structures at higher frequency. A potential impact of the high frequency e-seals is to have more uneven and smaller spatial regions of signal variations.

Another important observation from the 916 MHz study is that when a dipole antenna oriented in the Z direction (i.e. along the vertical surface of the container backdoor) is used in the simulation, RF can be excited in the gap and propagate effectively to outside. This is contrary to the 433 MHz results (Figure E.3.3.7), which show that no excitation is feasible with such dipole orientation. The understanding is that 916 MHz is above the cut-off frequency of the waveguide modes in the cavity/waveguide formed by the gap, thus making the excitation of RF possible. Therefore, higher frequency e-seals have better coupling efficiency in the gap and may be more effective radiation devices for the on-rail scenario

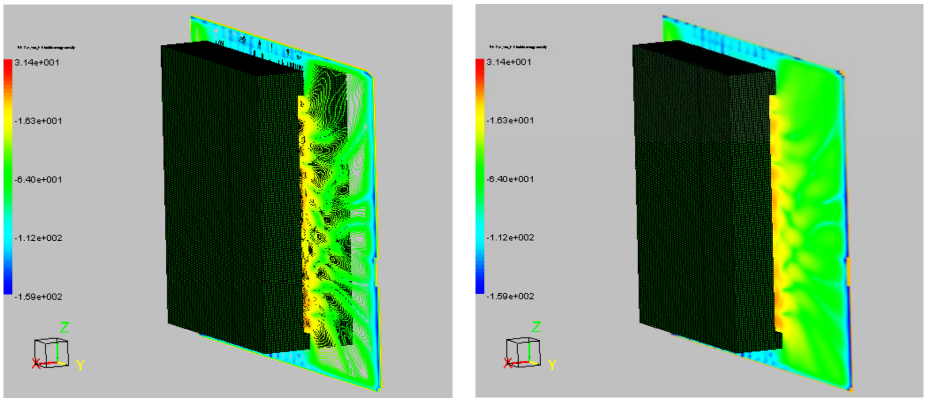

916 MHz – Dipole in X – X=40 plane Cut 10

Figure E.3.3.8 E-seal frequency=916MHz X cut at 40

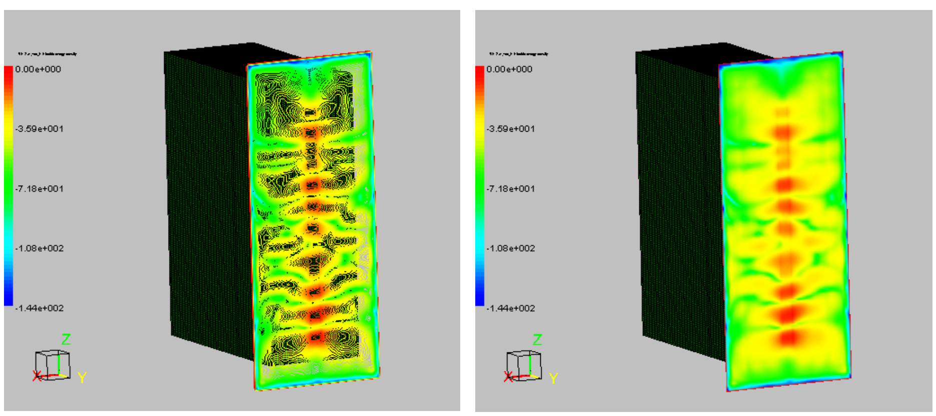

916 MHz – Dipole in X – Y=54 plane Cut 11

Figure E.3.3.9 E-seal frequency=916MHz Y cut at 54

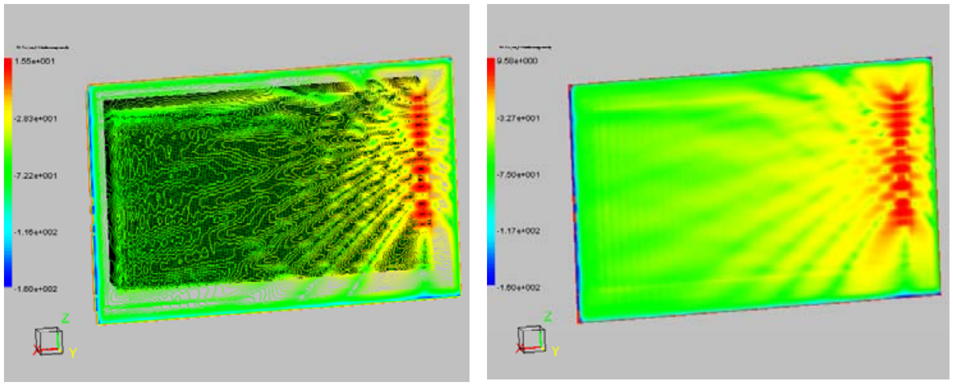

916 MHz – Dipole in X – Y=39 plane Cut 12

Figure E.3.3.10 E-seal frequency=916MHz Y cut at 39

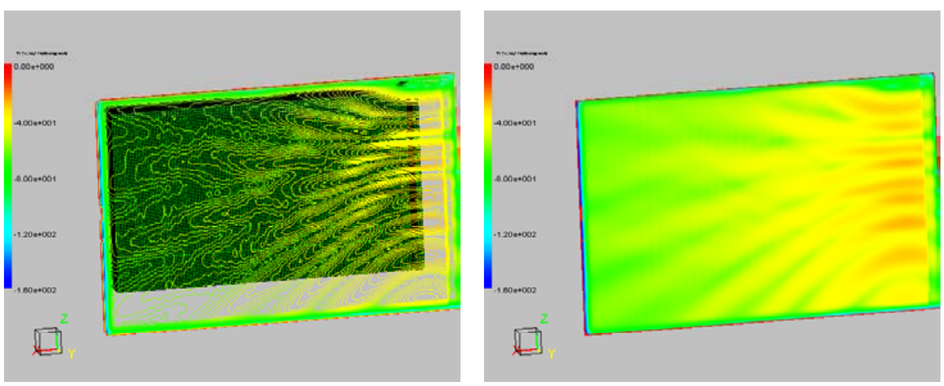

916 MHz – Dipole in X – Y=66 plane Cut 13

Figure E.3.3.11 E-seal frequency=916MHz Y cut at 66

E-seal at 2.44GHz Frequency

For this frequency, the CTLSS simulation was performed by placing an X-oriented dipole antenna in the gap. Figure E.3.3.12 shows signal intensity contours on the plane passing through the gap (X cut). The RF pattern shows fairly uniform signal intensity distribution coming out of the slot. Figure E.3.3.13 shows contour plots of signal intensity at Y cut plane (parallel to side surface of the container) outside the cavity slot. The RF pattern shows many very fine striations in front of the slot, which is consistent with the trend that intensity striations become finer in space as frequency increases. At 2.44 GHz, the striations are fine enough so that the overall RF distribution in space is somewhat uniform. Hence, higher frequency e-seal may be more desirable for the on-rail environment because of its signal uniformity outside the gap.

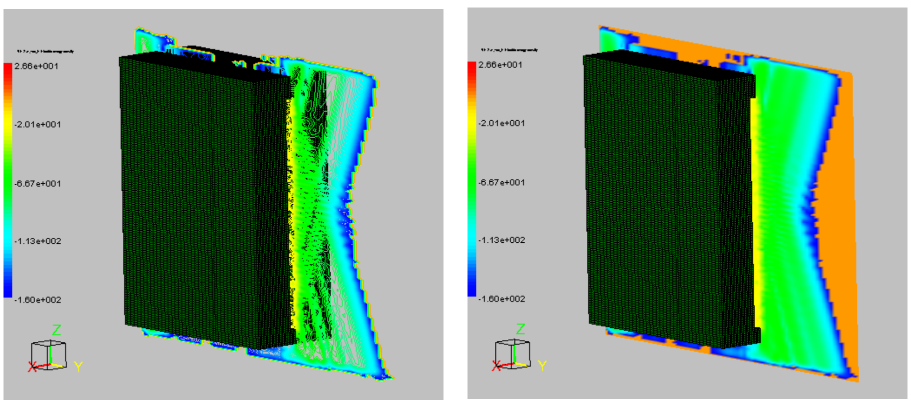

2.44 GHz – Dipole in X – Y=54 plane Cut 15

Figure E.3.3.12 E-seal frequency=2.44GHz Y cut at 54

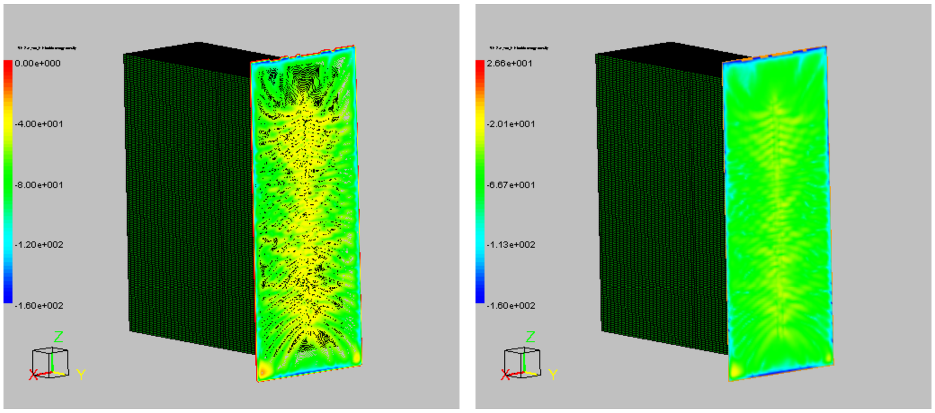

2.44 GHz – Dipole in X – Y=71 plane Cut 16

Figure E.3.3.13 E-seal frequency=2.44GHz Y cut at 71

E.3.3.3 On-Rail Conclusions

The on-rail simulation results show non-uniformity of signals observed alongside the container. This is due to resonance of RF signals in the gap between the containers and diffraction as the signals propagate out of this slot and to the outside. Because of these physical effects, higher-frequency e-seals may offer two advantages:

- Better coupling to the gap which acts as a microwave cavity; or better excitation efficiency in the gap cavity (or waveguide).
- More uniformity of signal distribution outside the gap, which may reduce sharp spatial variation of signal strength that can cause strong location dependency in reader responses.

E.3.4 On-Road Simulation

E.3.4.1 Scenarios and Configuration

The on-road simulation scenario is the same as the in-gate scenarios without obstructions. Hence, the configuration used for in-gate scenarios should be also applicable in the on-road environment.

E.3.4.2 Simulation Results

In this section we present results from the in-gate simulation run with no obstructions, in Z cut plane (Figures E.3.4.1.a-c). The results presented in Figures E.3.2.2 and E.3.2.3 are also applicable to the on-road environment. The Y cut plane is interesting, to examine the effects of reader antenna placement over the road. The patterns in Z cut planes are more interesting when looking at reader placement on the roadside.

The results again indicate that for lower frequencies (longer wavelength), contours are more uniform. At higher frequencies (shorter wavelength), signals are more directional, producing contours that are not as uniform. In the regions between the signal lobes the signal drops off, and that may result in no-reads in those regions. This needs to be validated against the read data collected at the terminal.

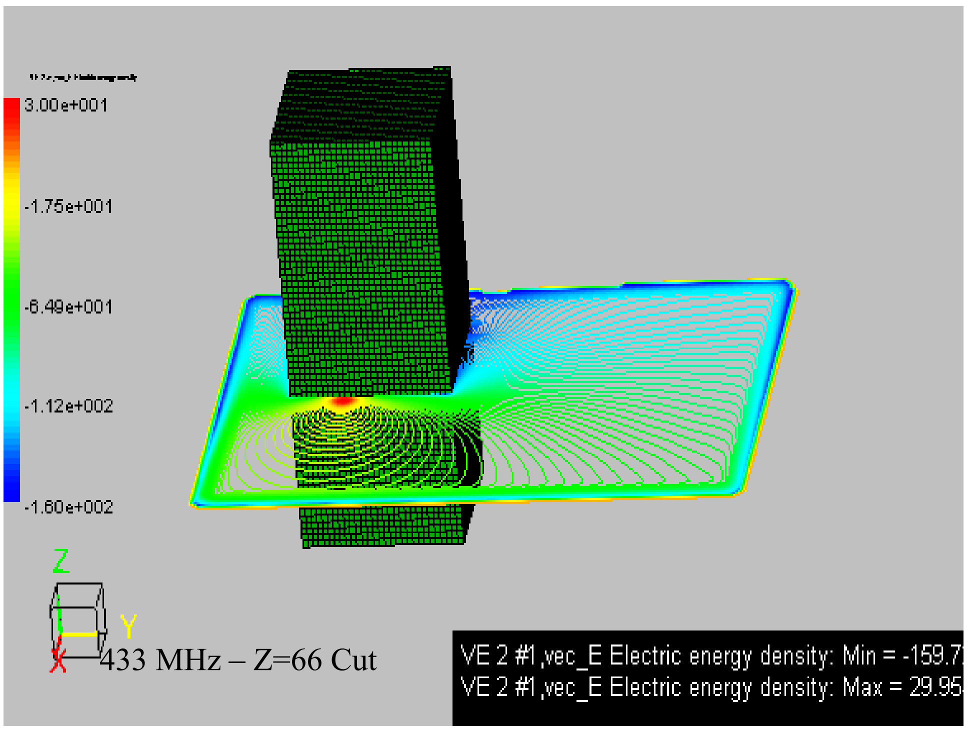

Figure E.3.4.1.a E-seal Signal Propagation with no Obstructions, 433MHz, Z cut at e-seal level

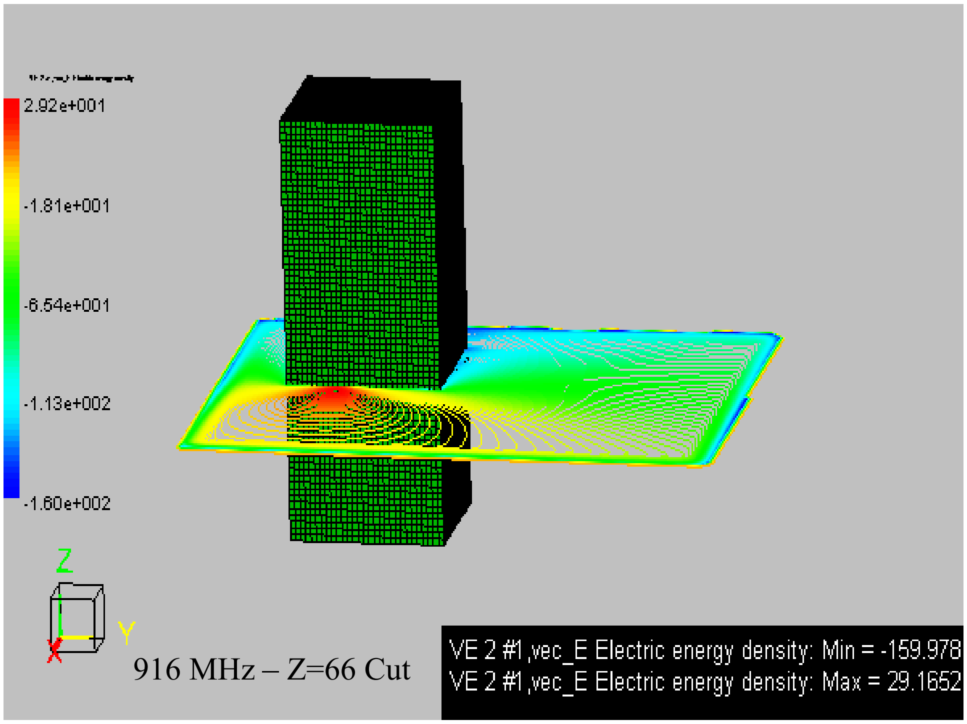

Figure E.3.4.1.b E-seal Signal Propagation with no Obstructions
(916MHz, Zcut at e-seal level)

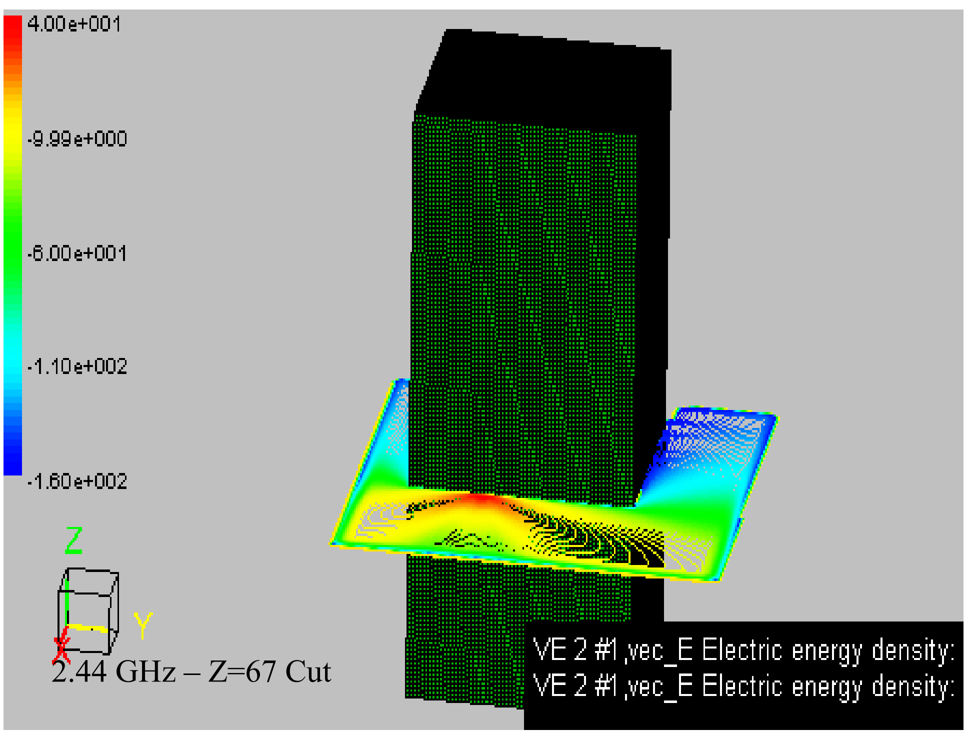

Figure E.3.4.1.c E-seal Signal Propagation with no Obstructions
(2.44GHz, Zcut at e-seal level)

E.3.4.3 On-road Simulation Conclusions

The results indicate that for lower frequencies (longer wavelength), contours are more uniform and spread out. At higher frequencies/ shorter wavelength, signals become more direct. For 2.44GHz frequency, gaps between direct signals may create regions with no-reads. The impact of the non-uniform patterns, resulting in no-reads, needs to be investigated against terminal read results.

E.4 CONCLUSIONS

The simulation effort investigated signal propagation and radiation patterns of three frequencies (433MHz, 916MHz and 2.44GHz) in the in-gate, on-rail, and on-road environments. The objective of the in-gate simulation was to investigate signal propagation in the terminal environment and, in particular, signal propagation and radiation patterns when signals reach obstacles commonly found in the in-gate area, such as booths and other containers. The objective of the on-rail simulations was to examine the effectiveness of e-seals in transmitting RF signals to the reader when the e-seal is in the gap between stacked-up containers. The on-road simulation scenario was similar to the in-gate scenarios with no obstructions.

For 433MHz signals, the in-gate simulation results show that signal strength contours, when there are no obstructions, are fairly uniform, and with a 69-cm wavelength, signals wrap around the edges of the container somewhat better then do signals for the other two frequencies. For 916MHz signals, radiation contours are less uniform. Finally, for 2.44GHz with a 12-cm wavelength), the contours evolving around e-seal are not uniform but have directional lobes. One reason is the reflection from the container door (backplane). The dipole has all three dimensions comparable to the wavelength and is offset from the container door by a few centimeters. This sets up a reflected “image” RF source that behaves as if it were “behind” the door. The combined radiation from the image source and the actual source can set up interference patterns, i.e., radial nodes of high and low signal strength. This directivity may create gaps where signal drops off sharply, and may result in regions with no-reads.

The patterns produced in the environment with structures are not as uniform as the patterns in the case where there are no obstructions. Pattern of RF intensity exhibits wave-like variations, which is typical of interference due to superposition with reflected signals from all the structures. Examining the patterns one can conclude that their propagation characteristics are somewhat similar. This is consistent with a rule-of-thumb in radio communications that operating effectiveness decreases by only 5%-10% as frequency increases from 433MHz –

2.44GHz. Hence, within the simulation region, we saw no great advantages of one frequency over the others.

The on-rail simulation results show non-uniformity of signals observed alongside the container. This is due to resonance of RF signals in the gap between the containers and diffraction as the signals propagate out of this slot and to the outside. Because of these physical effects, higher-frequency e-seals may offer two advantages:

- Better coupling to the gap which acts as a microwave cavity; or better excitation efficiency in the gap cavity (or waveguide).
- More uniformity of signal distribution outside the gap, which may reduce sharp spatial variation of signal strength that can cause strong location dependency in reader responses.

The on-road results also indicate that for lower frequencies (longer wavelength), contours are more uniform. At higher frequencies (shorter wavelength), signals are more directional, producing contours that are not as uniform. In the regions between the signal lobes the signal drops off, and that may result in no-reads in those regions. This needs to be validated against the read data collected at the terminal.

Since radiation patterns may vary significantly among various e-seals even at the same frequency, signal uniformity becomes an important factor. Uniformity helps ensure that if signal strength is maintained above a certain level for a particular distance along the road or rail, there should be no “no-read” regions within this distance as a result of poor signal strength.